THE UNIVERSITY OF MICHIGAN

INDUSTRY PROGRAM OF THE COLLEGE OF ENGINEERING

VORTEX RINGS FORMED BY FREE SURFACE INTERACTION

Hugh F. Keedy

A dissertation submitted in partial fulfillment
of the requirements for the degree of
Doctor of Philosophy in the
University of Michigan
Engineering Mechanics
1966

January, 1967

IP-765

Doctoral Committee:

        Associate Professor Walter R. Debler, Chairman
        Professor James W. Daily
        Associate Professor Arthur F. Messiter
        Professor James D. Murray

ACKNOWLEDGMENTS

TABLE OF CONTENTS

TABLE OF CONTENTS

LIST OF FIGURES

v

LIST OF FIGURES (CONT'D)

I. INTRODUCTION

A smoke ring is a rather commonplace phenomenon but seldom fails to catch the interest of an observer because of its intriguing properties. Although looked upon as a curiosity of nature, the smoke ring is but the most familiar example of the general classification known as vortex rings. Within recent years interest in vortex rings has increased as their presence and importance in nature has become more widely known. For example, the presence of vortex rings ranges from low temperature helium studies where the rings have diameters measured in microns to large scale thermal rings in the atmosphere.

The study of buoyant fluids, with specific applications to atmospheric studies, has been the general framework for most, but not all, vortex ring considerations. First investigations of the recent era involved continuous thermal point and line sources and led others to investigate discrete, rather than continuous, masses of buoyant fluid. Several studies of vortex rings emerged. Turner[18] and others introduced bouyant masses into the bottom of a tank in such a way that vortex rings were formed. The motion of these rings was studied and a theory developed.

In some of the early studies, brief mention is found that vortex rings could be formed by allowing drops to penetrate a free surface. However, special precautions were taken to avoid this type of formation from entering into the experiments. This present study concerns vortex rings formed by this free surface interaction with a falling drop of liquid. The density of the drop solution may be of greater, equal or lesser density than the solution providing the free surface. Therefore the rings studied may be considered as having either positive, neutral or negative buoyancy with respect ot the surrounding fluid. Thus, the buoyant force

can be chosen to act either in the direction of motion or opposite to it,
depending on the choice of drop and base solutions. This feature is not
known by the author to have been considered in other studies.

The general pattern followed by rings of this study begins with
a free falling drop hitting a free surface. As the mass contained in the
drop passes through the free surface and into the fluid below, there is a
change of shape from that of a drop to that of a torus, or ring. This
transformation of shape is completed within a very short time compared to
the total time of descent of the ring. The penetration into the base
during transformation is also small compared to the total penetration
of the ring. As the ring descends in the base solution the velocity of
the ring decreases and the diameter of the ring changes. A critical depth
of penetration (to be defined more precisely later) is reached at which
time the ring stops or begins a second transformation to a number of smaller
rings. The conditions under which the rings are produced are quite im-
portant in determining the characteristics which the ring will possess.

Two important features should be noted. The depth of penetra-
tion to critical depth is a function of the distance through which the
generating drop falls, but the surprising feature is that the relation-
ship of penetration to increasing free fall height plots as a curve with
definite sinusoidal characteristics. Secondly, the production of rings
of the types discussed is limited to a rather narrow range of free fall
distances.

In addition to the general characteristics exhibited by the rings,
several less frequently occurring phenomena connected with the study will
be described. These will include oscillations of the ring during descent,
unusual behavior of drops at the free surface and the appearance of very
small bubbles which descend with the ring.

II. SCOPE OF THIS RESEARCH

The purpose of this research is to investigate the behavior of vortex rings formed by the interaction of a free falling drop with a free surface. Variables which might be expected to affect this behavior are investigated and their effects discussed.

The study is confined to the formation of rings in a motionless base solution of uniform density, although the relative density of the ring and surrounding base solution may vary. The range of densities considered is quite small with the maximum density difference between the ring and base solutions being less than 1.5 percent. The density difference is one of the two major variables of the study.

The second major variable is the free fall distance of the drop before hitting the free surface. The range of free fall distances involved is quite limited, not by choice as in the case of the density differences, but by the fact that rings of the type discussed form within a range of less than two and a half inches of free fall. Outside this range occasional rings form but by a different process.

A third possible variable, the size of the drop used to produce the ring, was chosen as fixed. In the experimental part of the study a few observations using other size drops were made for comparisons but results will be given for only one size drop.

The study consists of two parts. The experimental phase was undertaken to observe the behavior of vortex rings formed by drops falling on a free surface. A primary purpose was the development of a basic knowledge of the behavior of such rings and a general understanding of their physical properties. A rather detailed description is presented, both by

written description and by a number of graphs designed to convey the prominent characteristics of the rings as indicated by the data collected. A second important aim of the experimental part was the collection of data for use in construction of a model and theory relating to that model.

The second part of the study concerns the construction of the model and related theory. A discussion of the agreement between theory and experimental results concludes the study.

III. LITERATURE SURVEY

The brief survey which follows presents a review of some of the early investigations involving the motion of vortex rings and some of the more recent analytic and experimental work which has been done. Two recent applications of vortex ring principles are cited to illustrate the far reaching areas of application and to indicate possible future studies using principles discussed here.

A. Early Investigations

The motion of vortex rings was a subject of interest in the period of the 1880's and several notable papers were presented during this era. Interest was largely due to the theory of vortex atom constitution of matter which was presented by Sir W. Thomson. The results of J. J. Thomson's efforts to investigate this theory more fully were published in a treatise <u>Motion of Vortex Rings</u> in 1882 and won for him the Adam's Prize.[17] A second contributor during this period was W. M. Hicks whose researches on the theory of vortex rings was published in two parts in Philosophical Transactions in 1884 and 1885.[5,6] Although the work of this period was done under the assumption of an ideal fluid, many of the results form the basis of later studies and many valuable insights were afforded. One item of special interest in the papers of Hicks is the possibility of "hollows" being formed under certain pressure conditions. In the course of this present study, very minute bubbles associated with the rings were observed. They will be discussed at more length later.

For a review of the results of this era the reader is referred
to the chapter on Circular Functions in Basset's works.[2] A similar but
less comprehensive review occurs in Lamb.[8]

B. Development of Buoyant Vortex Ring Studies

After the early investigations mentioned above the subject
seemed to remain rather dormant until the period of the second World War.
At that time interest was centered on studies of the effects of thermal
sources, both discrete and continuous, on the atmosphere. The vortex
ring, as one possible form which a discrete mass may assume, again became
a topic of interest.

Several early papers of this era concerned studies of contin-
uous thermal plumes rising through a fluid body at uniform temperature.
Following these, Morton, Taylor and Turner[11] investigated both contin-
uous and instantaneous sources of buoyancy in a fluid with a density
gradient, with application being made to the atmosphere. In the study
it was assumed that the source did not produce appreciable momentum.
Although the basic concern was with a heated source, the treatment was
made by using an equivalent density deficit with respect to the sur-
roundings. Following assumptions of previous work, the rate of entrain-
ment by the plume or cloud was taken to be proportional to a characteris-
tic velocity at the height concerned. Density differences of the plume
and surroundings were taken to be small. Results of discrete masses of
buoyant fluid in a fluid with linear density gradient indicated that the
cloud mass rose with a velocity which decreased with height, enlarged
linearly with height, reached a maximum height and settled there after
several oscillations about the level and entrained fluid in route at a
rate of the order of 0.3 times the average velocity of the cloud.

Scorer[15] and Woodward[20] conducted experiments with descrete thermal and buoyant masses and noted that the motion of the masses was much like that of vortex rings. From such observations there arose the vortex ring model used widely in investigations of the behavior of thermal and buoyant masses.

C. Studies of Turner and Morton

Turner[18] investigated buoyant vortex rings in a homogeneous fluid. Starting with known results for vortex rings in a perfect fluid as developed by Lamb, Turner also assumed constant circulation from which it followed that buoyancy increased the impulse. Entrainment effects due to viscosity were neglected.

A similarity solution was assumed from which it was concluded that the product of ring velocity V and diameter D is constant and related to circulation K through a constant factor C by VD = CK. A second conclusion was that the ring diameter is linearly related to the distance of travel h of the ring from a virtual origin by D = nh where n is constant. The study made on this basis indicated that increasing the buoyancy will lower the velocity of rise and icrease the rate of expansion of the ring diameter.

An experimental part of Turner's work involved releasing buoyant rings at the bottom of a tank. For the major part of the travel of the ring, (the final stages were not considered due to increased viscous effects), the values of c and n defined above were found to be constant for any given ring. Values of the constants were found to vary from ring to ring, however. The fluid used to form the ring was injected into the bottom of the tank in such a way that the circulation was the same for all rings, in keeping with the basic assumption of the similarity

solution used. The buoyancy was varied by the use of various density solutions for ring and ambient fluid. The time for rings to reach a specified height was recorded. Results indicated that for a certain density difference (about 3.5%) the time to reach a specified height was minimum with the time required increasing nearly linearly on both sides of this critical density relationship.

A similar analysis and experiment with a stably stratified base fluid revealed that buoyant rings rose to a height which was dependent on the density difference of the base and ring fluids. A maximum height of rise was noted for a density difference of about four per cent with a linear reduction of maximum height for density differences removed from this value. The maximum density difference of 1.5 per cent as used in this present study is well below the critical value found by Turner.

In an extension of results of his earlier paper, Turner[19] compared buoyant vortex rings and vortex pairs. For vortex rings in a stably stratified base fluid, the circulation was no longer assumed constant but was related to the density gradient of the base fluid. A development was made in which the initial buoyancy, initial circulation and the density gradient are variables which determine the behavior of the rings. By introducing a given initial circulation into a non-dimensionalized discussion, three distinct cases of behavior are found. The types are based on the relative times at which the circulation and momentum reach zero. When both reach zero together, a linear increase of ring diameter with distance is indicated, as in the case of uniform surroundings. When momentum becomes zero before the circulation, the

rings enlarge less rapidly but nearly linearly with distance until the point of zero buoyancy, after which the ring diameter decreases to zero as the ring travels a short distance further. If circulation becomes zero before the momentum does, the ring is indicated as increasing in diameter more rapidly but nearly linearly until the point of zero buoyancy. At this point the ring stops but the diameter increases quite rapidly to a large value. Turner felt that the physical reality of the latter type is doubtful.

Morton[10] presented an analysis for weak vortex rings, (as opposed to the strong rings discussed by Turner), generated from an instantaneous point source of heat. Density variations due to temperature were considered small and taken into account only through the buoyancy terms. Both kinematic viscosity and thermal conductivity were included in the analysis and a similarity solution assumed. The results indicated a constant circulation, linear increase of ring diameter with height, and vertical ring velocity inversely proportional to height. The rings expanded more rapidly with height than the stronger rings of Turner. Growth of the rings was attributed to thermal and viscous diffusion rather than to entrainment of fluid by the ring as indicated by Turner.

A significant difference is found in the studies conducted by Turner and Morton. While the rings investigated by Turner were turbulent except perhaps in the early stages, those discussed by Morton were considered to always be laminar.

The assumption of a similarity solution in which the distributions of the circulating and turbulent velocities remain similar at all heights was basic to the work of Turner and Morton. Many other

investigators working with isolated thermal and buoyant masses, including Woodward and Scorer, used this assumption as the basis of their studies and produced results which were experimentally verified. A second possible assumption which Turner[18] proposes arose from observations made by Dr. E. G. Bowen (and reported by Turner) of smoke rings formed by explosions. His observations suggest that the vorticity containing region has a constant volume. Since the volume of a torus is given by $V = 2 \pi^2 Ra^2$, the implication is that the product Ra^2 (R is the ring radius and a the core radius) be constant. Turner, however, found that the assumption of a similarity solution better fitted his laboratory results.

D. Mechanics of Drops

It will become evident in the description of the formation of the rings that the interaction of the drop and the surface is very strongly affected by the shape and mode of motion of the drop at the time of contact. It is not the purpose of this study to investigate the behavior of free falling drops but in the interest of a broader understanding of the underlying mechanisms of the phenomena a brief description of some of the important properties of falling drops is presented. A more extensive discussion of the topic may be found in an article by Hughes and Gilliland.[7]

The dynamics of a free falling drop, neglecting drag, are expressed by the familiar relationships:

$$v = (2gh)^{1/2} \quad \text{and} \quad h = gt^2/2$$

where h is the free fall distance. For this study, the maximum free

fall distance was about two and a half inches so that terminal velocity

was not approached and the above relationships considered applicable.

A free falling drop does not maintain a constant shape, but

rather oscillates about an equilibrium configuration. Surface tension

tends to make the drop spherical but the presence of drag during free fall

results in an equilibrium configuration which is spheroidal rather than

spherical. The deviation from the spherical shape can be expressed by an

eccentricity defined as the ratio of the length of the axis in the direc-

tion of motion to the length of the transverse axis. For the sphere the

eccentricity so defined would be unity. The eccentricity for the equilib-

rium configuration is greater than unity.

The surface tension forces at the time of release of the drop

from the generating needle induce distortions of an oscillating nature

about the equilibrium form. The drop changes from spherical through

the equilibrium form to vertically oblate, then returns through the

spherical shape to horizontally oblate and back to spherical in one oscil-

lation. As the surface tension effects damp out during free fall, the

variation about the equilibrium configuration decreases and the eccen-

tricity approaches a constant value, that of the equilibrium configura-

tion. See Appendix A.

Hughes and Gilliland report that a 3 mm. water drop (very

nearly the size used in this study) experiences a decrease in amplitude

of oscillation of about one half in a free fall distance of about 60 cm.

in air, or during 0.35 seconds. Since the maximum time required for free

fall in this study is about 0.11 seconds (a free fall of about 7 cm.) the

oscillations are quite important. Further, Hughes and Gilliland concluded that the oscillations do not severely affect the overall motion of the drop but that their effect on the internal motion could be quite large. It was found in this study that these conclusions were valid. Agreement with theoretical free fall times was very good. The effect of internal motion was found to be one of the major determining factors in the characteristics of the rings formed.

For the case of a free falling drop in air, the important variables are considered to be the frequency of oscillation f , the radius of the equivalent sphere a , the density of the drop ρ and the surface tension of the drop σ . These four variables may be arranged into a non-dimensional parameter $f^2 a^3 \rho/\sigma$ from which the frequency may be expressed as:

$$f = (\text{constant})(\sigma/\rho a^3)^{1/2} \text{ cycles/second}$$

Lamb[10] presents a general form for all modes of vibration of a liquid drop in air. From this formulation, the primary mode of vibration is found to be of frequency:

$$f = 3.87 \ a^{-3/2} \text{ cycles/second}$$

with a the radius of the equivalent sphere in centimeters. This is in agreement with the above relationship. From Lamb's presentation, the next four higher modes have frequencies 1.6, 3.0, 4.2 and 5.5 times those of the fundamental oscillation.

E. Applications of Vortex Ring Theory

Vortex rings or elements of vortex ring theory occur frequently in nature. The vortex ring studies noted earlier were conducted to provide insight into thermal effects in the atmosphere. Also, vortex ring forms are found in some demolition explosions. An explanation for the way in which birds can soar for long periods of time without moving their wings is based on the existence of large vortex rings of long life. By circling in such a manner that the kinetic energy supplied by a region of updraft is just sufficient to overcome drag on the wings, the bird can maintain altitude or even gain altitude without effort of its own.[4]

Whereas atmospheric vortex rings are usually very large scale, a recent theory regarding the flow of charged particles in superfluid helium concerns vortex rings whose diameters are measured in microns. In working with low temperature helium (0.3 to 0.6°K) Rayfield and Reif[11] found that charged ions behave in an unexpected manner. Experiments showed that the velocity of a charged carrier is very low compared to the velocity of uncharged ions, that this velocity is approximately inversely proportional to the energy of the carrier, and that this relationship of velocity and energy is unique. It is concluded that charged ions behave almost like free particles and the assumption was made that the electric charge is coupled to the surrounding liquid in the form of a vortex ring. Analysis made on the basis of classical hydrodynamics suggested that each ring contains precisely one quantum of circulation. As the energy of the ring is increased, the velocity decreases and the radius increases but the circulation remains one quantum. Experiments in liquid helium have been conducted for the purpose of comparing results

with vortex ring theory but the conclusions, although encouraging, are still inconclusive.[12] Efforts are presently being made at the University of Michigan to model vortex rings in water to gain insight into the behavior of vortex rings in the theory of superfluids.

Another area in which no mention is made of vortex ring formation or theory but which exhibits many characteristics of the early stages of ring formation is that of high speed impact. In a study of solid projectiles impacting a solid surface at various velocities made by Charters,[3] three regions stand out. In the low speed region, the projectile deforms but is unbroken during penetration. Penetration is found to vary directly with velocity. As velocity of the projectile is increased, a second region is found in which the projectile cannot withstand the forces of impact and deforms radically or breaks up. Penetration decreases for a time with increasing velocity but then begins to increase again, tending toward a rather uniform rate of increase but less than that of the first region. The final region, with highest velocities, is the fluid impact region characterized by a large crater with complete disintegration of the projectile into a flowing metal which coats the surface of the crater and sprays outward around the top. In the same vein with this last region, a study by Anders[1] concludes that the meteorite responsible for Meteor Crater in Arizona can be reasonably well described from the size and shape of the impact area. Both the shape of the meteorite and its orientation at impact are considered important.

In this present study the free surface behavior of the falling drop closely resembles the first region described by Charters. The behavior of the surface and drop beyond the range of free fall heights which produce vortex rings resembles well the transition and fluid impact regions. It is found in this study that the geometric configuration at impact with the free surface has great influence on the rings produced.

IV. ORIGIN OF PRESENT WORK

The subject of this thesis arose from what began as some prelimi-
nary investigations with dyed jets introduced into a horizontal flume
flowing with a stratified fluid. The water level would eventually fall
below the level of the surgical needle through which the vertical jet was
issuing. At sufficiently slow flow rates, the jet, when clear of the sur-
face, would produce drops rather than a continuous stream. These drops
upon hitting the free surface were observed to produce vortex rings of a
consistent nature for a given free fall height of the drops. As the level
of the base solutions dropped further, the characteristics of the vortex
rings changed. Finally a free surface level was reached at which no
further rings were produced.

The effects observed were so unusual and interesting that it was
decided to investigate further the behavior of rings produced under con-
trolled conditions of drops falling on a free surface. To simplify the
observations and data, the base solution (into which the drops fell) was
chosen of constant density and motionless. However, the density of the
base and drop solutions was allowed to vary. The range of densities of
the solutions used was also a product of the evolutionary nature of the
study and is approximately that of the range of density within the strati-
fied base of the origin study.

As the number of observations increased and more data were col-
lected, several characteristics of the rings appeared with regularity.
Other phenomena connected with the rings were also observed. It is with
these characteristics and phenomena that this study is concerned.

V. EXPERIMENTAL PROGRAM

A. Apparatus

The apparatus constructed was for the purpose of producing vortex rings caused by free falling drops hitting a free surface. The conditions under which the rings were produced were controlled so that the effects of certain variables on the behavior of the ring could be studied and data collected for use in development of an appropriate model. The rings were generated by dropping drops of salt water of known salinity from the tip of a hypodermic needle into an aquarium containing a base of known salinity. See Figure 1. The apparatus, although quite simple and easy to use, allowed good control of the ring characteristics.

In most cases the drop generator was a hypodermic needle whose end had been filed to a blunt tip. Unless specified otherwise, a standard No. 20 needle was used. A few observations were made using larger and smaller needles and even a section of 1/4" diameter copper tubing. The results for these generators were qualitatively in agreement with those of the No. 20 needle.

The generating needle was mounted on a vertical bar which was in turn mounted on an angle iron base. This entire assemblage rested on the top of the aquarium and was moved by hand to position the generating needle as desired. The vertical bar to which the generator was mounted had an attached vernier giving vertical displacements to the nearest 0.001 foot, or approximately 1/64 inch.

The solution for the drops was supplied to the generator by means of a 1/4" rubber tube siphon from a supply bottle mounted on a ring stand. The supply bottle could be adjusted vertically to control the
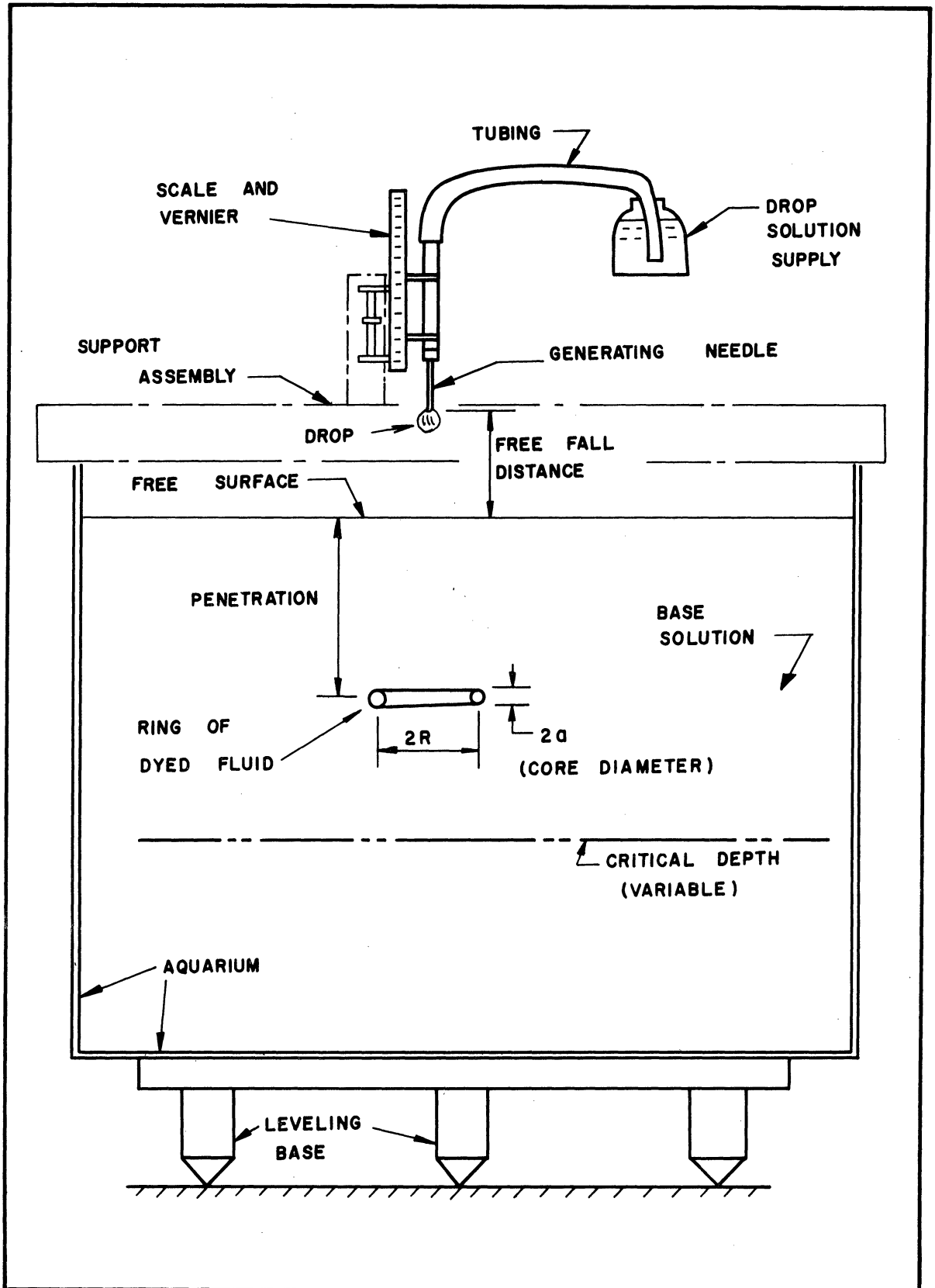
Figure 1. Definition Sketch of Equipment.

rate at which drops were formed. In practice the drops were formed at least two seconds apart, usually much longer. This procedure reduced internal momentum effects within the drops and served to standardize release conditions, especially the drop size. Also, the time between drops was used to move the angle iron base and still have ample time for vibrations induced while relocating the needle to damp out before the next drop fell. Moving the position of the generating needle between drops allowed each drop to penetrate a portion of the free surface which had not been disturbed or contaminated, at least for a time, by a previous drop.

The base solution was contained in a standard aquarium 11-1/2" by 8" by 9-1/2" deep. The manner of filling the aquarium was either by a slow flow through a siphon tube or by pouring the solution directly from a bucket. It was found that the former method produced internal currents which were essentially damped out in an hour or so. The second method produced a base solution free of objectionable internal currents after setting overnight. The dyed vortex rings, as they slow down, are excellent indicators of any currents present. (The currents were never completely absent, even after a period of several days, but were generally of such slow velocities as to not alter the results materially.)

After filling, the entire aquarium and needle assemblage was leveled by means of a three point support. This assured a constant distance from the needle tip to the free surface of the base solution for any position of the needle. To minimize wall effects, care was taken to avoid forming rings within an inch of the aquarium sides, a safeguard visually observed to be adequate.

Solutions for both the drops and base were made from a stock solution prepared by thoroughly mixing 8.0 pounds of general purpose salt into 10 cubic feet of water. The stock solution was stored in gallon jugs and then diluted, by volume, to produce the desired solutions. Solutions used ranged from 0.025 pounds of salt per cubic foot to 0.800 pounds per cubic foot.

In order to present the combinations of variables used in an experiment briefly, the following notation was adopted and will be used. The solutions used for the drops and base were designated by a density number from 0 to 32. To convert to salt content, multiplying by the factor 1/40 will give the number of pounds of salt per cubic foor of water. The other major variable, the fall height, completes a triplet. For example, DOB8F.08 indicates a drop with zero salinity falling into a base solution containing 0.20 pounds of salt per cubic foot from a surface to needle distance of 0.08 feet. The range of density differences of drop and base is therefore from D32B0, designated as +32, to DOB32, designated as -32.

The apparatus reduced the number of variables under investigation to three; namely, the size of the needle, the distance from needle tip to the free surface and the density difference between the drop and base solutions. Actually, a given density difference could be produced by several combinations of drop and base solutions. It will appear in the discussion that the combination as well as the density difference affects the behavior of the ring although the latter is generally the predominant effect.

B. <u>Observations</u>.

The experimental part of this study was conducted by dropping a large number of drops onto a free surface and observing the behavior and the characteristics of the vortex rings formed. Some characteristics were found to be common to all rings while other characteristics were found to vary with the conditions used to generate the rings. The observations which originally inspired the theoretical part of this study and which support the theoretical analysis are of two types, visual and photographic. These will be discussed.

1. Visual observations.

In general visual observations were used for obtaining data when the velocities were small or extreme precision was not necessary. Thus this method was used in determining critical depths (to be defined later) of the rings, and for observations of the number of secondary rings produced or for the presence of air bubbles that occurred as a by-product of the ring's formation.

Data involving the depth of penetration of rings into the base for various free fall heights were all obtained visually. A discussion of problems encountered is contained in the section on measurements. An important depth, known as the critical depth, was defined as that depth where the translatory motion of the ring ceased or some entirely new ring characteristic appeared.

In practice, the critical depth could be anticipated by the observer. If the drop and base solutions were identical, the rings enlarged noticably just before the critical depth was reached. The development of small vortex rings, or secondary rings, was used to denote the

critical depth when the drop solution was more dense than the base solution. If the drop solution was of less density than the base solution, the original ring stopped and secondary rings rose from it. The depth at which the ring stopped was considered the critical depth.

The determination of the critical depth was made by superposing two vertical scales in the line of sight. A grid of horizontal lines a quarter inch apart was attached to the rear of the aquarium to measure distance from the surface. Plastic scales were placed on the front of the aquarium to measure from the surface. As a ring descended, one could lower the eye to keep the ring and two corresponding depth marks together to obtain a depth reading free of parallax effects. As the ring reached critical depth, the scale reading was noted and recorded.

No other measurements were made visually. However, many behavior patterns became evident from the many drops observed. Among these are the formation of the secondary rings, the behavior at critical depth, the appearance of small air bubbles and other effects. These will be described and discussed later.

This method was used to determine the critical depth of rings formed at various free fall heights over the entire range of formation. Data obtained will be presented later in the form of a series of penetration graphs.

2. Photographic observations.

Although many features of the vortex rings could be noted by visual methods, the speed involved in some of the more critical periods of the history of the drop and ring made photographic techniques a necessity. Several photographic arrangements were tried involving both motion

pictures and still cameras. It was found the best quantitative data could be obtained from a multiple exposure with a still camera while qualitative details of surface interaction and of ring formation were best shown by high speed movies.

a. Still pictures:

Some early photographs were made using 35 mm film and Polaroid film but it was found that a 4" by 5" Graflex camera produced negatives of better size and quality. Kodak Contrast Process Ortho film was used to produce negatives of maximum contrast.

Due to a very limited depth of field, it was very important that drops were made to fall at the same point for each picture. A series of guides and stops made it possible to position the generator at a chosen point between drops when a picture was to be exposed. As only one drop (i.e. ring) was photographed per film sheet, the generator was removed as soon as the drop fell. Sufficient time was allowed between exposures to allow the spot of penetration to return to a relatively undisturbed state and for the dye residue of the previous drop to diffuse into the sur-roundings.

The method of measuring the size of the rings needs to be noted. A plastic scale was immersed vertically at the spot immediately below the needle. The camera was then positioned in such a way that the image of the immersed scale appeared full size on the ground glass back. With the camera position unchanged, the scale was removed and photographs of the rings were made. Ring dimensions were measured directly from the full size images on the negatives. This technique was used since the introduc-tion of any kind of measuring device near the axis of the ring would have introduced undesired effects on the behavior of the ring.

Lighting was provided with a Type 1532-B Strobolume actuated by a Type 631-BL Strobotac. The Strobolume was located about 4" from one end of the aquarium with the axis of the source at the center of the picture area and normal to the camera axis. A cylinder of white cardboard served to channel the light into the region of interest. It was found that a background of ordinary brown wrapping paper produced good results. The timing of the flash rates was checked by the use of the built-in reed calibration system for the more rapid flashing rates and by stopwatch for the slower flashing rate.

The purpose of this series of photographs was to produce negatives each recording a number of positions of a single ring at regular time intervals. With the lighting described set at high intensity, it was found that up to about 16 positions (each flash recording a position) could be recorded. In order to insure as much detail as possible, the number of positions was usually restricted to 10 or 12. The medium dark background seemed to reduce the "washing out" of a recorded position by other flashes of the exposure and yet provided suffecient contrast for clarity.

For 10 flashes, f/8 was found to be most satisfactory as a shutter setting. The exposures were made on open shutter for the number of flashes desired. The use of open shutter made it essential that the light level in the room during exposure be as low as possible. However, complete darkness was not practical as it was necessary to check the needle position and determine when to begin the exposure as the drop left the needle. Some general fogging of the film was induced but was not considered objectionable.

Due to the wide variation in velocity over the region of penetration it was necessary to use two exposures to study the full life of a given

type ring. A flash rate of 600 per minute (0.1 seconds between images) produced well spaced images during the early stages of penetration. In low velocity regions overlapping occurred at this rate. For these regions of low velocity 120 flashes per minute (0.5 seconds between flashes) gave only chance images in the upper regions of penetration but produced well spaced images as the ring slowed. A study of the two negatives for a given set of variables was made to determine if they were compatible in overlapping regions and if the region of critical depth was in agreement with the visually observed critical depth of rings of that type. If there were discrepancies, a repeat series of two negatives was made.

Only two bases, B0 and B8, were used during the photographic study. With each base solution, a range of drop solutions from B32 to B0 was used to give ten different combinations of drop and base solutions. In addition, two free fall heights were used. One was in the region of 0.08' where the critical depth occurs after|maximum penetration. The other free fall was in the region of 0.10' where the critical depth occurs after minimum penetration. The actual free fall to produce maximum penetration to critical depth or minimum penetration to critical depth was determined visually just prior to the taking of the pictures. Slight variations in free fall were found for various combinations but the free fall heights remained close to the regions noted.

The negatives were studied individually and in pairs to obtain data concerning the penetration characteristics, velocity and size of the rings. Measurments were made with a scale divided into fiftieths of an inch and with a 6X comparator. Data obtained was used to produce Figures 5 through 24.

b. Motion pictures.

Motion pictures were made of the drop as it fell to the surface, as it penetrated the free surface as seen from above, and as it penetrated the free surface as viewed from below. Through the generous cooperation of the Department of Aerospace Engineering arrangements were made for the use of a Fastax camera, a high speed camera. For this study the maximum speed was about 2650 pictures per second.

Exposure was made on 100 foot rolls of Dupont 931A reversal film. Exposure was checked by a trial run of about 25 feet of film which was hand developed in DK-50 developer. Lighting was supplied by two No. 2 photoflood bulbs in metal reflectors. One reflector was placed a few inches from a sheet of 1" styrofoam placed against the back of the aquarium. The second reflector was placed on a line about 60° above the horizontal and directed toward the needle. The camera was mounted on a tripod and directed normal to the front of the aquarium.

Two series of motion pictures were made. The first series was made at about 480 frames per second. A D8BO combination was used. Extension tubes were used on the camera to have the region from needle tip to the surface fill the frames of the film. Two rolls of film were taken of the forming of a drop on the needle, its release and free fall, and the penetration of the surface. One roll was taken of drops with free fall distance of 0.085 feet (in the region of maximum penetration) and one with free fall distance of 0.105 feet (in the region of minimum penetration). Two additional rolls were exposed to record the formation of rings from the same two free fall heights as viewed from below the surface level. Drops were produced about two seconds apart so that each roll recorded 4 or 5 drops.

A second series was made at approximately 1350 to 1500 frames per second. A B8 solution was used for all sequences. Two rolls were taken of D16 drops hitting the surface from free fall heights of 0.085' and 0.105'. At these heights, rings form well. A third roll was taken of the surface being hit by drops from 0.205', from which height rings will not form. Two rolls were taken of the surface effects as viewed from below using free fall heights of 0.085' and 0.105'. A final roll was taken of a special case which had arisen from time to time; namely, the tendancy for the drops to hit the surface but remain there for a short time as spheres before penetrating the surface. For this case DO drops were used from a free fall distance of 0.021'.

C. Description of Phenomena of an Individual Ring

Certain patterns of ring behavior emerge from the visual observations made and from the data collected from the photographic studies. Some of these patterns and characteristics are common to all rings while others are definitely related to the combination of variables used to produce the rings. The following will present a description of the life history of a ring from the time the drop leaves the tip of the generating needle to the time when the vortex ring dissipates into the surroundings. Although much of the description is based on qualitative observations (mostly visual) several important quantitative results will be presented in their proper places. The history of a ring is divided into three quite distinct parts and will be discussed by these parts. A description of some unusual effects will complete this section.

1. <u>From Needle to Free Surface.</u>

Care was taken to form drops on the needle slowly to prevent momentum effects from causing a premature release of the drop. In this way drops were nearly identical with respect to size and initial conditions. The drops of course begin their free fall when surface tension can no longer hold the drop to the needle. Frame by frame studies of high speed movies showed a conical distortion at the top of each drop as it detached from the needle. Once the drop was free, this distortion induced an oscillation of the drop as surface tension forces pulled the drop toward a spherical shape. The sperical shape was overshot and the drop became horizontally oblate. The effect then reversed and the drop progressed back through the spherical form to a vertically oblate form, this time of less eccentricity than previously. This process repeated during the full period of the free fall with the magnitude of the oscillations decreasing with each cycle. The period of the oscillations was found to be constant, however, and is given below. The geometry of all drops at any given time measured from release was found to be identical and assured uniformity of drops for the study.

The period of oscillation of the primary mode as calculated from the movies was in excellent agreement with the formula previously noted in Lamb. For drops from a No. 20 needle, theory indicates a period of 0.0155 seconds while the motion pictures indicated a period of about 0.015 seconds. The total time of free fall was also in good agreement with free fall theory although slightly greater. (See Appendices A and B).

The shape of the drop shortly after release although uniform from drop to drop was not truly ellipsoidal but rather exhibited flat regions and occasional prominences. Later these were damped out and within about two

complete oscillations the form was essentially ellipsoidal in the motion
pictures. It is worthy of note that the cycle of shapes assumed was not
divided uniformly by times of maximum, zero and minimum eccentricity.
The vertically elongated shape was present for considerably more time than
the horizontally elongated shape. The time ratio of vertical to horizontal
elongation is approximately 5:3.

During one period of oscillation of the drop, the spherical shape
was momentarily present twice. In one instance the form was progressing
from vertical to horizontal elongation while in the other the opposite
transition was taking place. A very important observation from the study
of the movies was that the spherical shape was present at the time of con-
tact with the free surface for both maximum and minimum penetration of the
rings formed. For minimum penetration, the form was progressing from ver-
tically to horizontally elongated. However, for maximum penetration the
form was progressing from horizontally to vertically elongated.

The studies of the drops used to form the vortex rings indicated
several important properties of the drops in determining the characteristics
of the vortex rings formed. These were found to be the height of free fall
of the drop, the period of oscillation of the drop (which is dependent on
drop size but maintained constant for this study), and the shape of the
drop at impact as well as the direction of motion of the boundary of the
drop at impact.

2. Free Surface Behavior.

The interaction of the drop with the free surface was studied
by the use of high speed movies since the duration of the interaction was
too short to allow for detailed visual analysis. The study was restricted

to filming the interaction from above and from below the surface for two

free fall heights of the drop. One height was chosen as typical for the

production of rings of maximum penetration to critical depth and the

other height as typical of rings of minimum penetration to the critical

depth. The films were examined carefully for characteristics of a quali-

tative nature to compare the interaction for the two extremes of penetration

expected. It was not feasible with the arrangement used to make anything

more than crude measurements from the films.

Drops falling on a free surface have been photographed many times

and excellent pictures published.[3] However, in all such pictures known

to the investigator the free fall heights were much greater than in this

study. In such cases, the drops either form large craters or rebound in

a spout upon hitting the surface. This behavior is found to begin to ap-

pear at the upper ranges of the free fall heights of this study when rings

of the type discussed here can no longer be formed with regularity.

Selected frames of the interaction as seen from above are shown

in Figure 2. Although this series was taken with a free fall height of

0.085' the series for 0.105' was so similar as to not be included here.

The interaction of the drops is very similar for all cases. As

the drop contacts the surface it begins to depress the surface and at the

same time spread out along the walls of this depression. This momentarily

gives the appearance of a Mexican sombrero resting on the indented surface.

The center of the form continues downward as the center region becomes

thinner and the drop fluid continues to move outward from the center of

impact. During this time a single wave appears on the surface and begins

to move from the point of impact. How and when the drop solution actual-

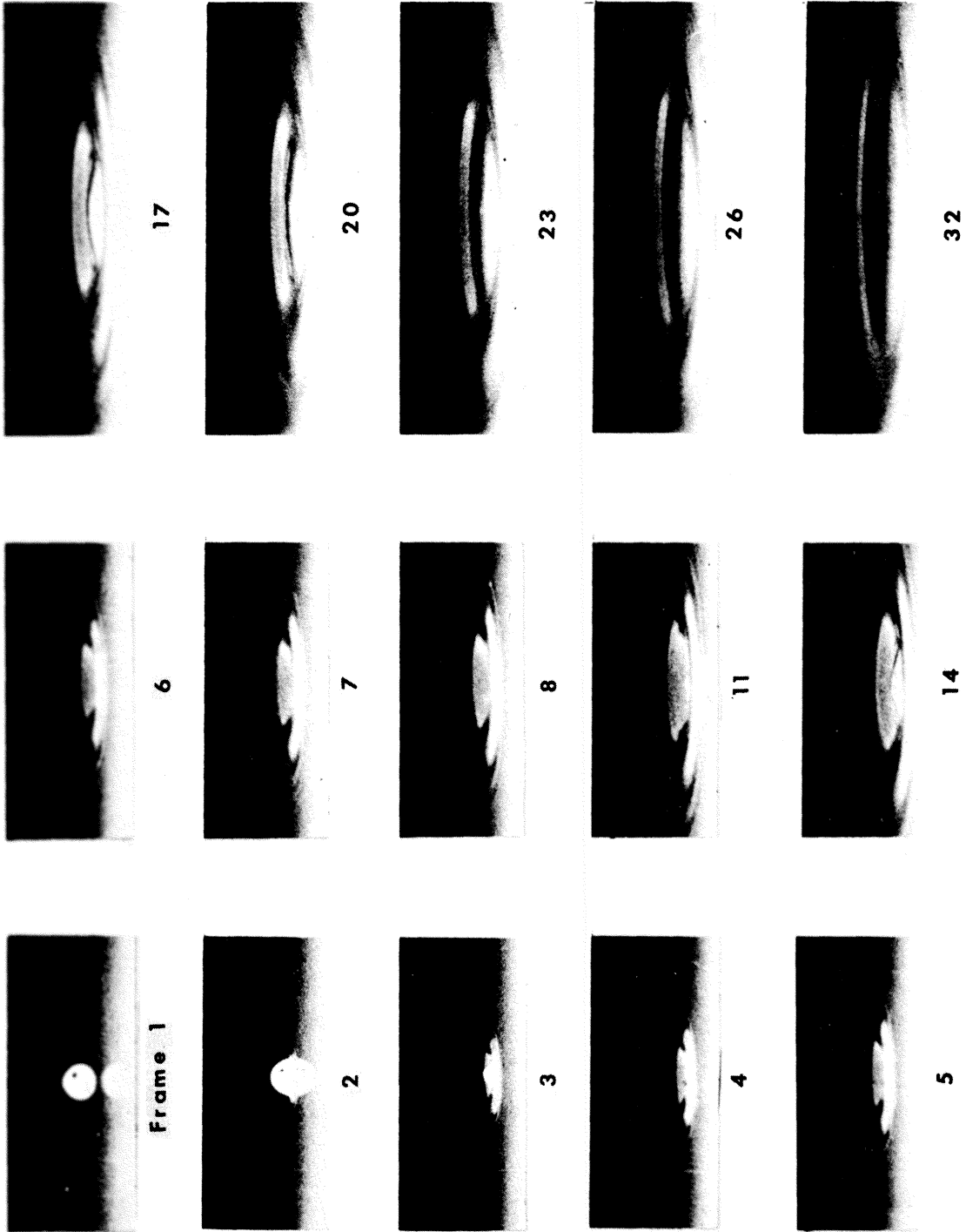ly passes through the free surface was not revealed in the movie frames

Figure 2. Surface Interaction of Drop from Free Fall of 0.085' as Viewed from Above.

but evidently takes place at or near the time when the depression in the
surface is greatest. After maximum depression is reached, the center of
the crater rises and reaches a level slightly above the original surface
level. When rings are being formed by a given fall height, the center
which rises is of large curvature. As the heights are increased above the
range for which rings are formed, the curvature of the center portion be-
comes greater and peaks into a spout, possibly with a ball of fluid at the
top. When rings are formed, the surface in the area of impact smooths very
quickly, leaving only the receding and diminishing solitary wave.

Measurements of individual frames failed to produce conclusive
observations concerning the size or velocity of the wave in either case
filmed. However, it appears that for the case of maximum penetration the
depression in the free surface is of less depth, the center of the depres-
sion rises more quickly, and the whole interaction is completed more quick-
ly than for the case of minimum penetration.

Figures 3 and 4 show the interaction with the free surface as
viewed from below for free fall heights of 0.085' and 0.105' respectively.
Although similar in many ways, these series present two notable differences
in the interaction for the two fall heights. First, the turbulence level
as indicated by the amount of dye residue is more pronounced in the case
of minimum penetration. Secondly, the velocity of descent from the sur-
face is greater in the case of maximum penetration. Both of these effects
are easily seen by visual observation and are important distinguishing
features of the two types of rings.

In either case the lower portion of the drop solutions assumes a
rounded shape as the surface is first penetrated with the fluid moving from
the center regions to the outer edges to form the rotating ring. As the

Frame 15

20

26

32

38

Frames 1-7   Frames 8-14
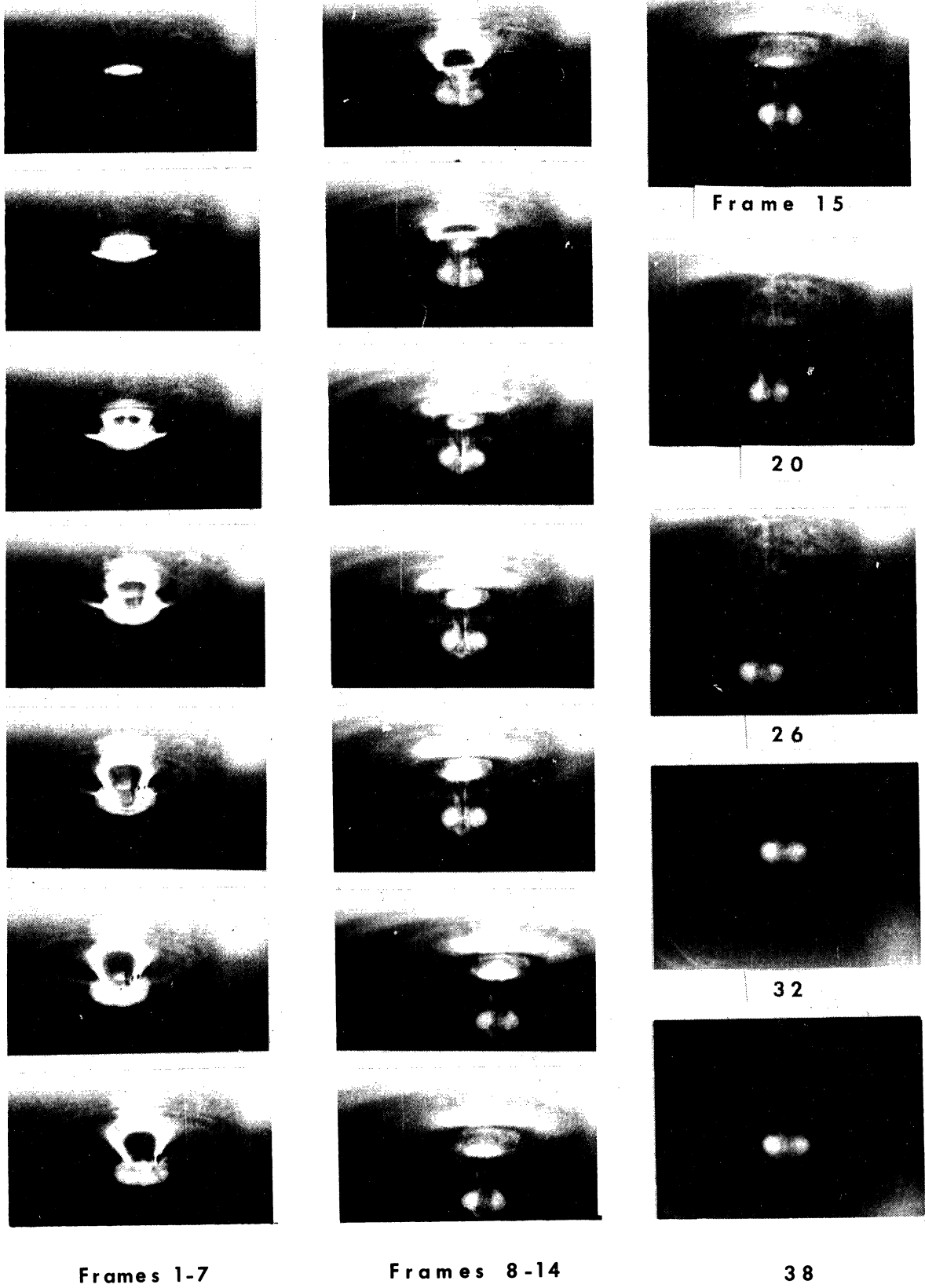
Figure 3.   Surface Interaction of Drop from Free Fall of 0.085' as Viewed from Below.

15

19

25

31

61

Frames 1-7   Frames 8-14   61
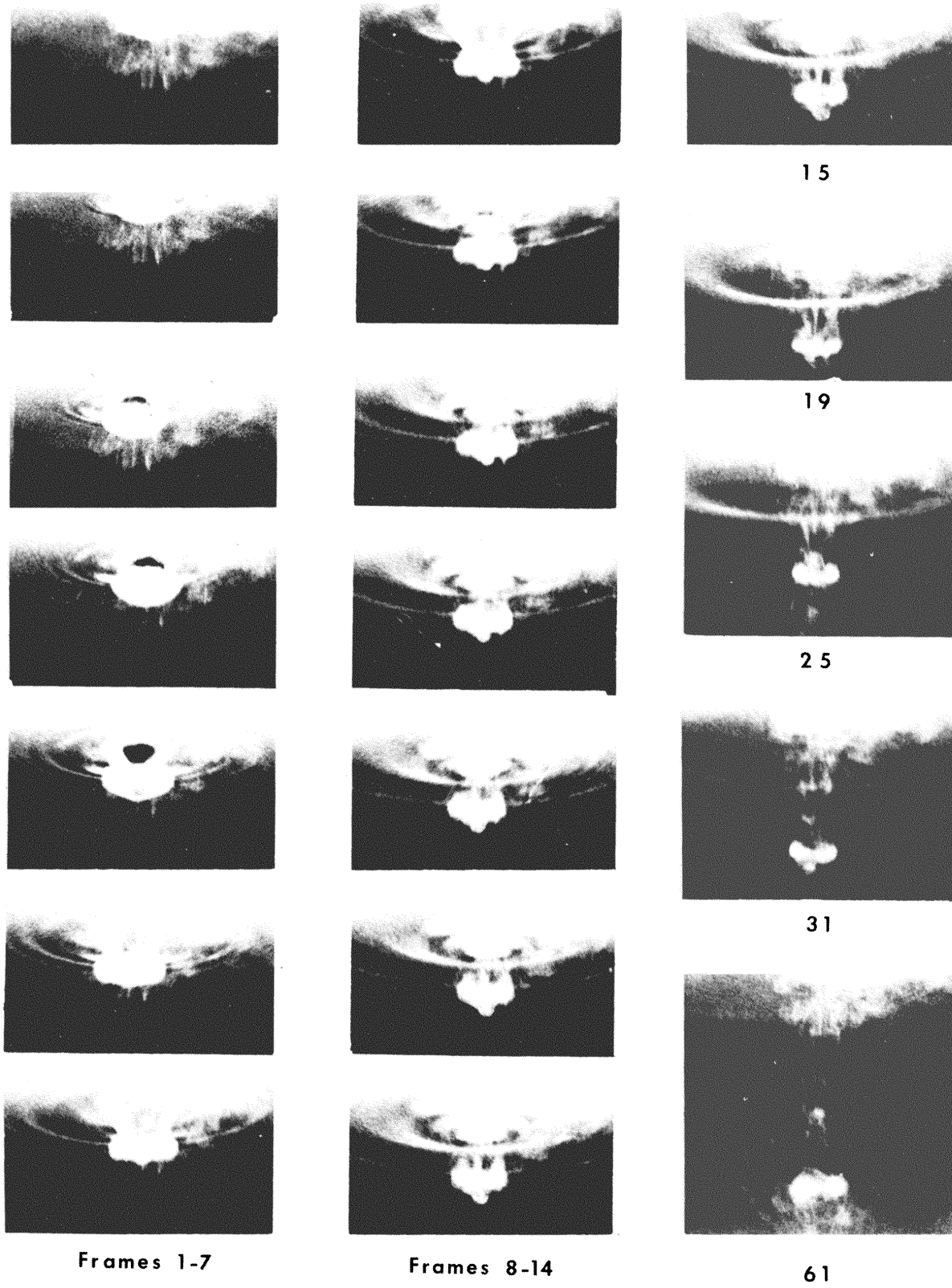
Figure 4.   Surface Interaction of Drop from Free Fall of 0.10' as Viewed from Below.

ring descends, the surface closes back over it. It appears that the transformation from drop to ring is substantially complete by the time the form is one to two ring diameters below the free surface level.

3. Descent of the Rings.

a. Presentation of graphs

Before entering into a description and discussion of the ring as it descends into the base, a series of graphs constructed from the data obtained in the experimental work will be presented. These will be helpful in the description of the behavior of the rings and later in the theoretical considerations. The graphs presented are selected to provide a cross section of behavior so that by comparing various graphs certain trends may be seen.

1) Selected Behavior Patterns (Figures 5 through 24).

These graphs show the relationship of the penetration of the ring into the base and:

1. The ring diameter at that level

2. The velocity of the ring at that level

3. The elapsed time from contact with the surface to that level.

The graphs were constructed from data taken from the multiple exposure films. For any given film, the diameter of the ring, the diameter of the cross section of the ring, and the distance from the surface to the center of the ring were recorded for each image on the film. Data was recorded to the nearest 0.01". With the time between images known, the elapsed

Figure 5.   Penetration Depth Velocity and Ring Diameter as
            Related to Time   D32B8F.08 .

Figure 6.   Penetration Depth, Velocity and Ring Diameter as
            Related to Time.   D32B8F.10.

TIME
(SECONDS)

RING DIAMETER
(INCHES x IO)

VELOCITY
(INCHES / SECOND)

PENETRATION FROM FREE SURFACE

Figure 7.   Penetration Depth   Velocity and Ring Diameter as
             Related to Time.   Dl6B8F.08 .

Figure 8.   Penetration Depth, Velocity and Ring Diameter as
            Related to Time.   D16B8F.10.

Figure 9.   Penetration Depth, Velocity and Ring Diameter as
Related to Time.   D8B8F.08.

Figure 10.   Penetration Depth, Velocity and Ring Diameter as Related to Time.   D8B8F.10 .

Figure 11.   Penetration Depth, Velocity and Ring Diameter as
Related to Time.   D4B8F.08.

Figure 12.   Penetration Depth, Velocity and Ring Diameter as Related to Time.   D4B8F.10.

Figure 13. Penetration Depth, Velocity and Ring Diameter as Related to Time. DOB8F.08.
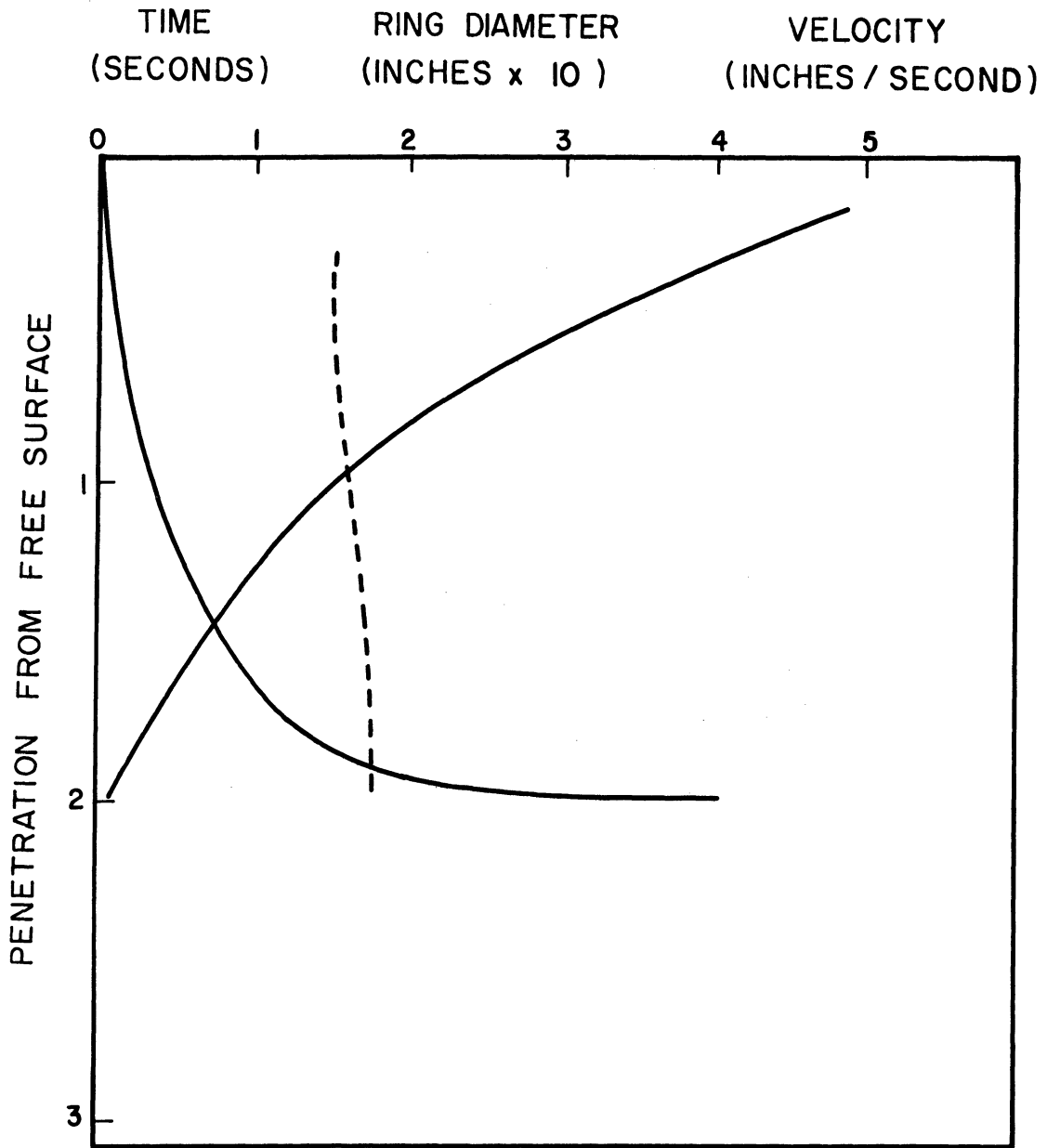
Figure 14.   Penetration Depth, Velocity and Ring Diameter as
              Related to Time.   DOB8F.10.
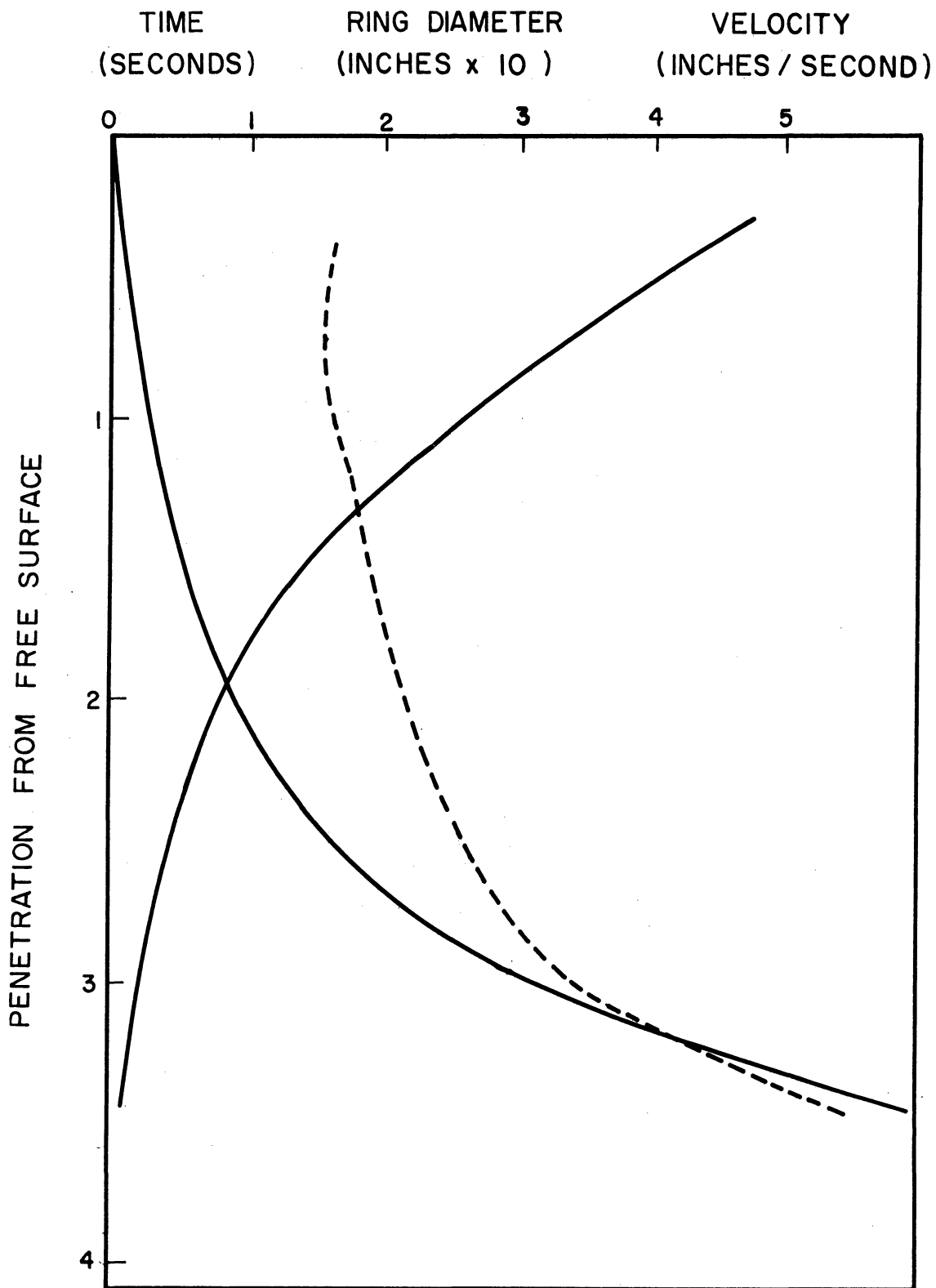
Figure 15. Penetration Depth, Velocity and Ring Diameter as Related to Time. D32BOF.08.
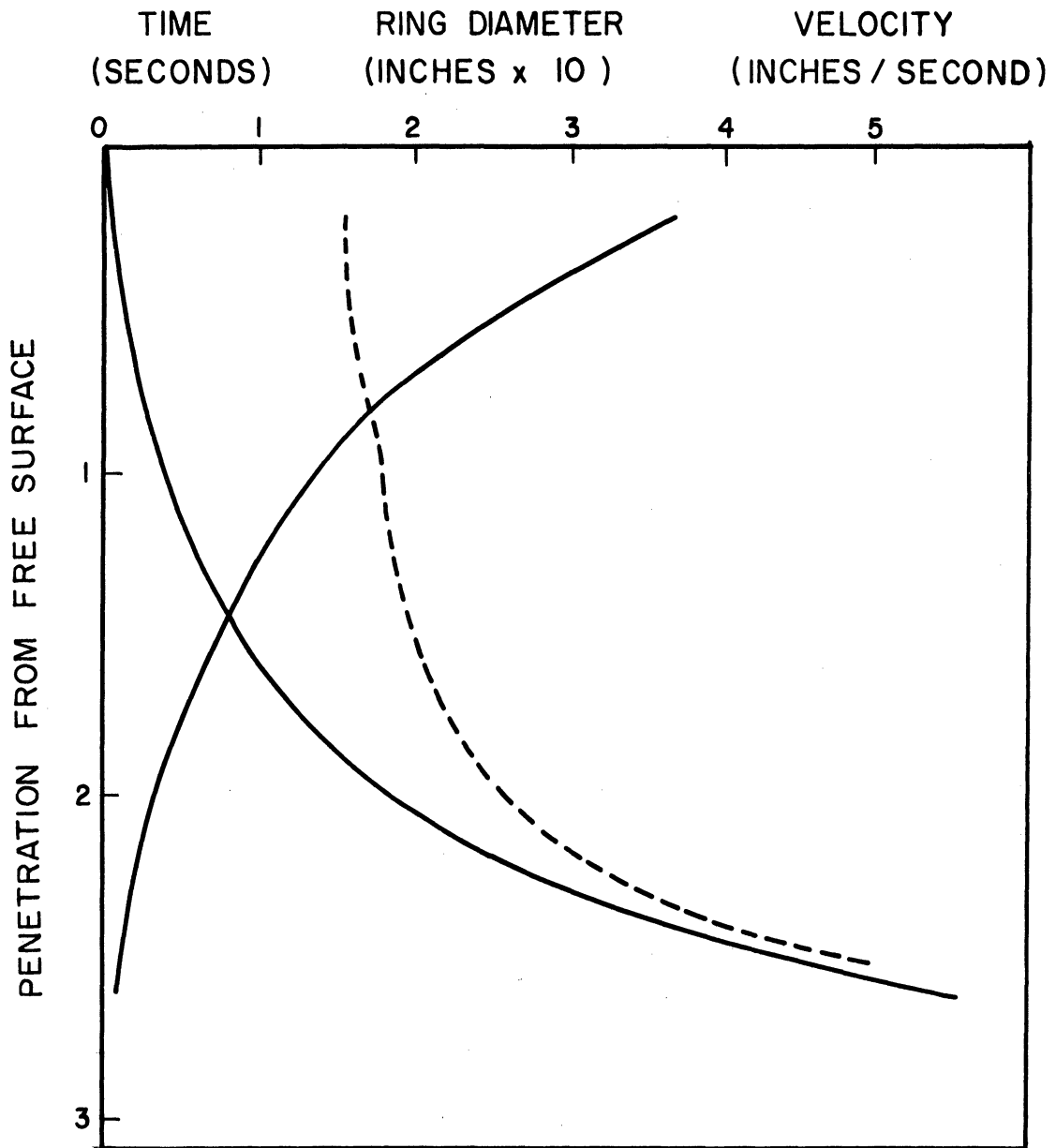
Figure 16.   Penetration Depth, Velocity and Ring Diameter as
Related to Time.   D32BOF.10.
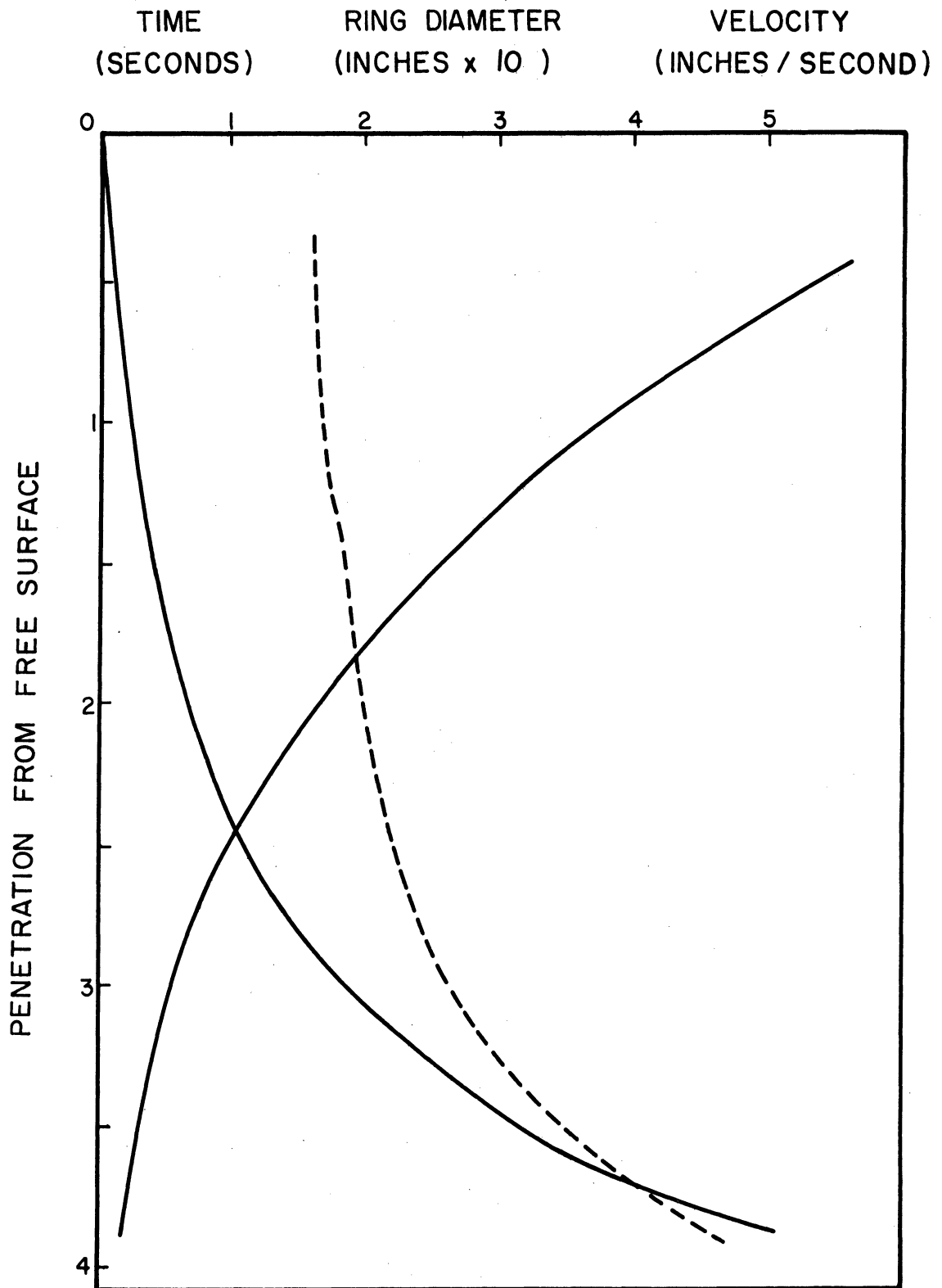
Figure 17.   Penetration Depth, Velocity and Ring Diameter as
             Related to Time. D16BOF.08.
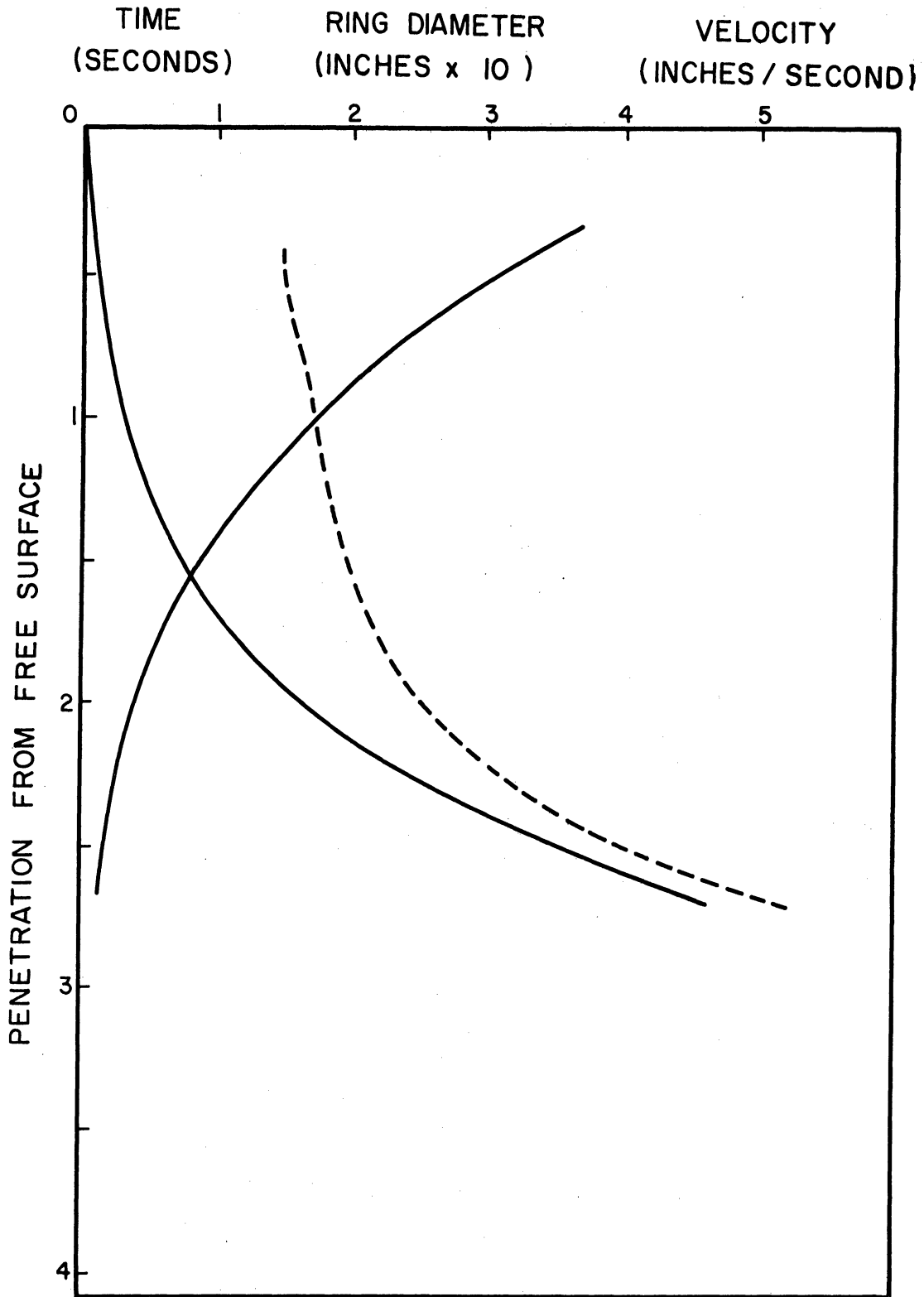
Figure 18. Penetration Depth, Velocity and Ring Diameter as
           Related to Time. D16BOF.10 .
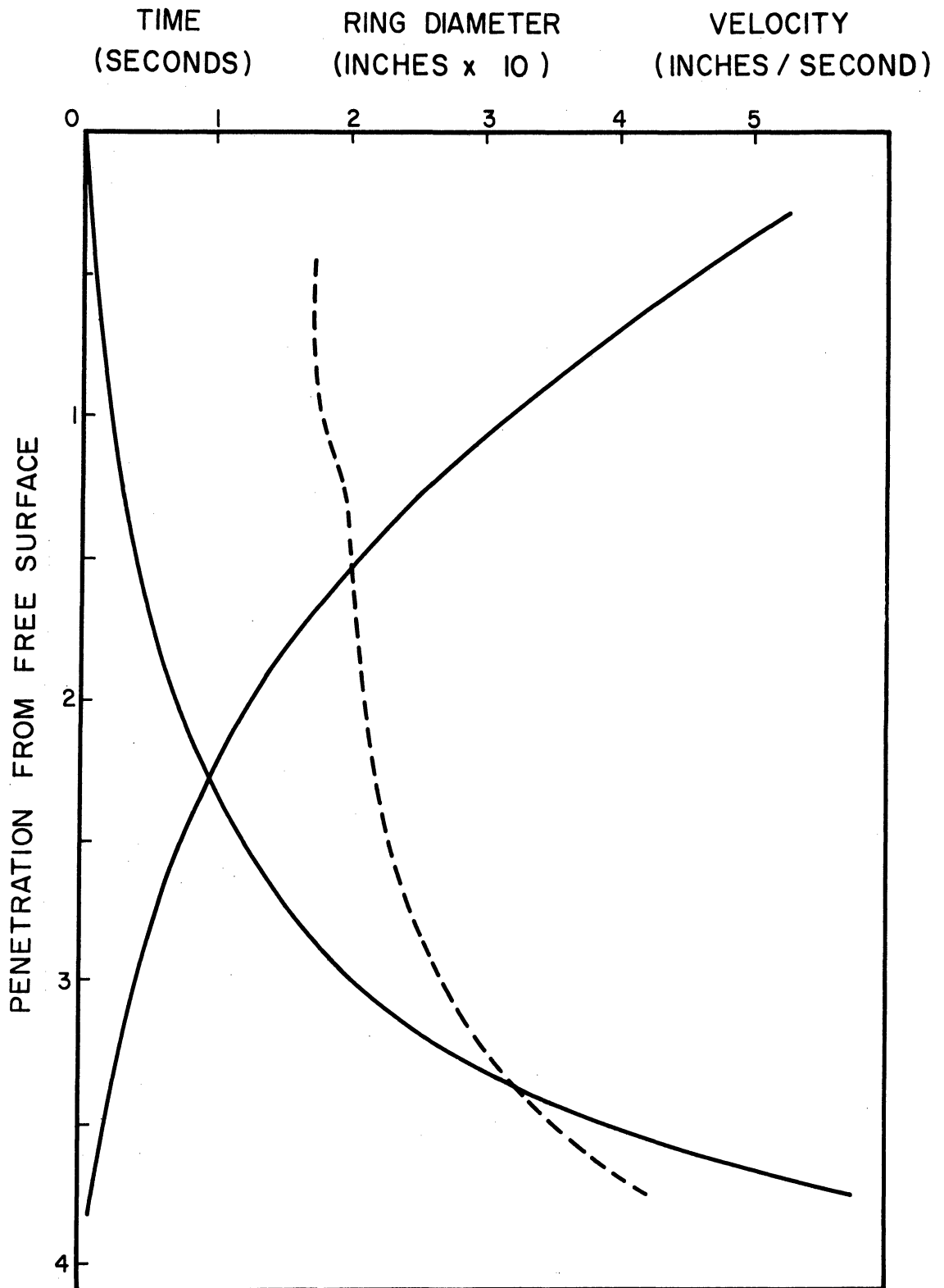
Figure 19.   Penetration Depth, Velocity and Ring Diameter as
Related to Time.   D8BOF.08.
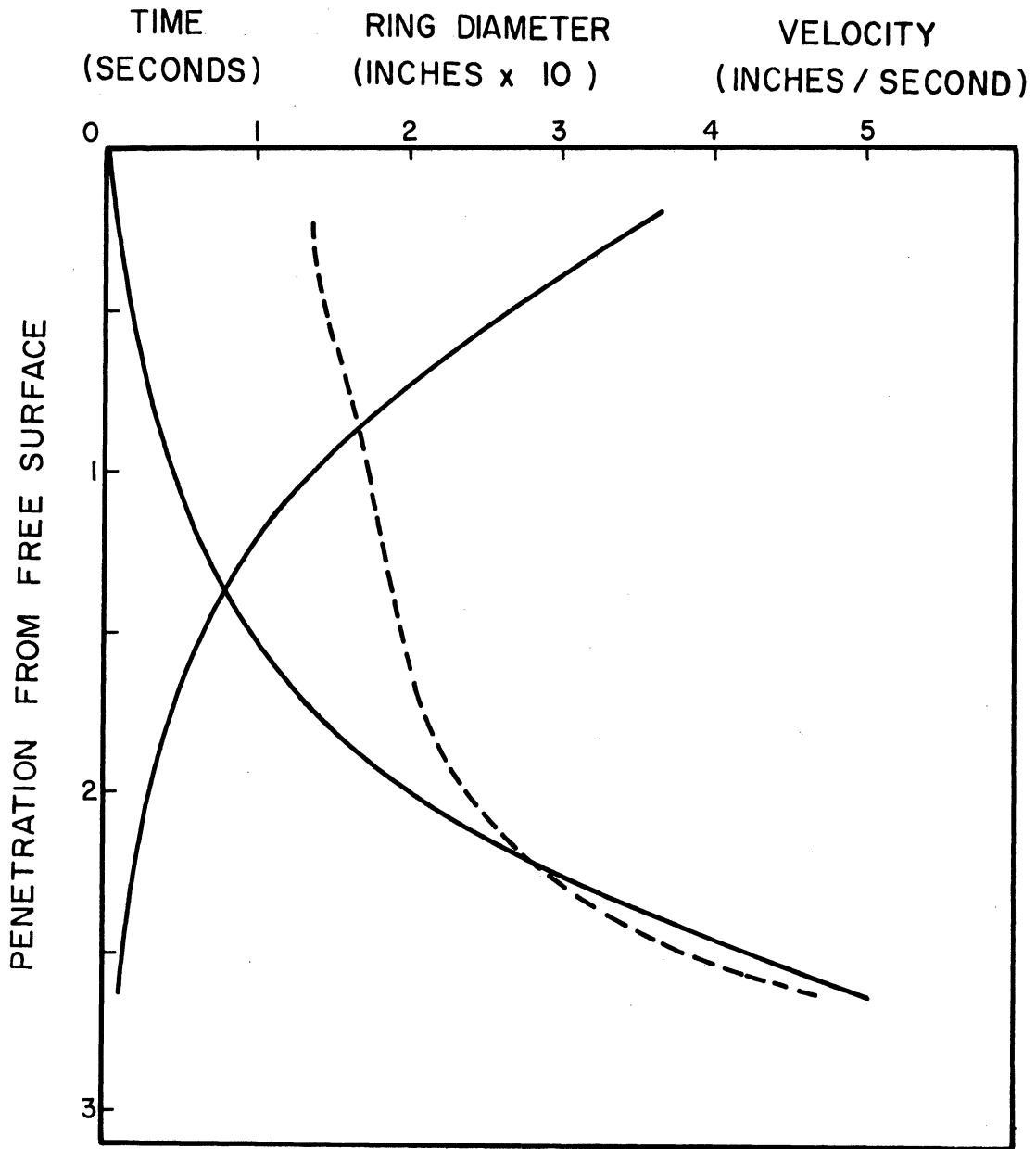
Figure 20. Penetration Depth, Velocity and Ring Diameter as Related to Time. D8BOF.10.
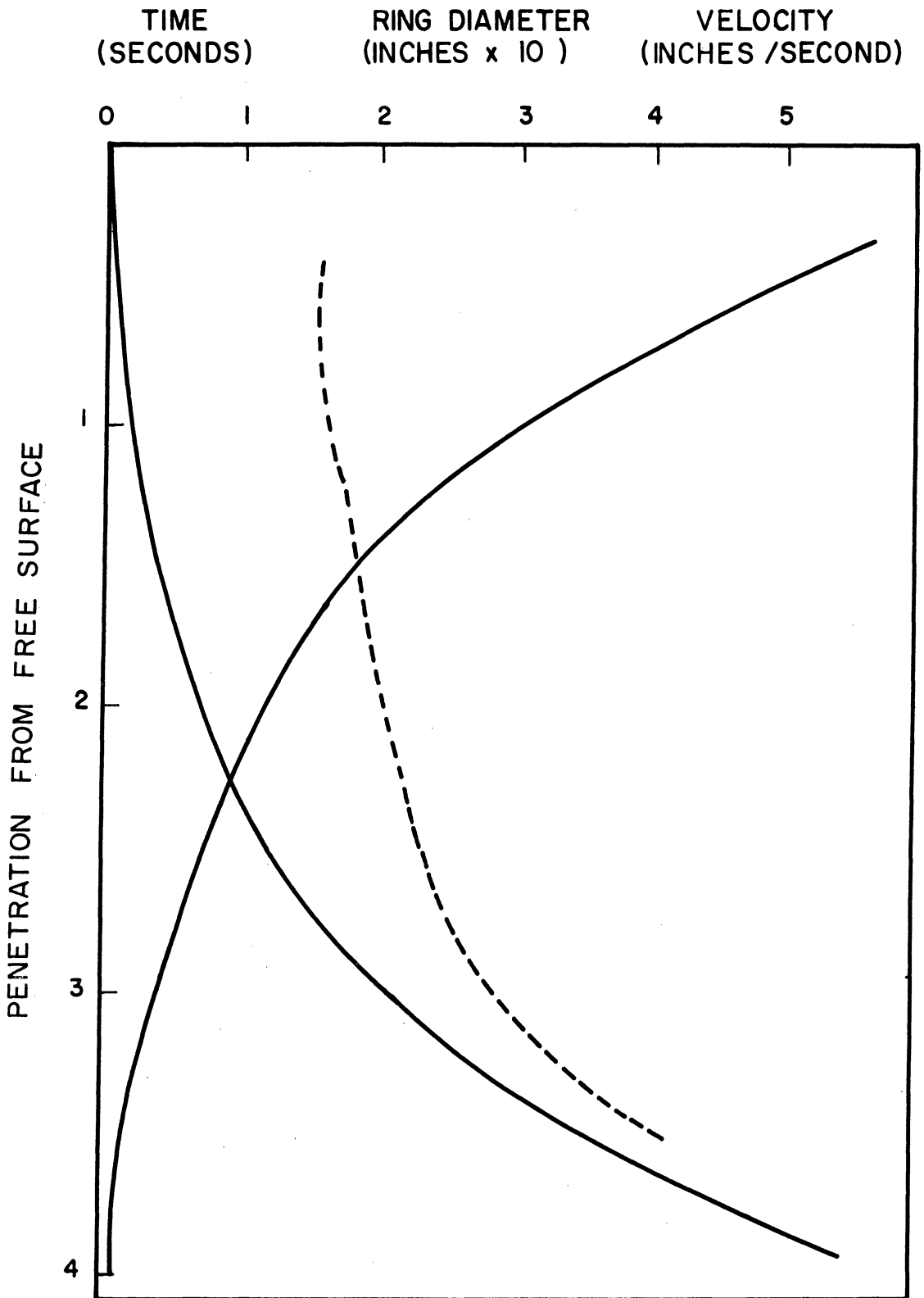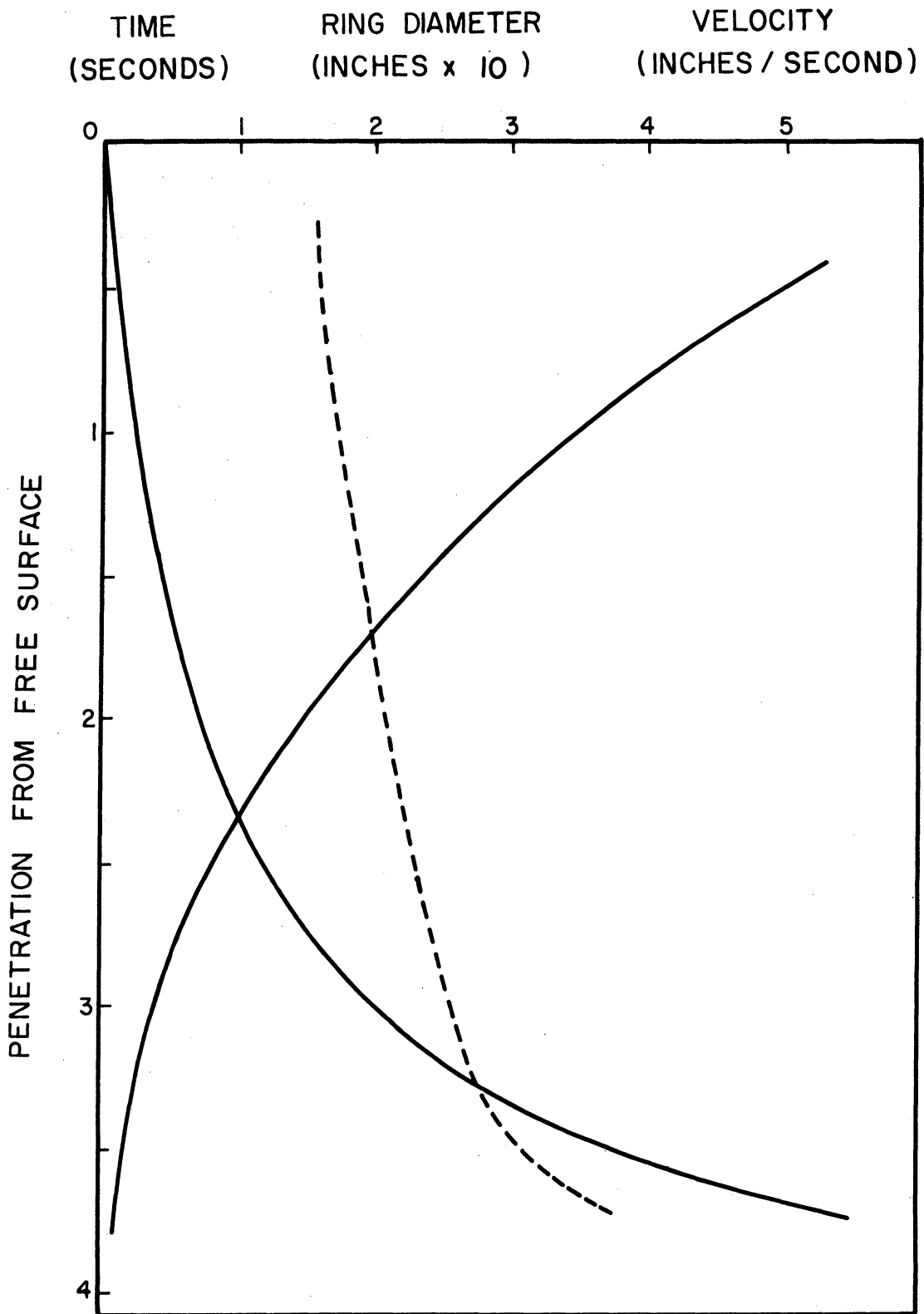
Figure 21.   Penetration Depth, Velocity and Ring Diameter as
Related to Time. D4BOF.08 .
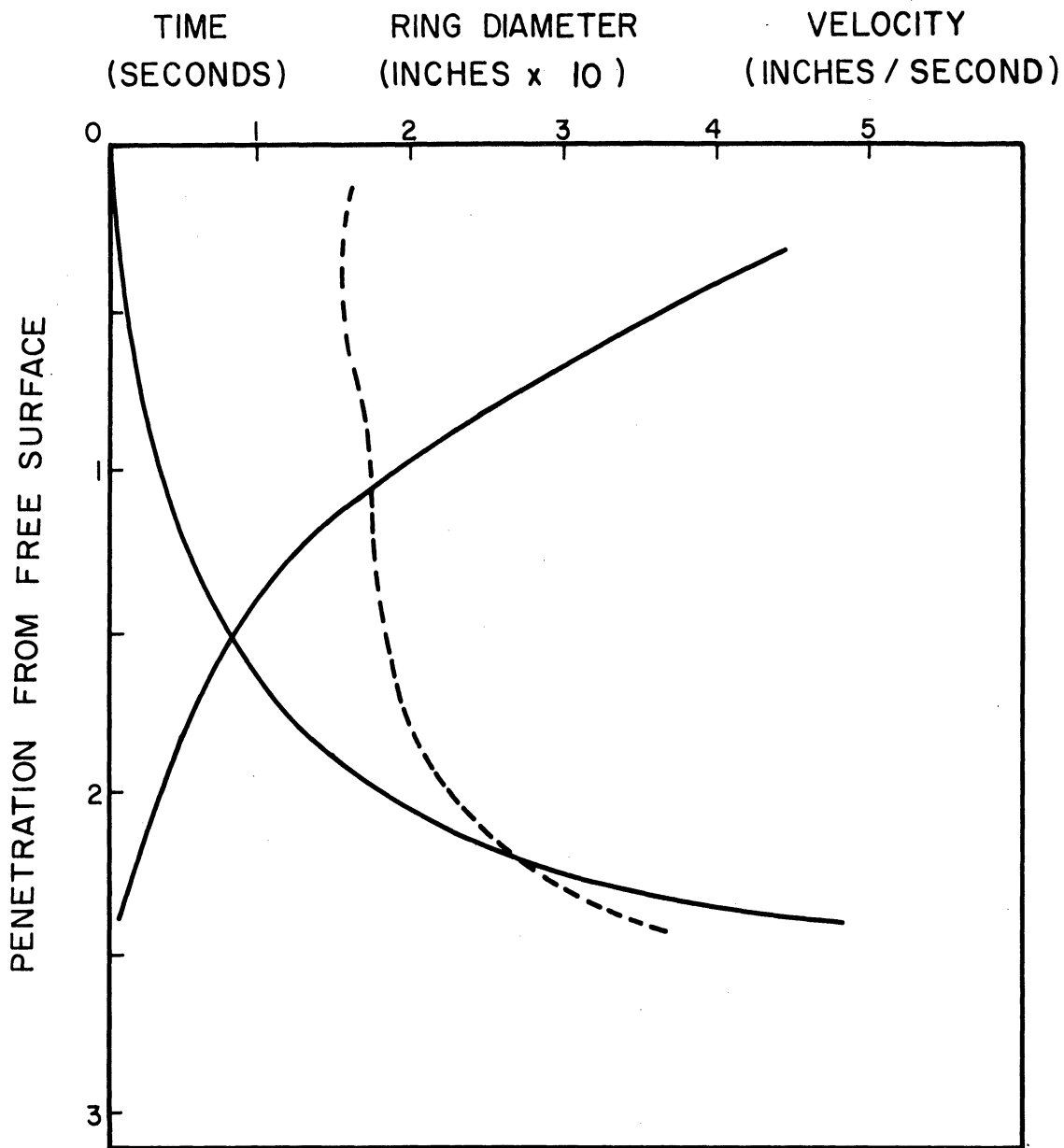
Figure 22.   Penetration Depth   Velocity and Ring Diameter as
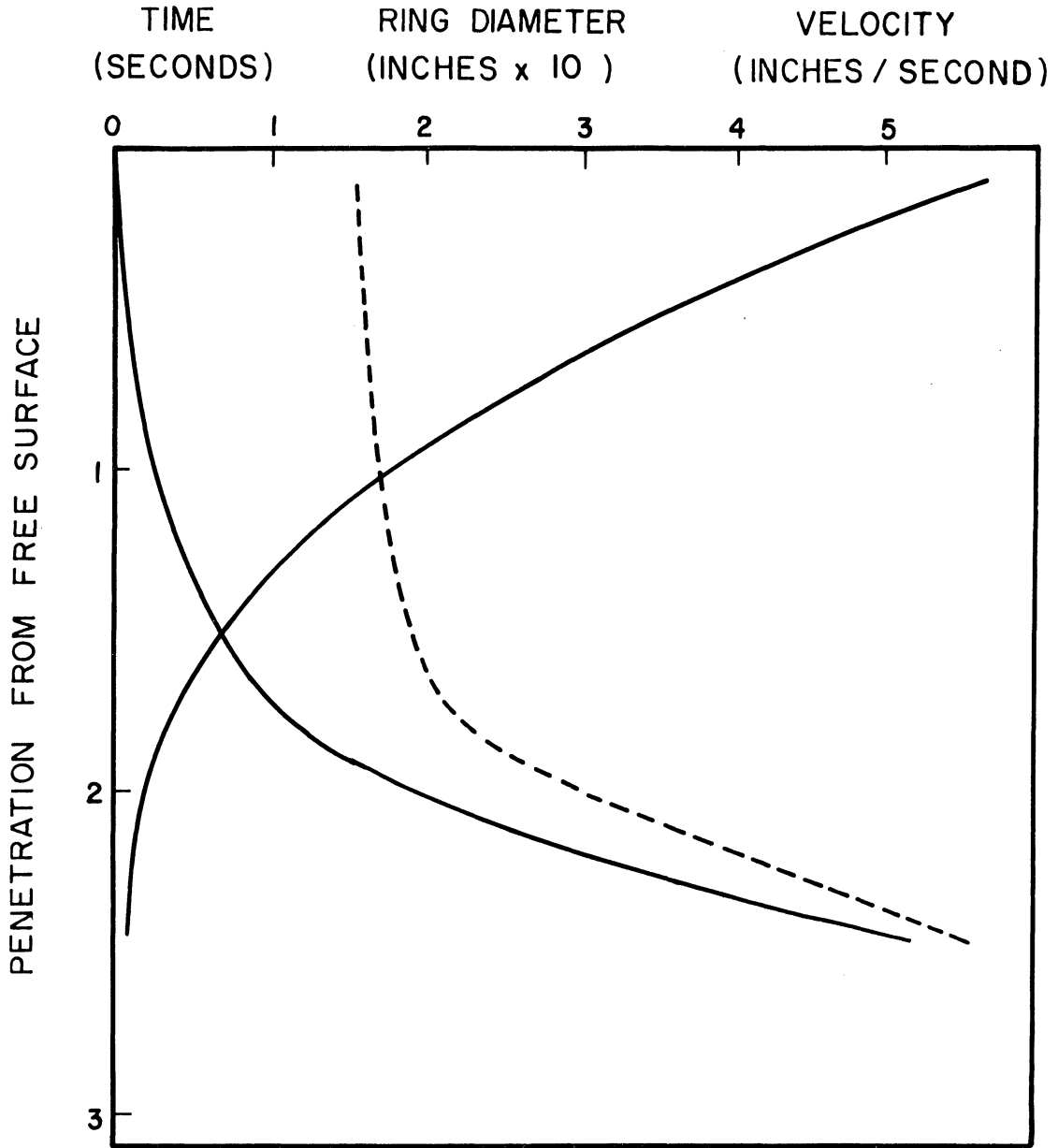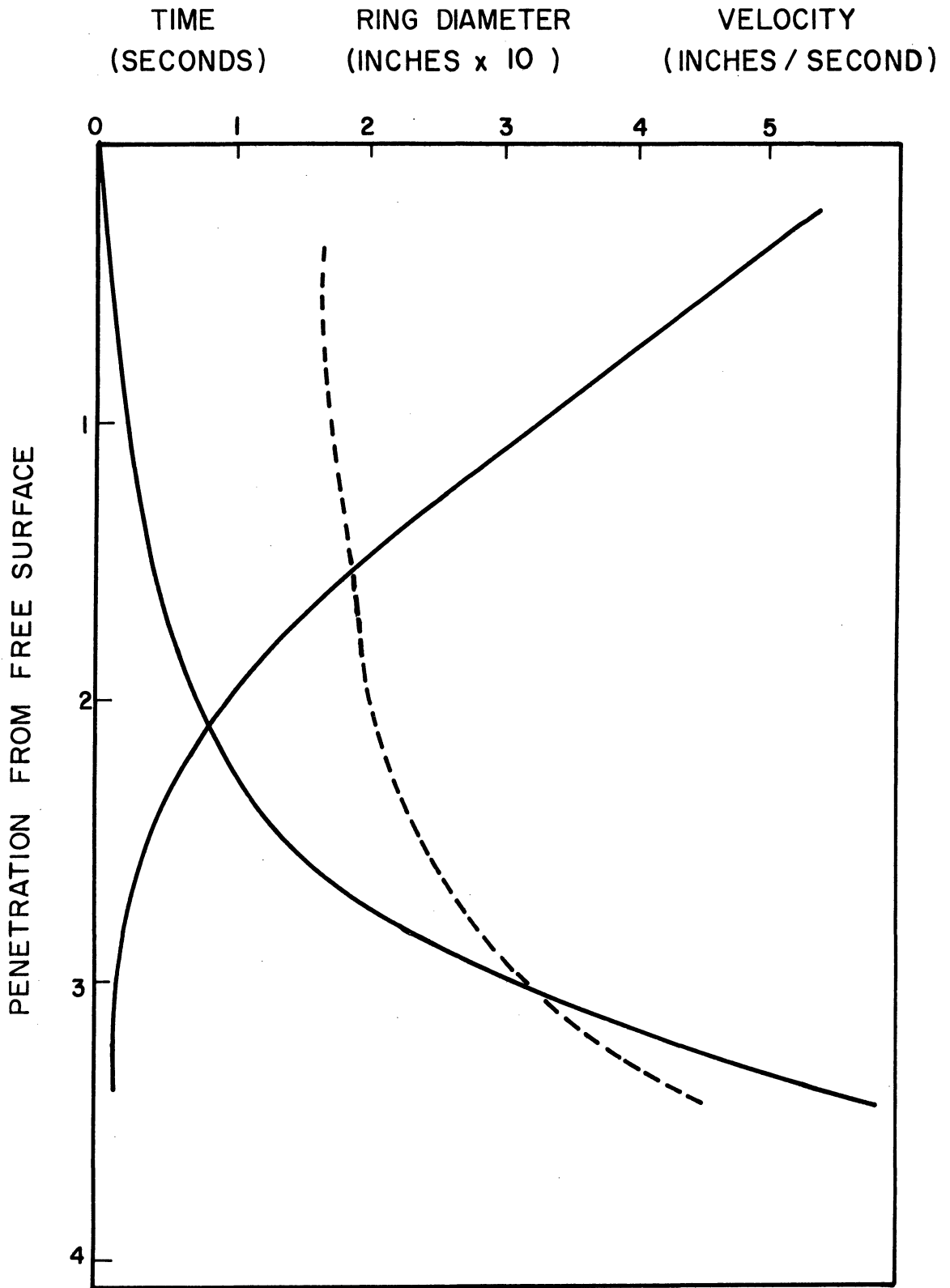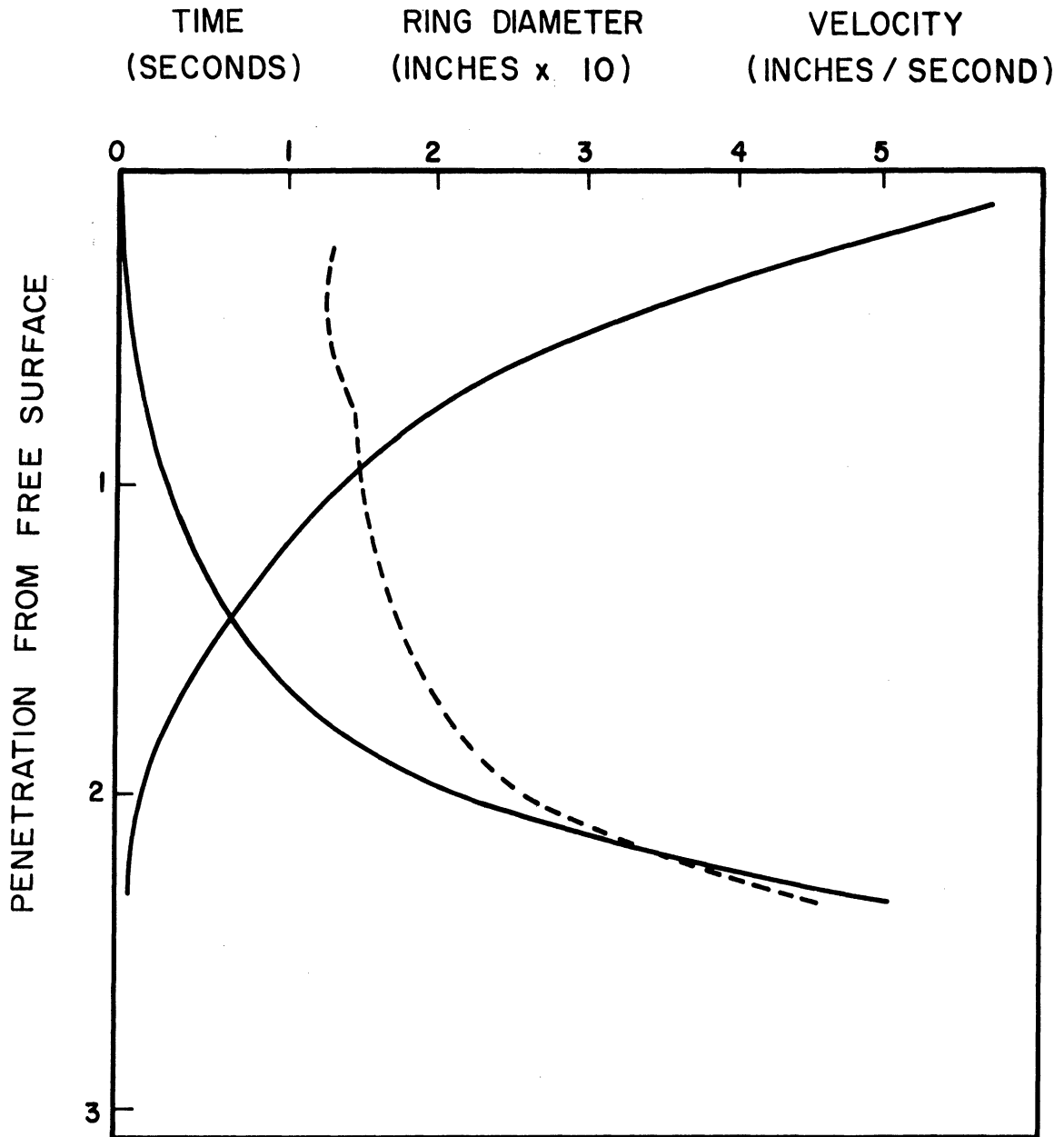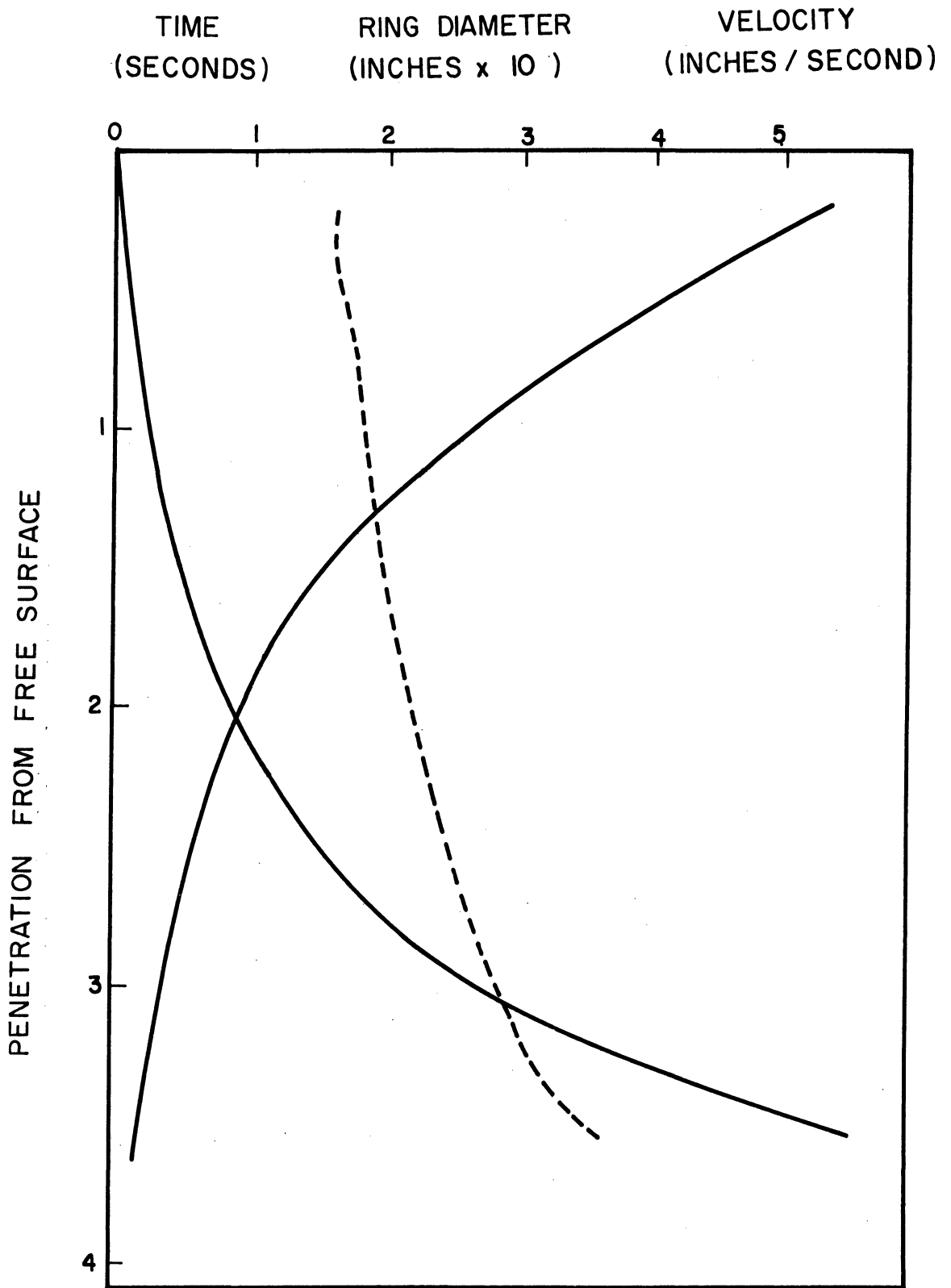Related to Time.   D4BOF.10.
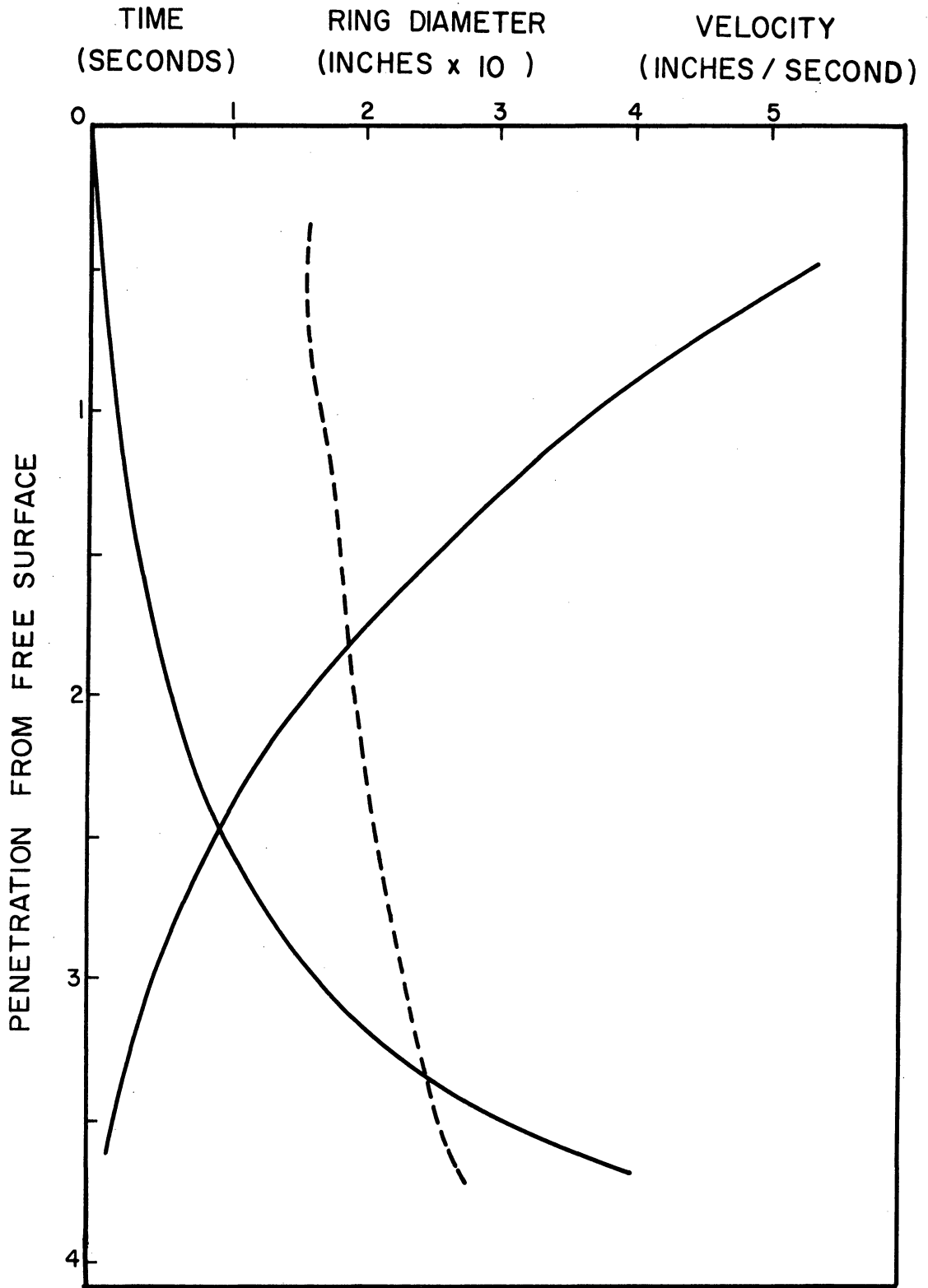
Figure 23.   Penetration Depth, Velocity and Ring Diameter as
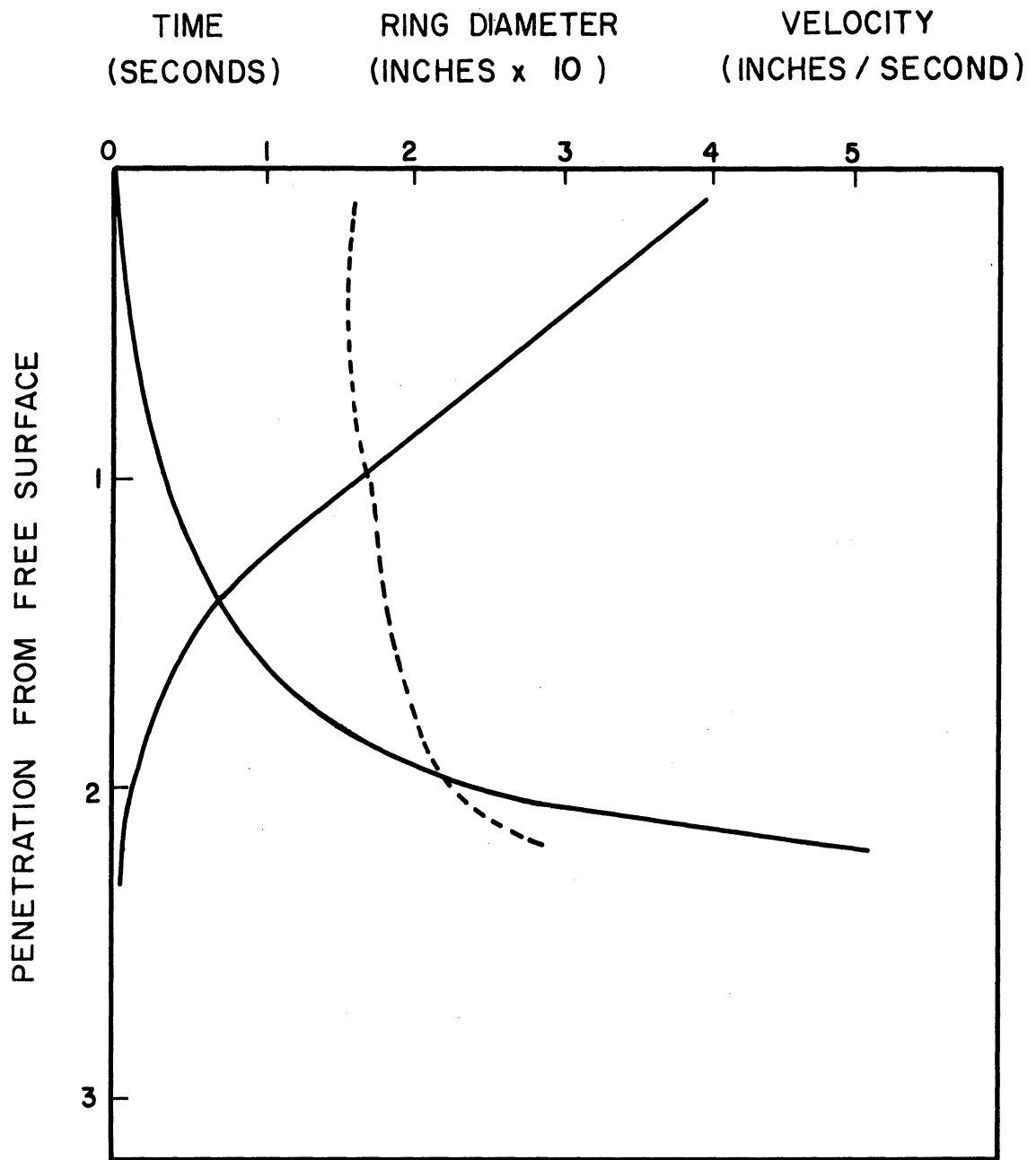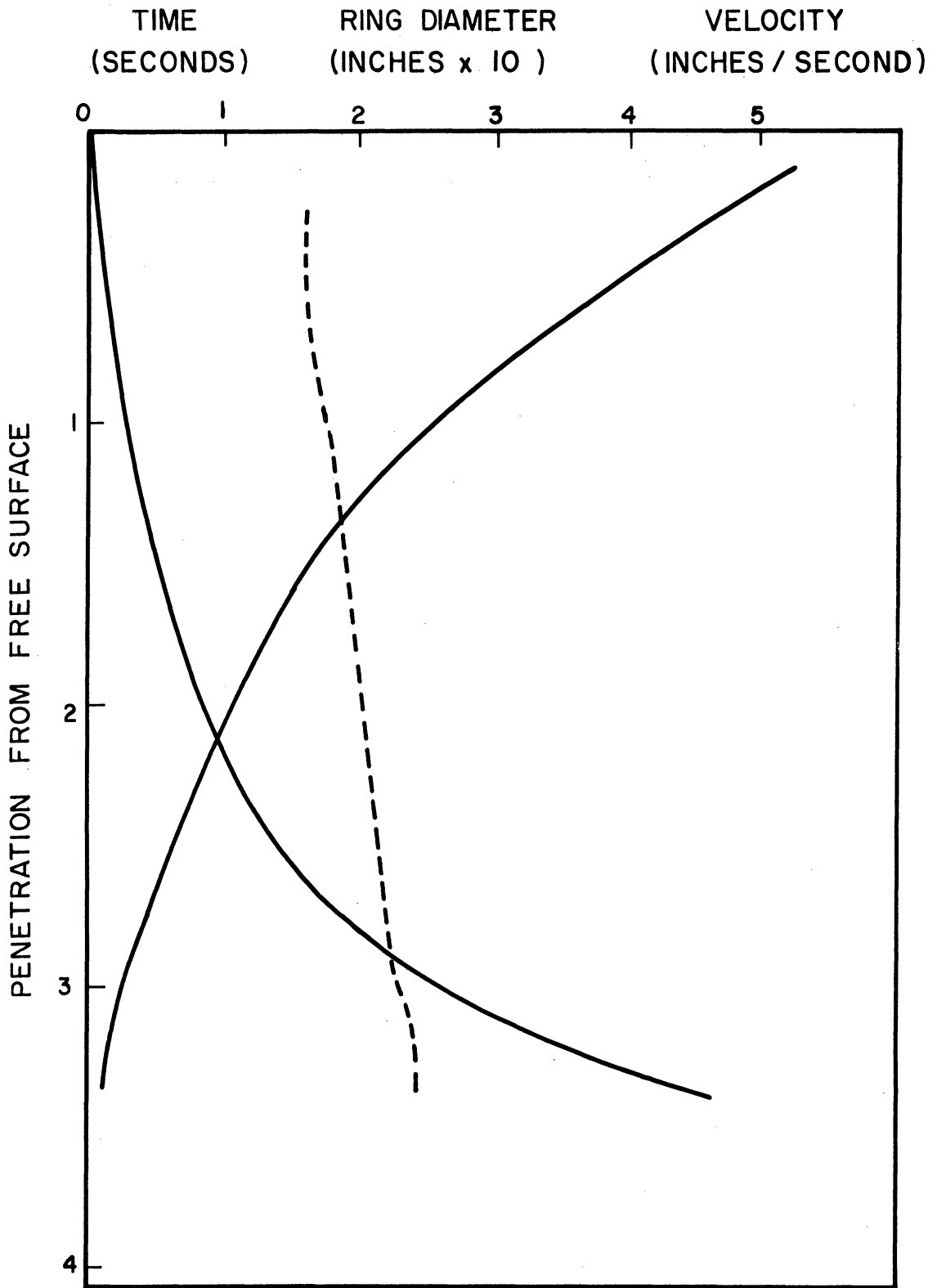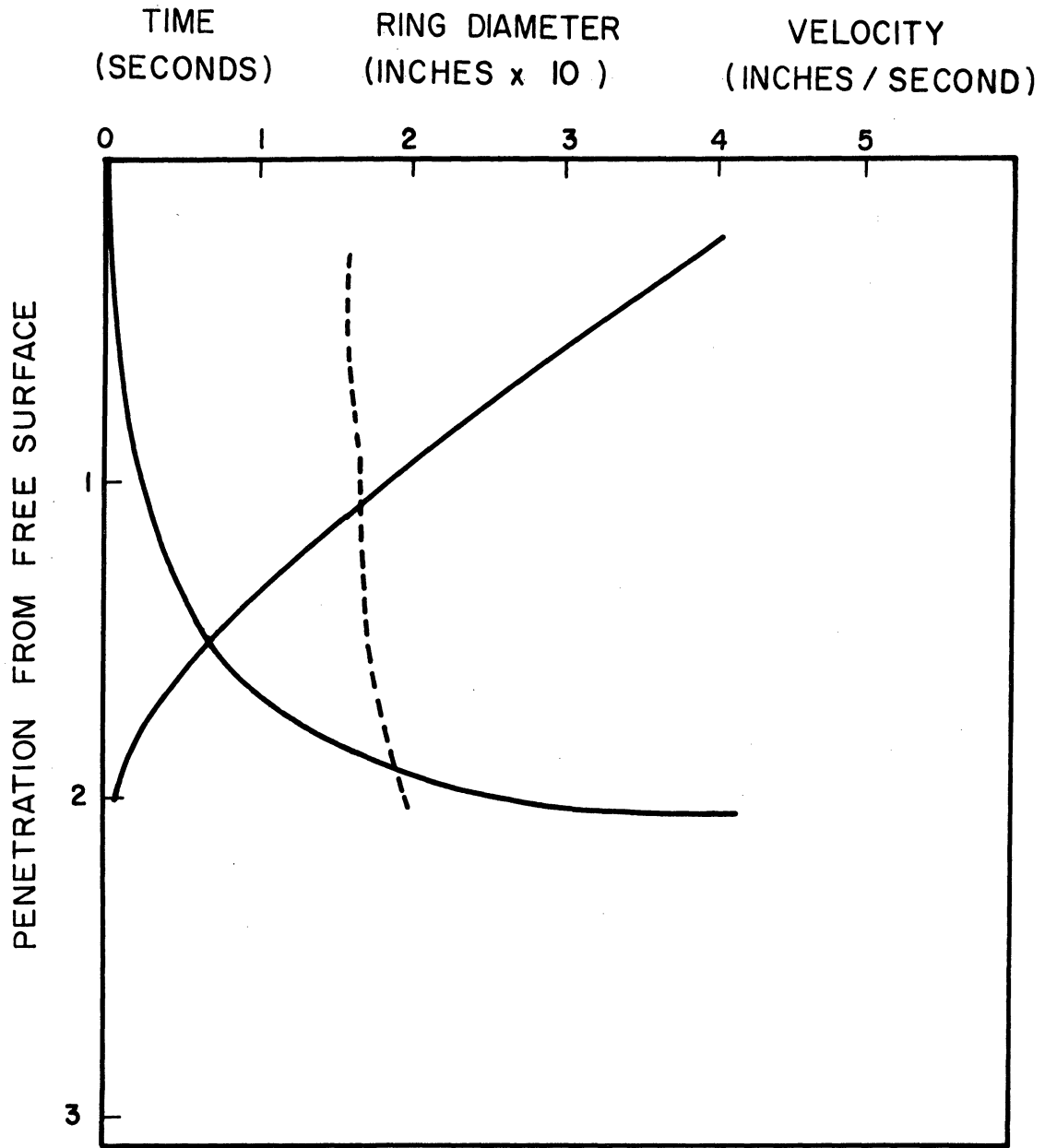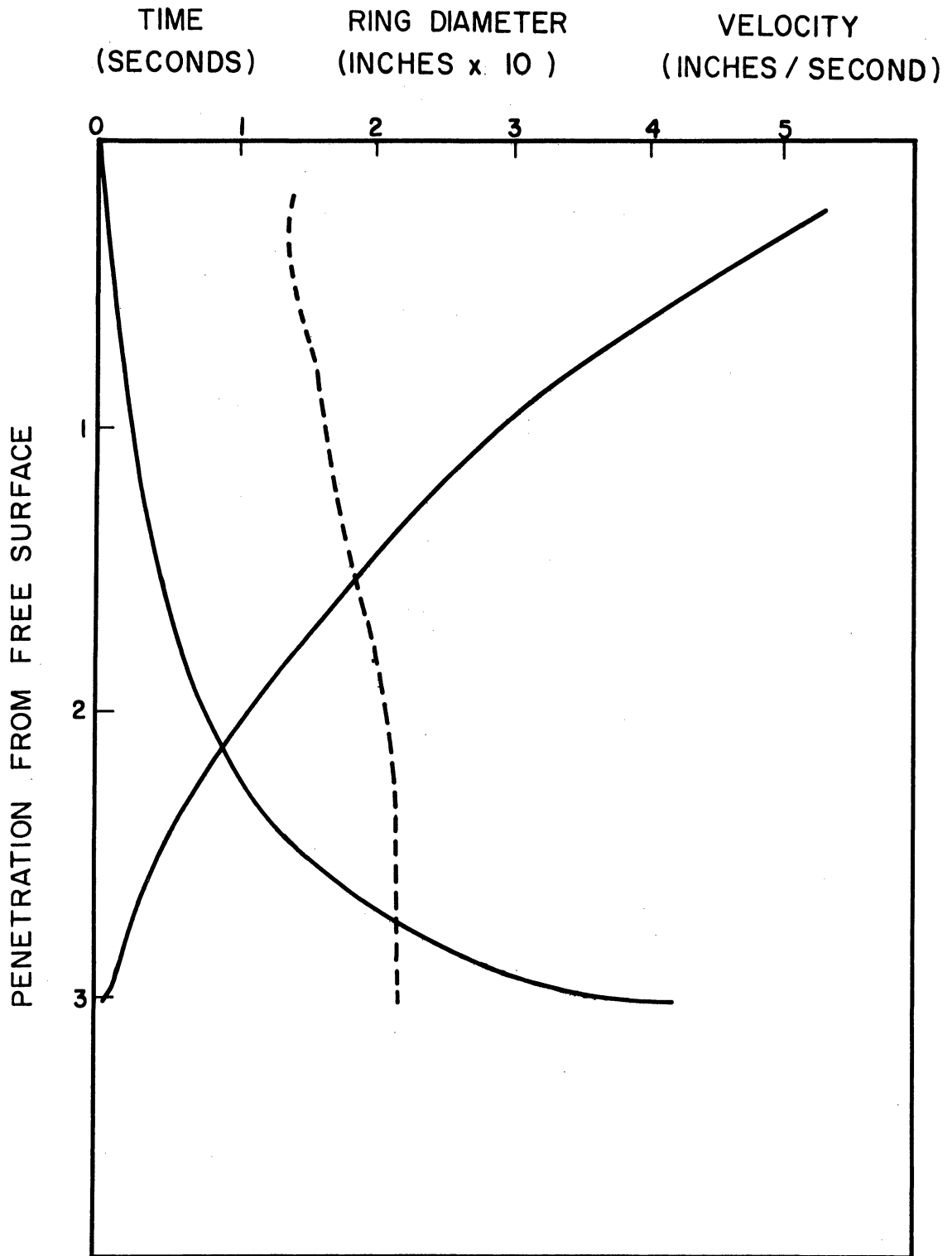   Related to Time. DOBOF.08.
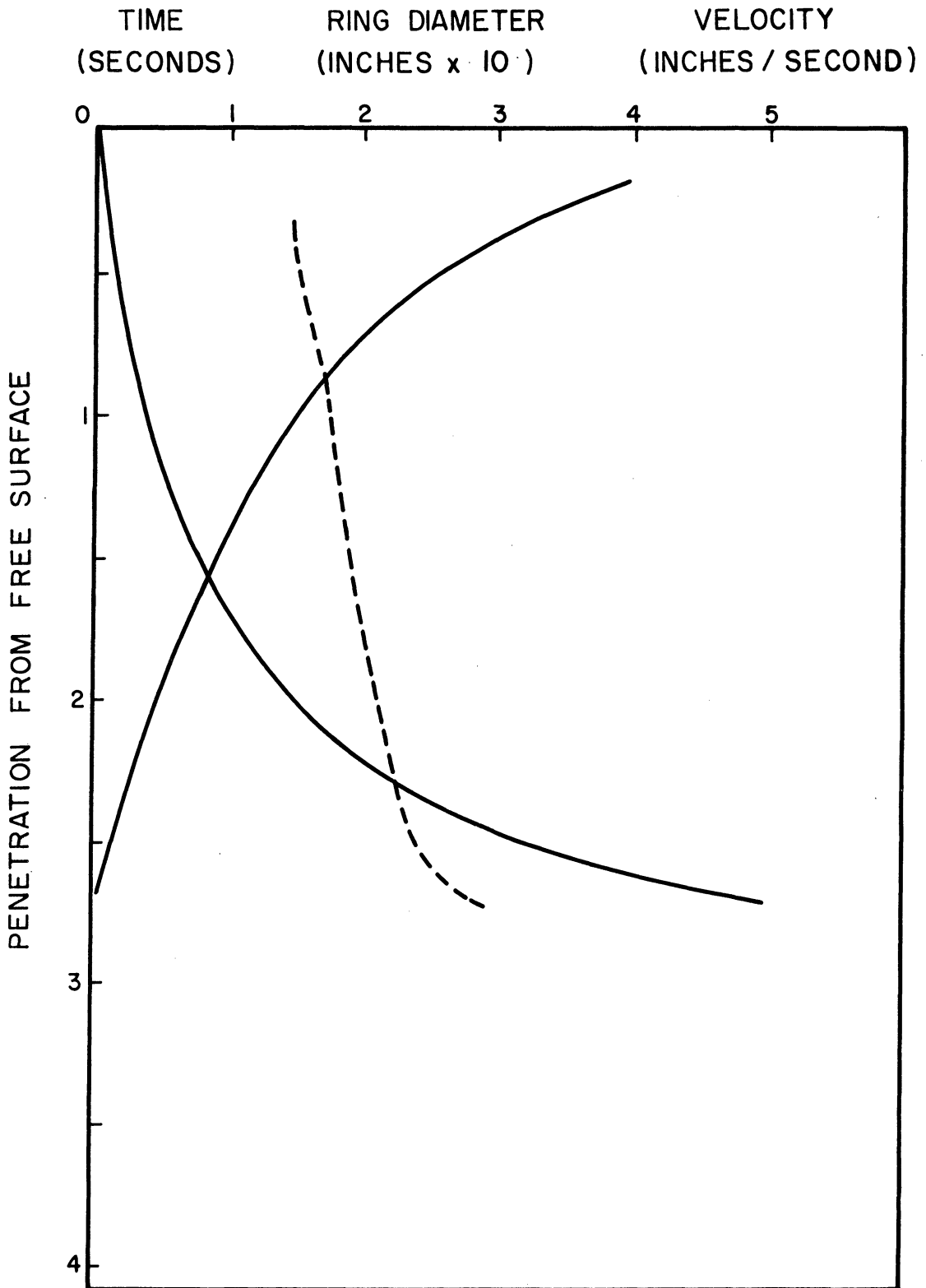
Figure 24.   Penetration Depth, Velocity and Ring Diameter as
Related to Time. DOBOF.10 .

time to any level was easily obtained. The velocity curves are based on average velocities at the midpoint of the distance between images by dividing the distance between successive images by the time between images. Since the time from surface contact to the first image was not known exactly, the first part of the velocity curves were extrapolated from points occurring later.

The graphs are shown for only two free fall heights: namely, 0.08' (rings with maximum penetration to critical depth) and 0.10' (rings with minimum penetration to critical depth). For each of these free fall heights, two base solutions (B0 and B8) were used in combination with five drop solutions (D32, D16, D8, D4, and D0).

To interpret these graphs draw a horizontal line through any penetration depth to intersect the three curves for diameter, velocity and time. Vertical lines through the three points of intersection, when extended to the upper scale, will give for that level of penetration the diameter in inches, the velocity in inches per second and the elapsed time to that level in seconds.

Although the data used to construct these graphs were the result of careful and precise measurements, quantitative comparison of two graphs may or may not be too reliable. The main utility of such comparisons is the establishment of basic and common characteristics or of trends suggested by several graphs. There was no check on the drop filmed as being typical of the average drop produced under the given conditions until the negatives were developed. At that time, any obvious discrepancies of the filmed images from visual observations of typical critical depth were refilmed but the generally accepted range of variation for a given combination was taken to be 1/4" from the usually observed critical depth.

2) Penetration graphs (Figures 25 through 41.)

These graphs show the relationship of penetration to critical depth and free fall height for various combinations of drop and base solutions. The combination range from D32B0 to D0B32.

The graphs are plotted from data obtained visually by noting the level of penetration at which critical depth was judged to occur. For a given free fall height sufficient drops were released to allow several checks to be made on the recorded critical depth. If some rings of a series were not within this range (due to the presence of internal currents or other effects) the series was continued until a reasonable average could be determined.

The free fall heights were begun at the point where the drop would just leave the needle before contacting the free surface and continued by increments of 0.005' until rings were no longer formed with regularity. In some regions the critical depth was found to change very rapidly with free fall height. Especially in the regions of minimum penetration to critical depth was this effect noticeable. In such regions, increments of 0.001' or 0.002' indicated the presence of a possible secondary oscillation of much less amplitude but greater frequency than the primary oscillation. The effect is indicated on one graph (Figure 41). The remaining graphs indicate only the effect of the primary oscillation on critical depth.

3) Composite Penetration Curves (Figures 42 through 44.)

These graphs indicate the location of relative maximum and minimum points of penetration as composite representations of Figures 5 through 24. In each of this series, one variable of the D-B-F
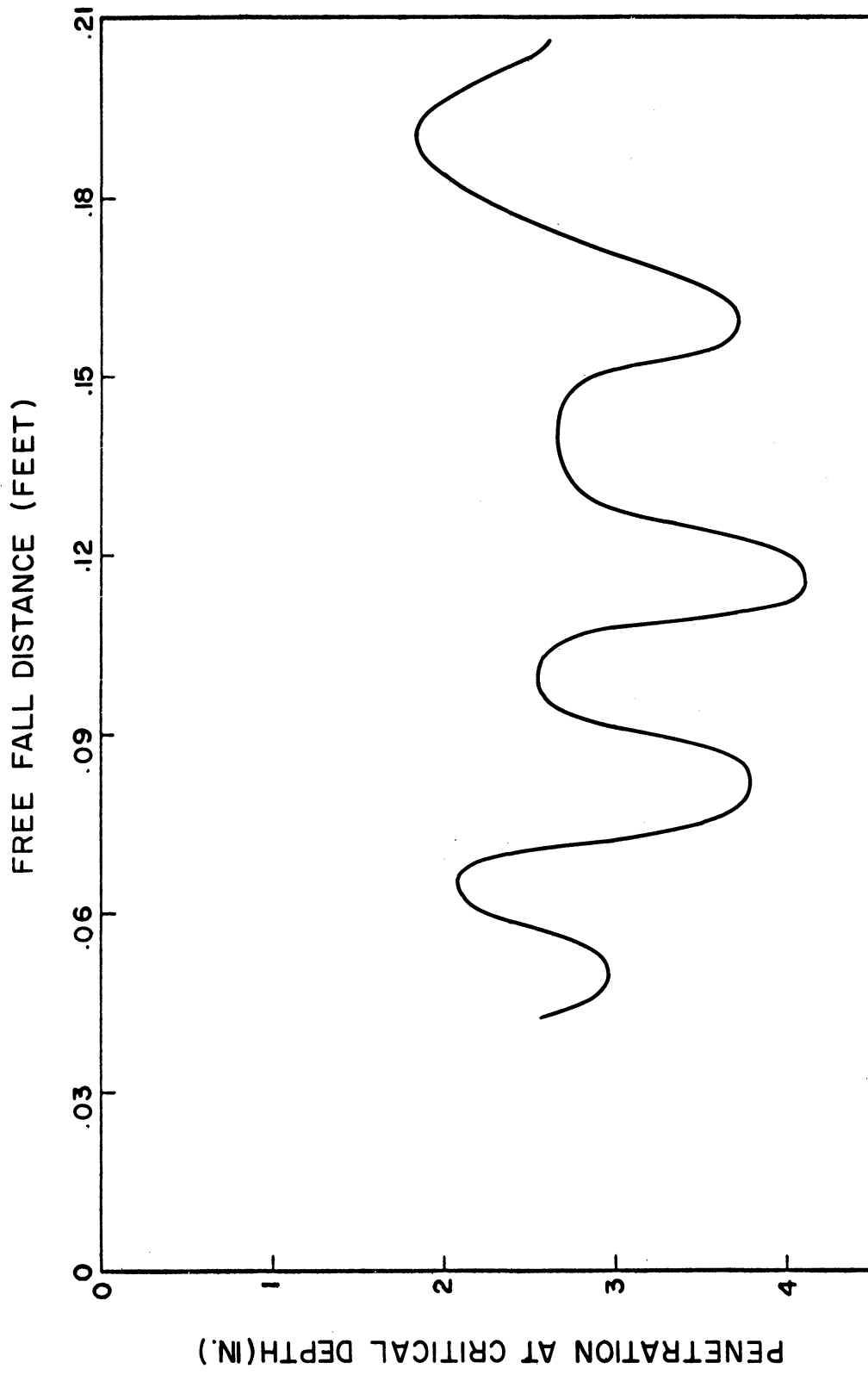
Figure 25. Variation of Ring Penetration with Free Fall Distance for D32B0.
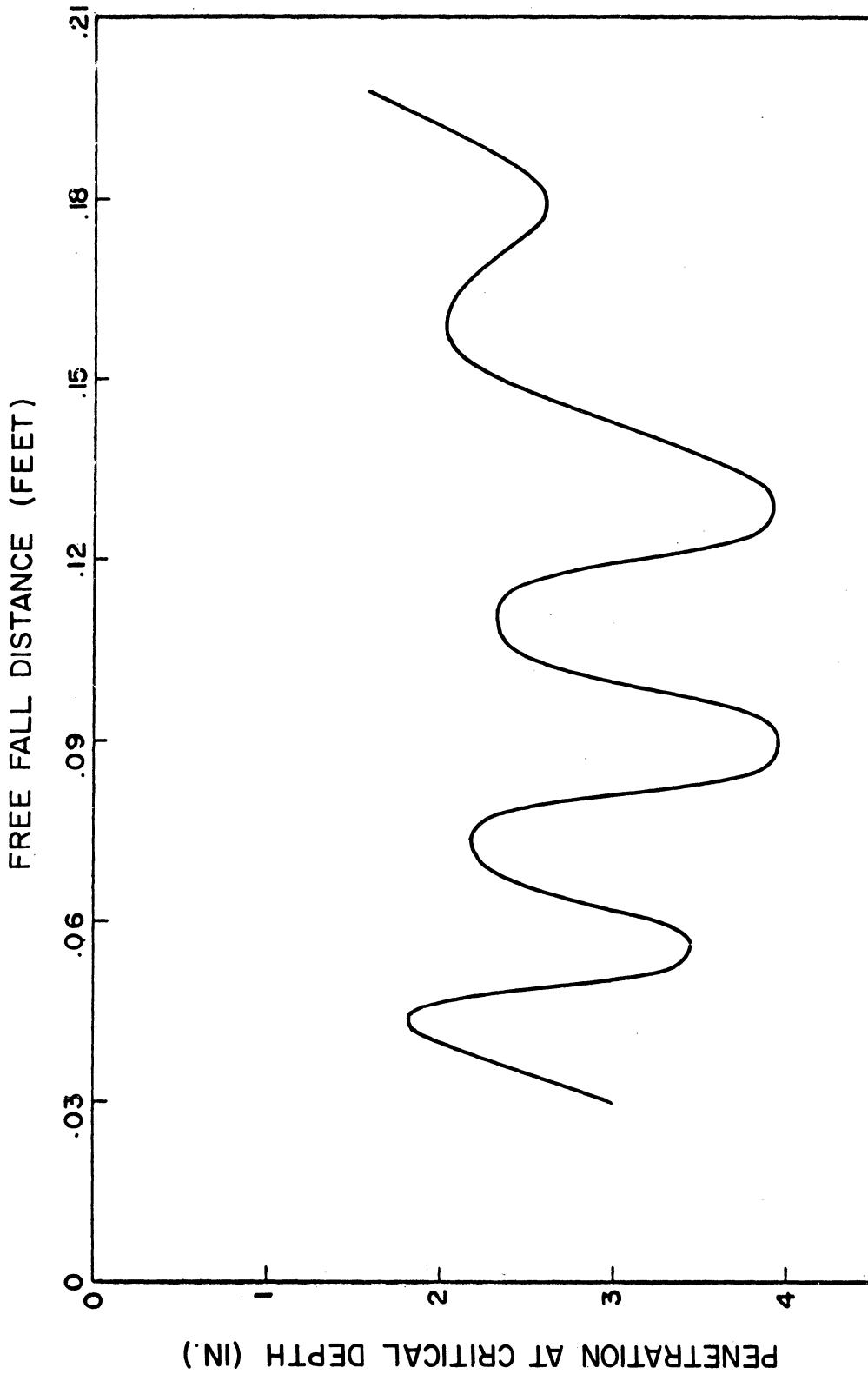
Figure 26. Variation of Ring Penetration with Free Fall Distance for D32B16.

FREE FALL DISTANCE (FEET)

PENETRATION AT CRITICAL DEPTH (IN.)
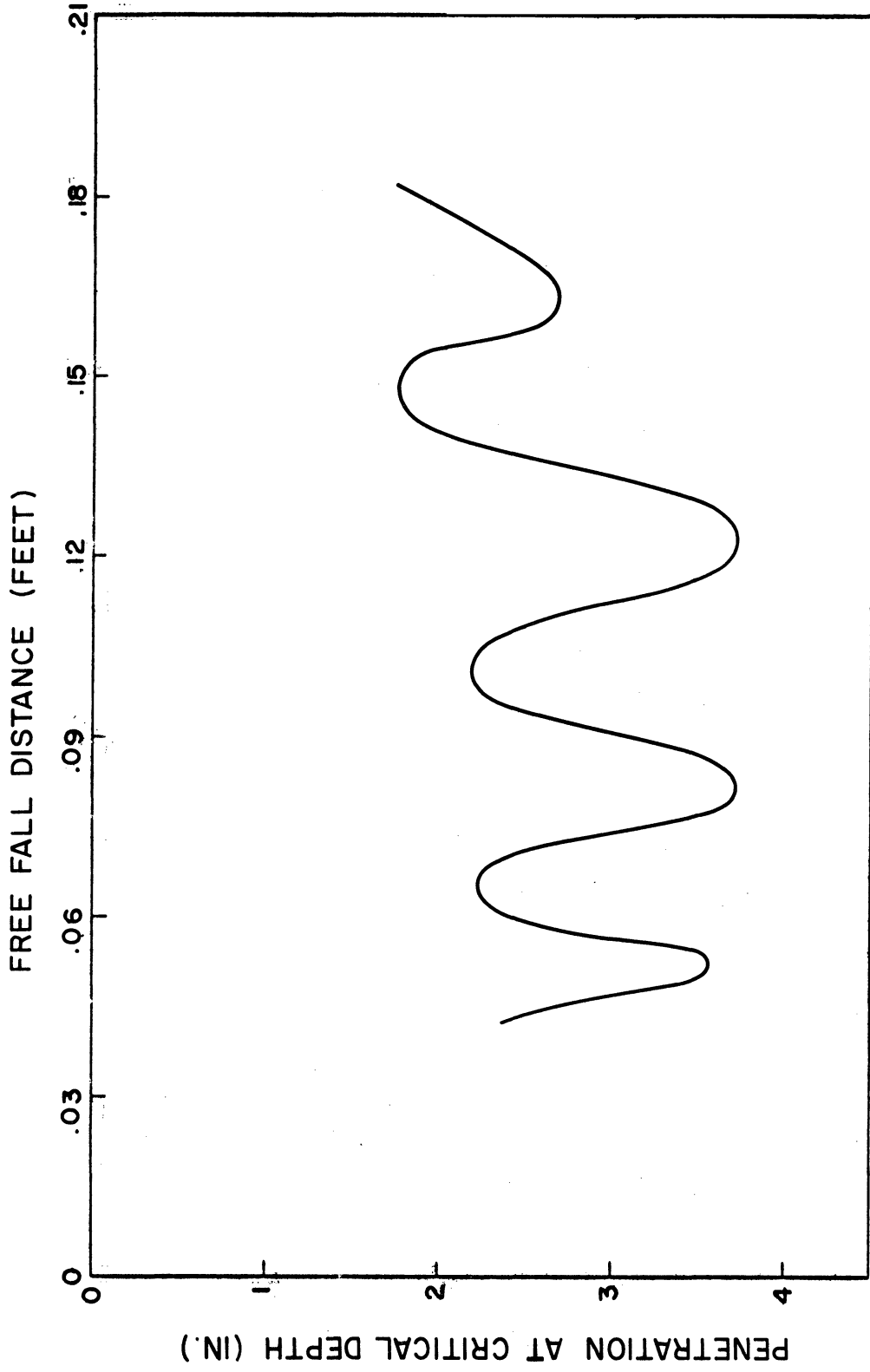
Figure 27. Variation of Ring Penetration with Free Fall Distance for B16B0.
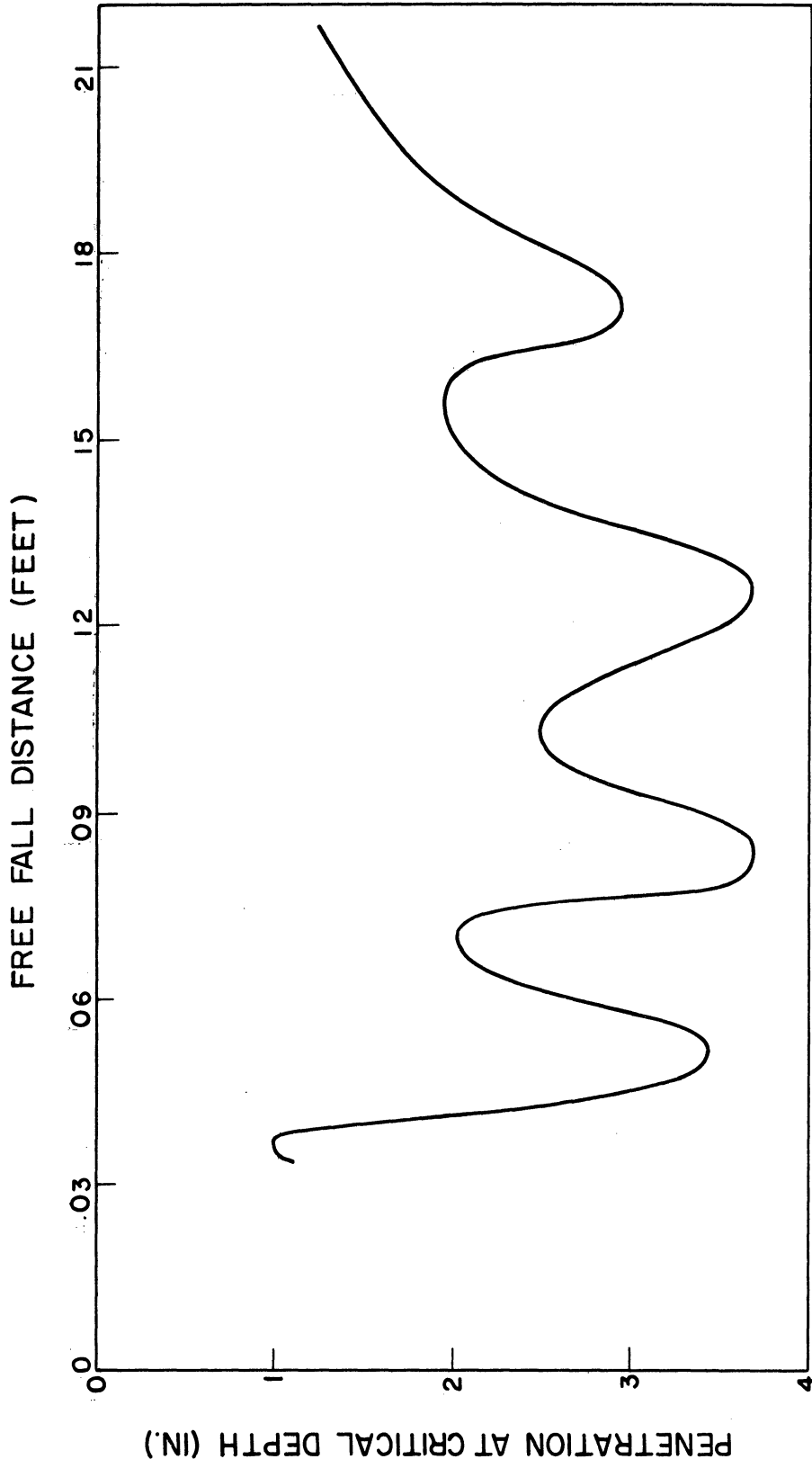
Figure 28. Variation of Ring Penetration with Free Fall Distance for D16B4.

FREE FALL DISTANCE (FEET)

PENETRATION AT CRITICAL DEPTH (IN.)
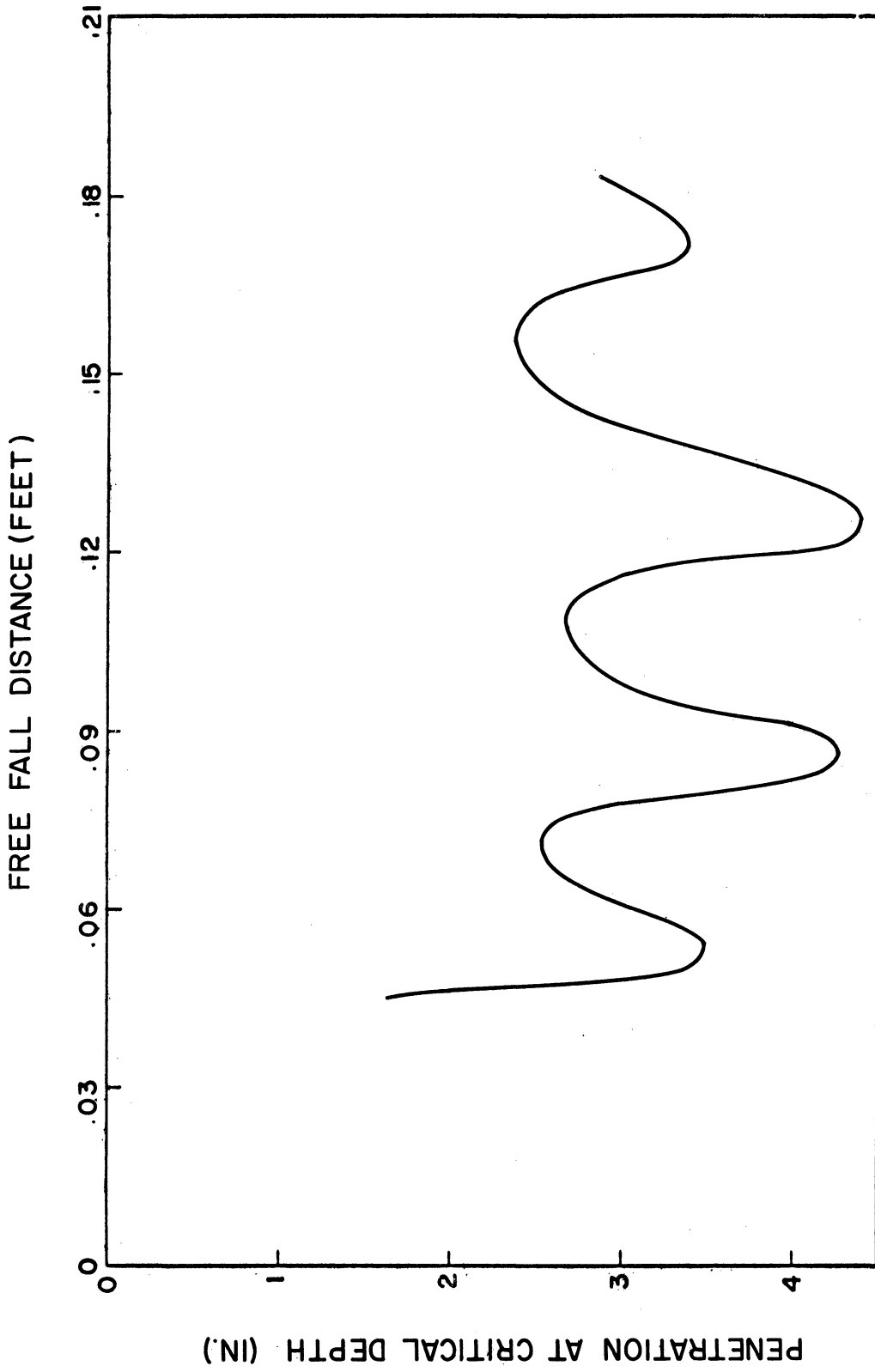
Figure 29. Variation of Ring Penetration with Free Fall Distance for D12BO.

FREE FALL DISTANCE (FEET)

PENETRATION AT CRITICAL DEPTH (IN.)
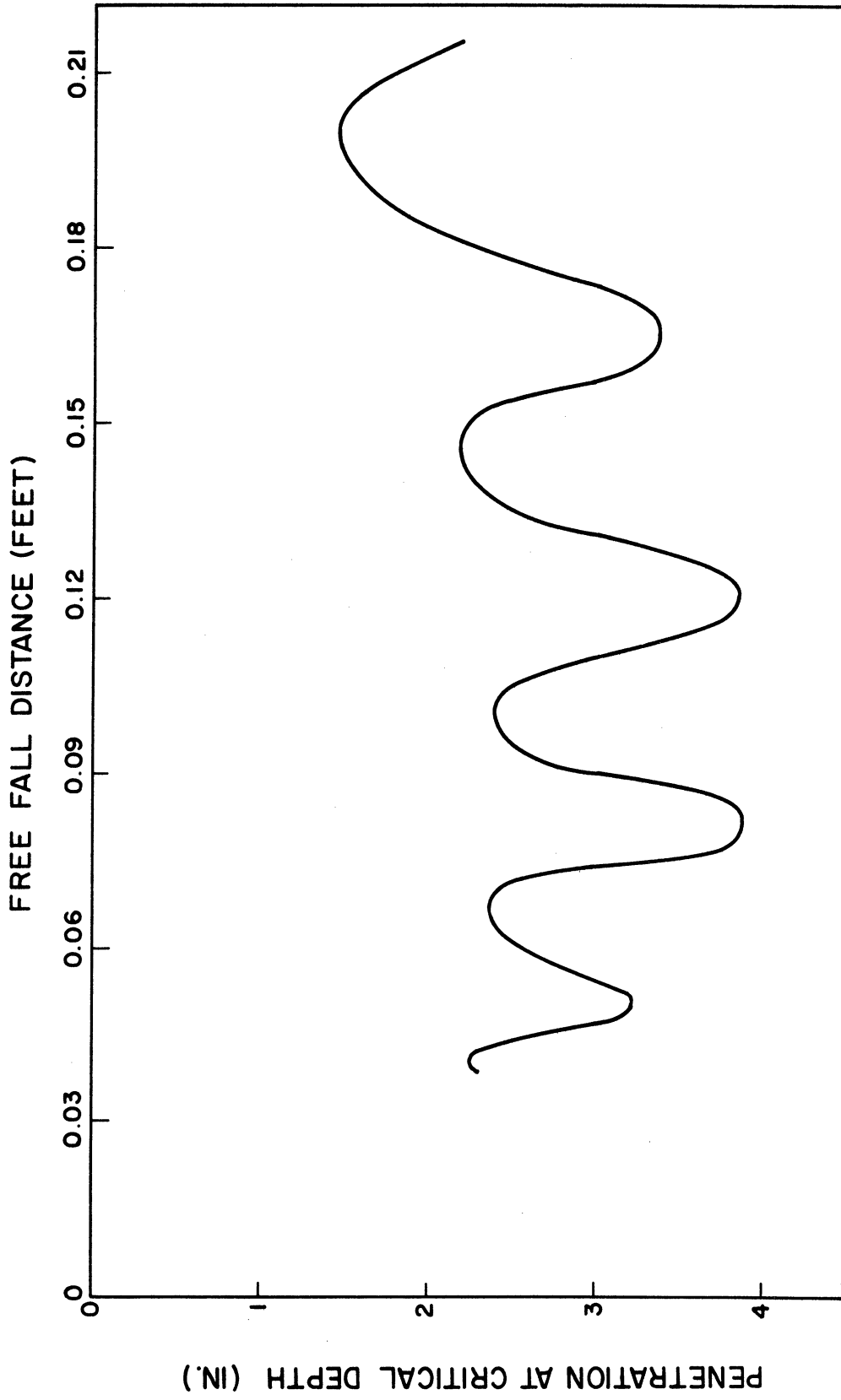
Figure 30. Variation of Ring Penetration with Free Fall Distance for D12B4.
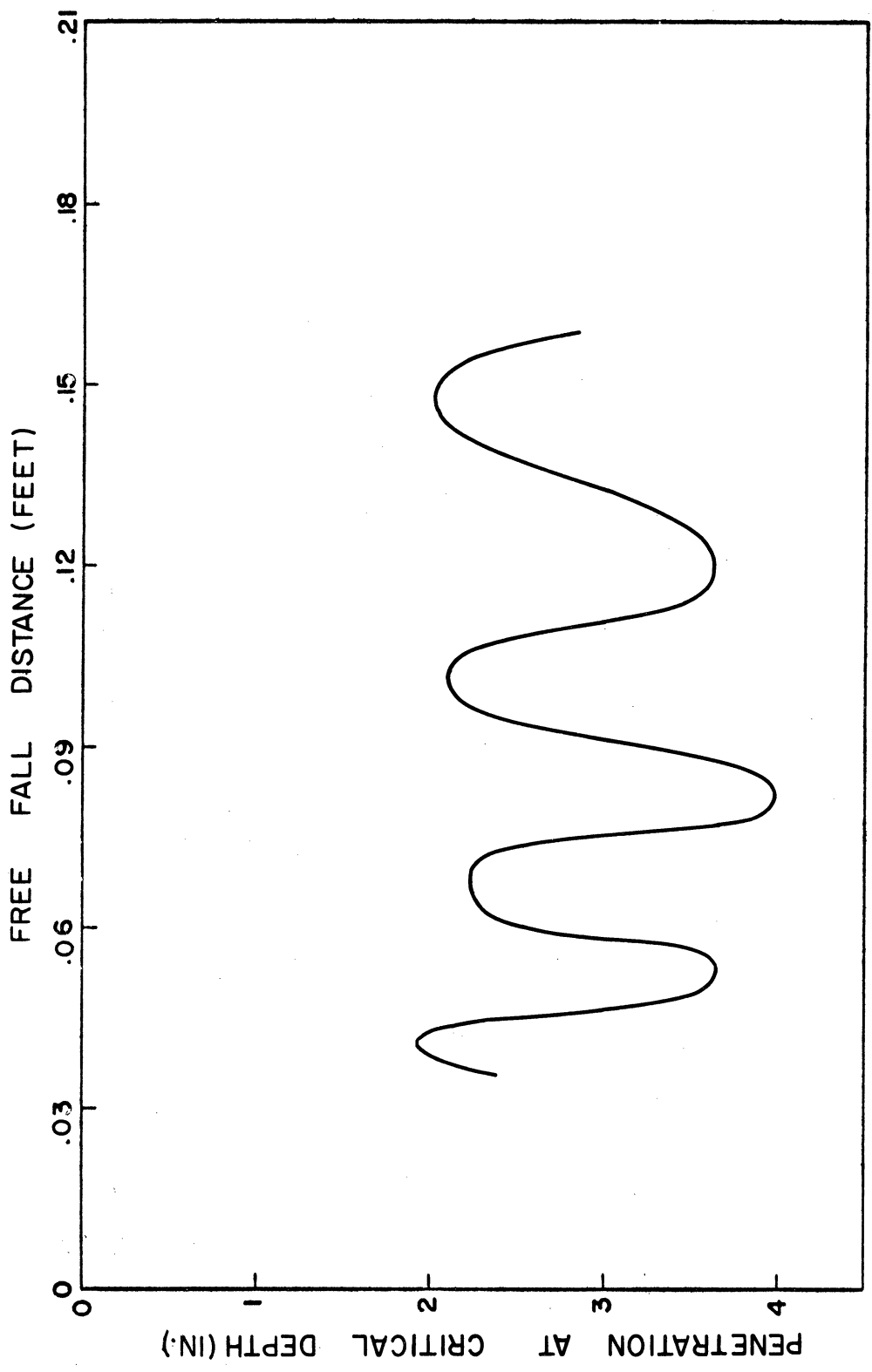
Figure 31. Variation of Ring Penetration with Free Fall Distance for D8B0.
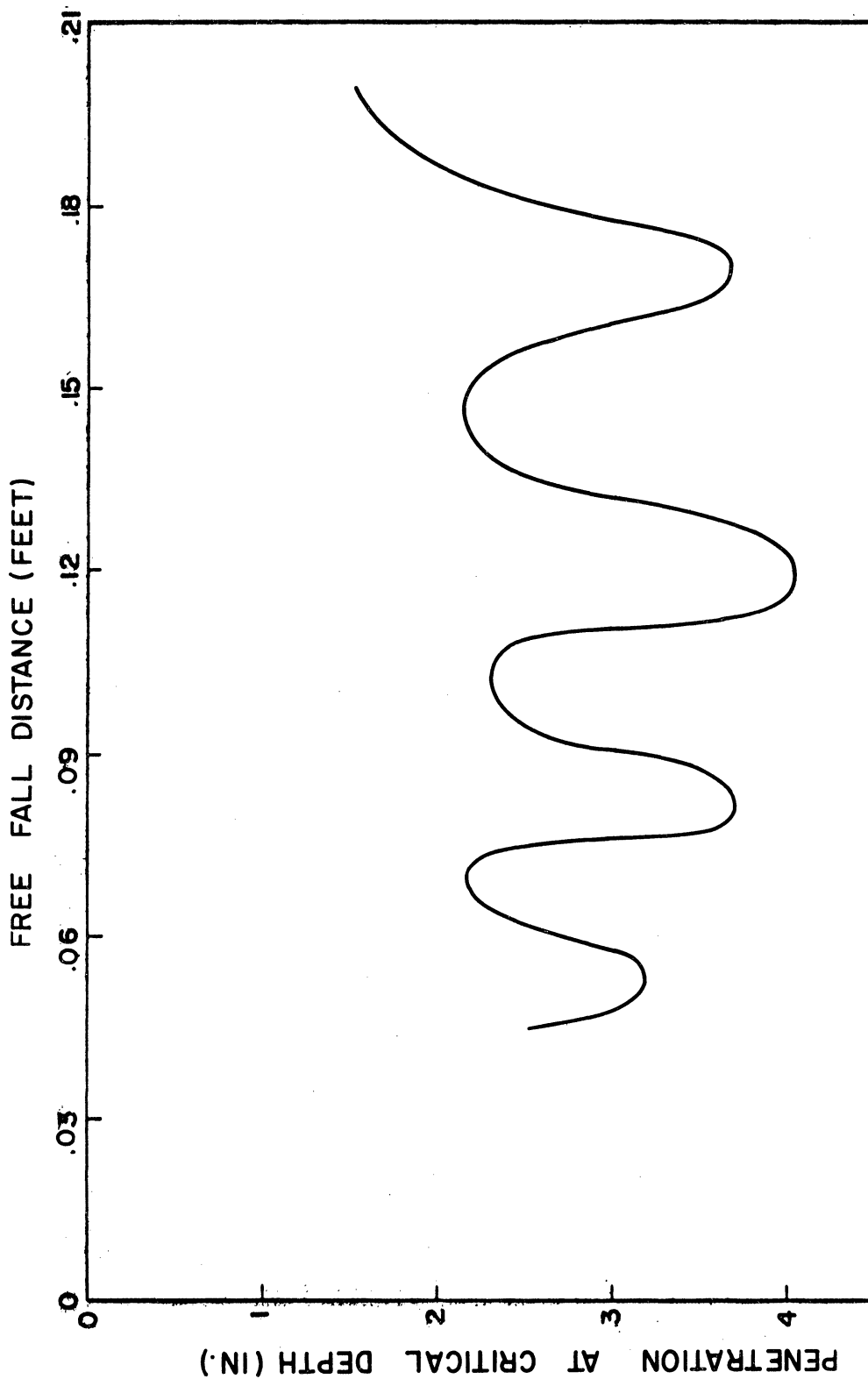
Figure 32. Variation of Ring Penetration with Free Fall Distance for D8B4.
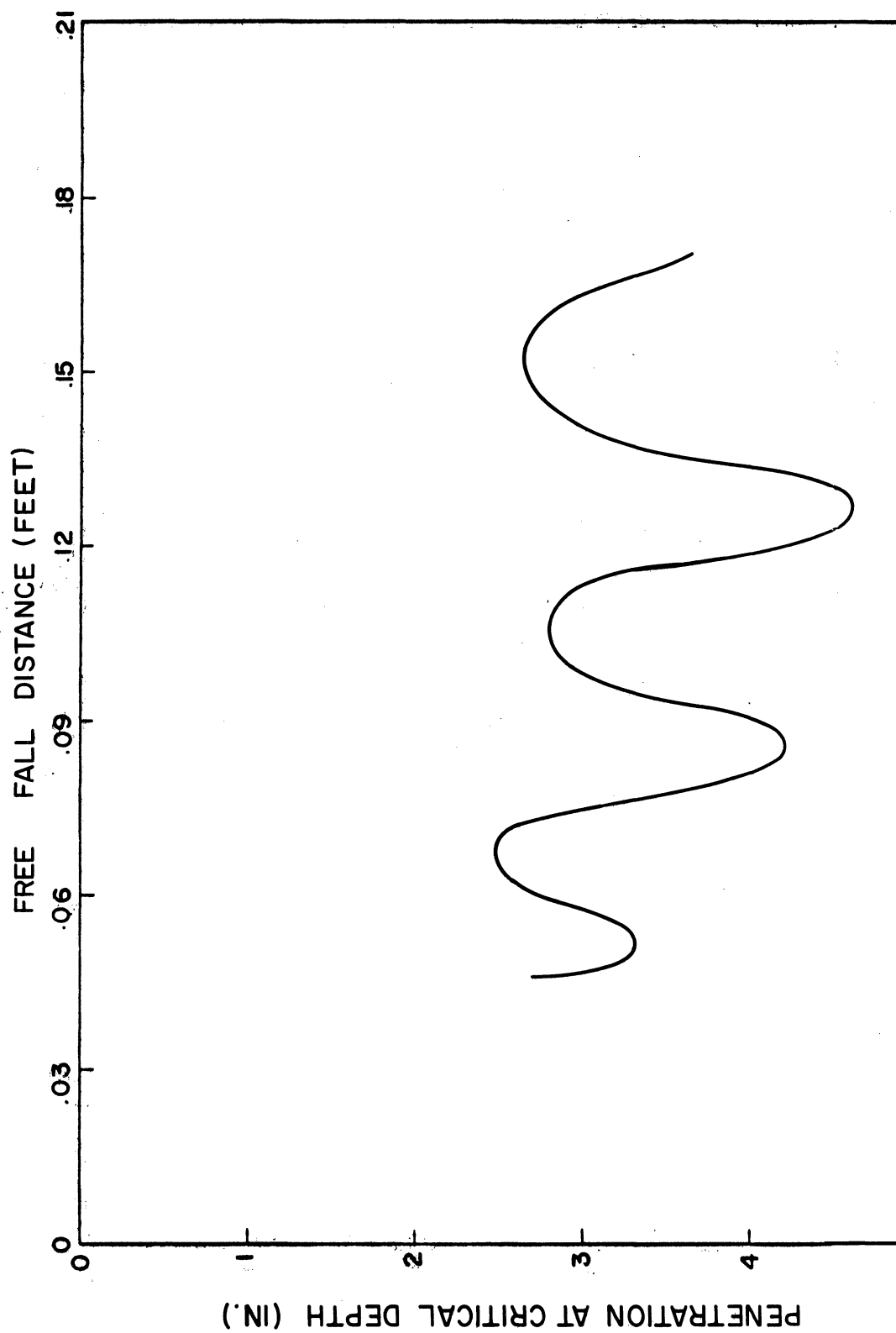
Figure 33.   Variation of Ring Penetration with Free Fall Distance for D4BO.
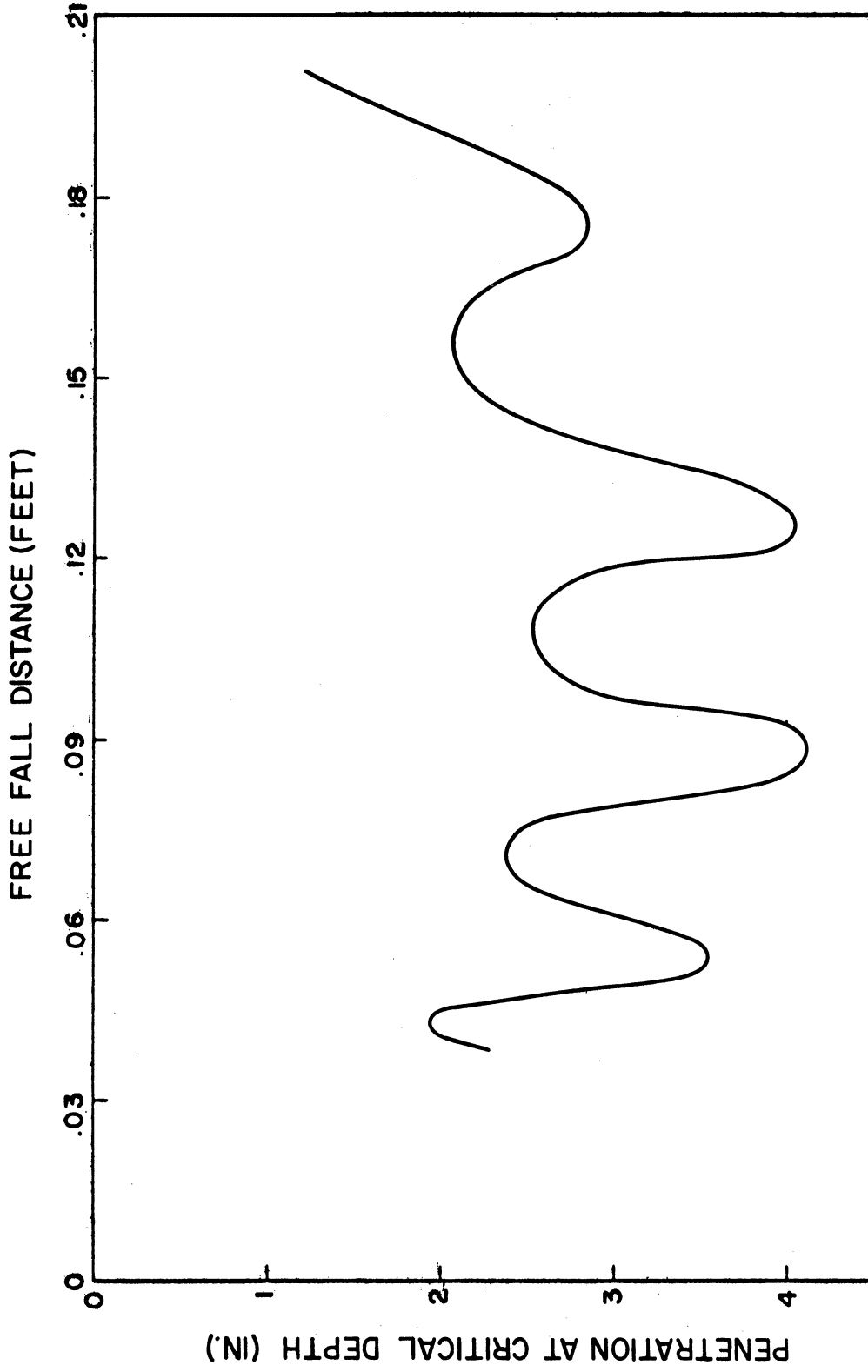
Figure 34. Variation of Ring Penetration with Free Fall Distance for D32B32.
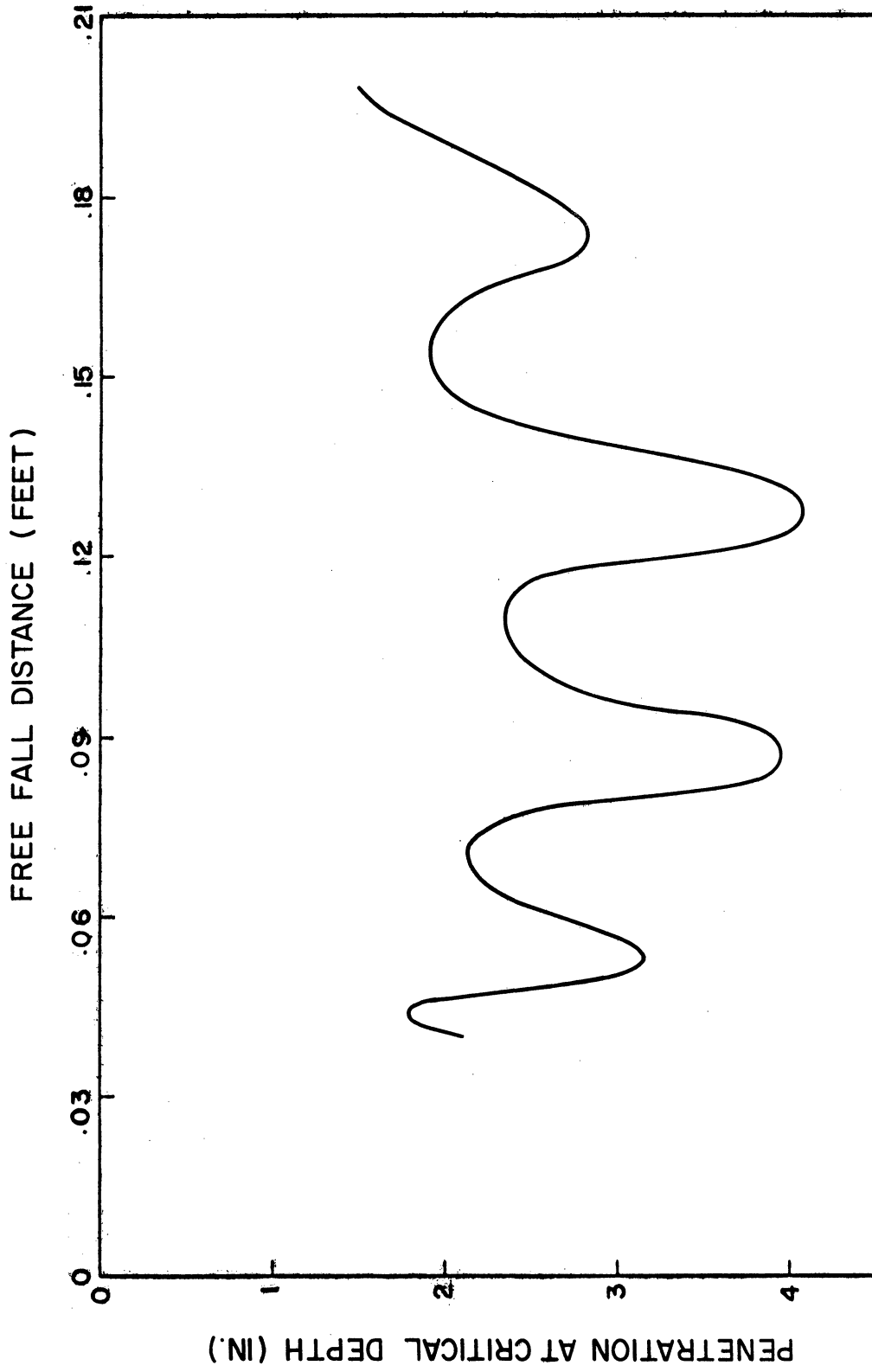
Figure 35. Variation of Ring Penetration with Free Fall Distance for D16B16.
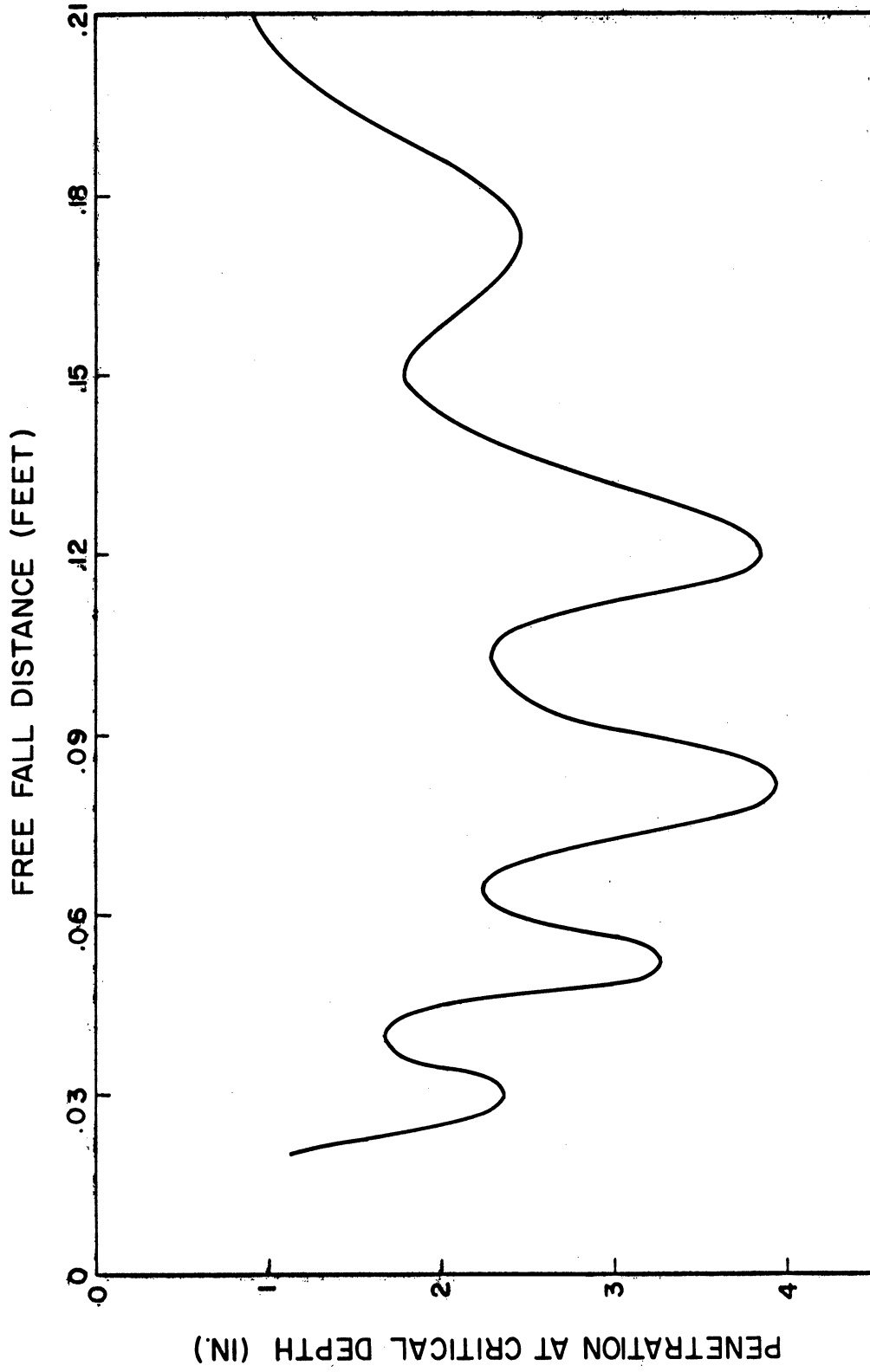
Figure 36. Variation of Ring Penetration with Free Fall Distance for DOBO.
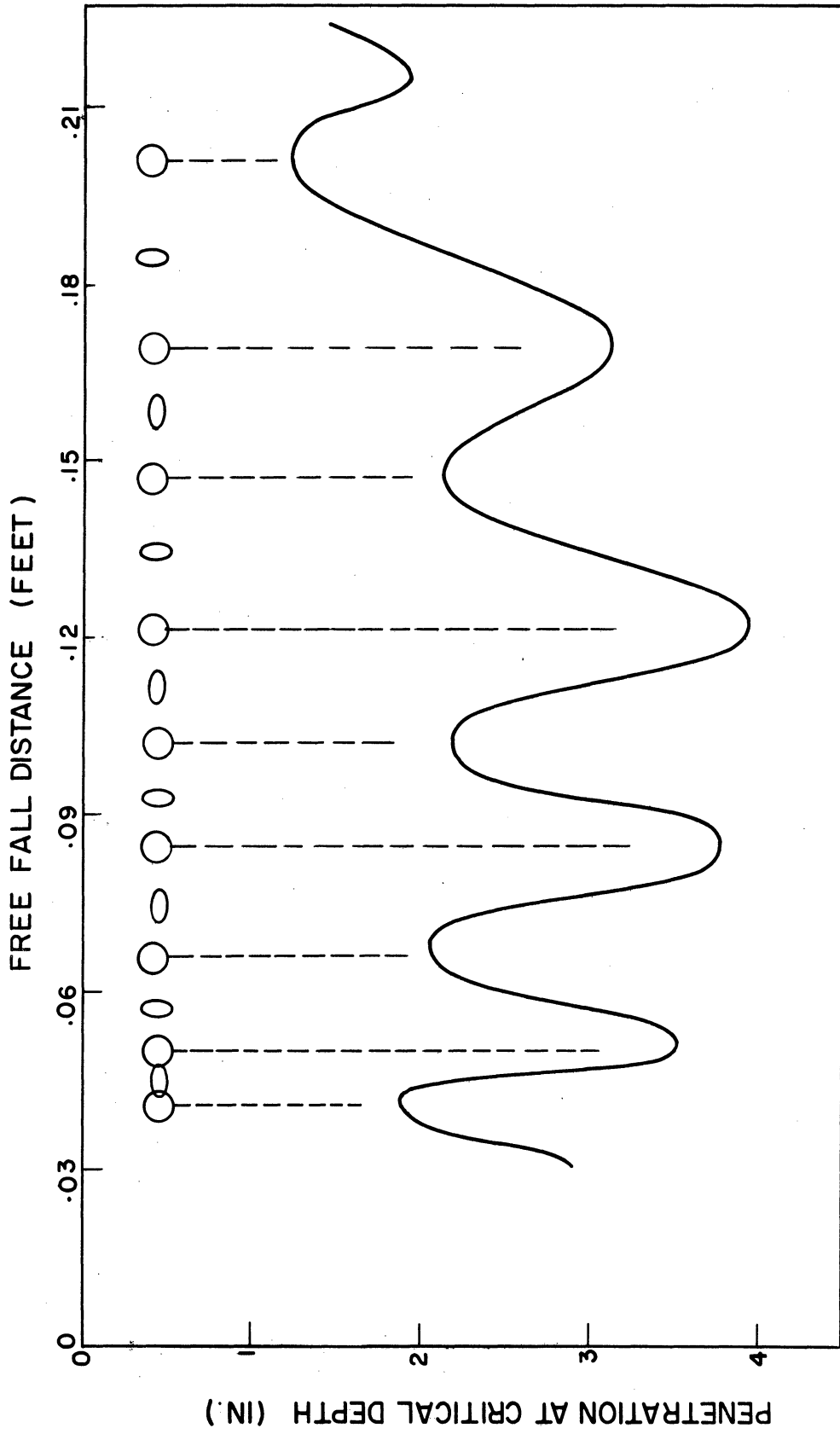
Figure 37. Variation of Ring Penetration with Free Fall Distance for D12B16.
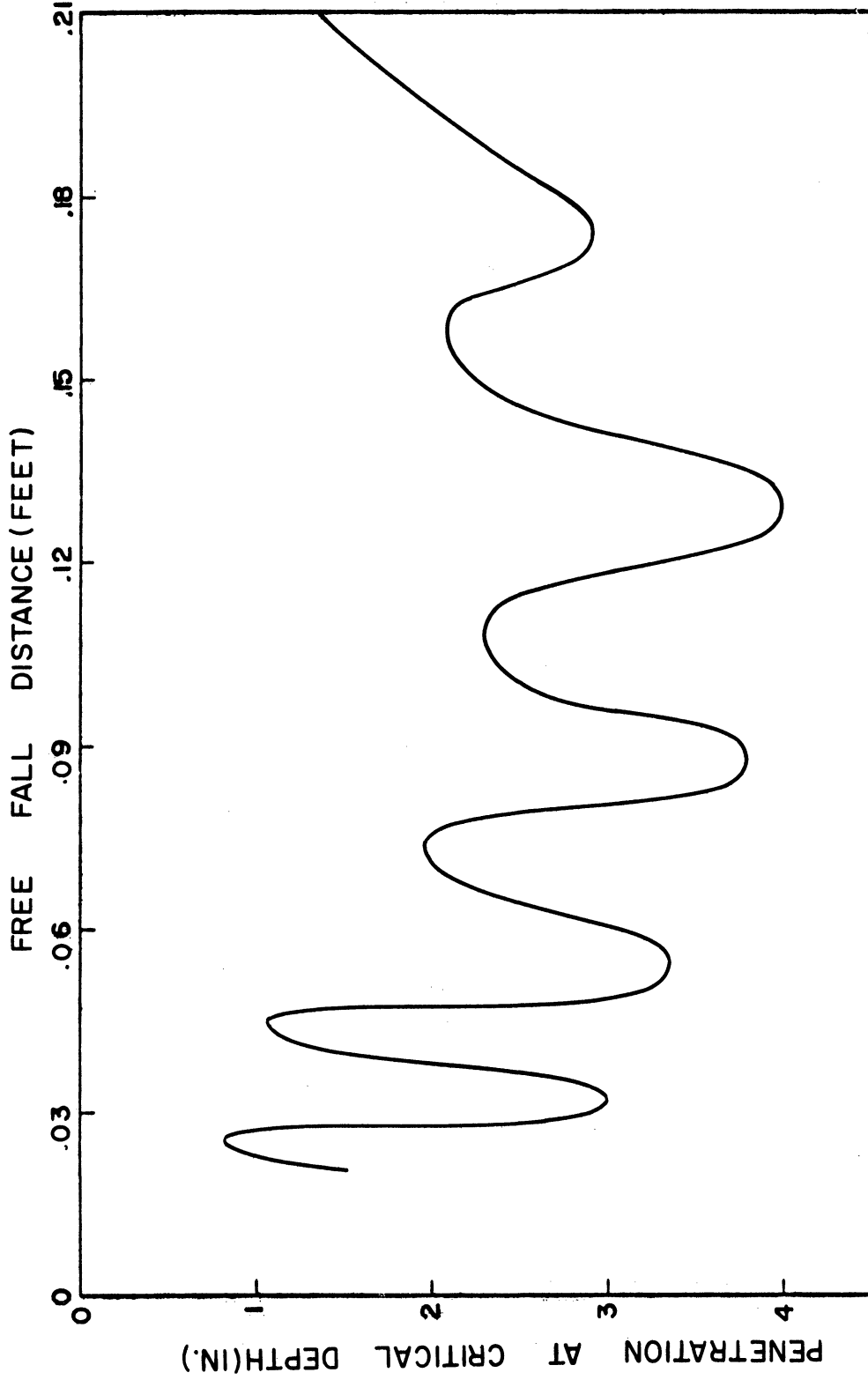
Figure 38. Variation of Ring Penetration with Free Fall Distance for D8B16.
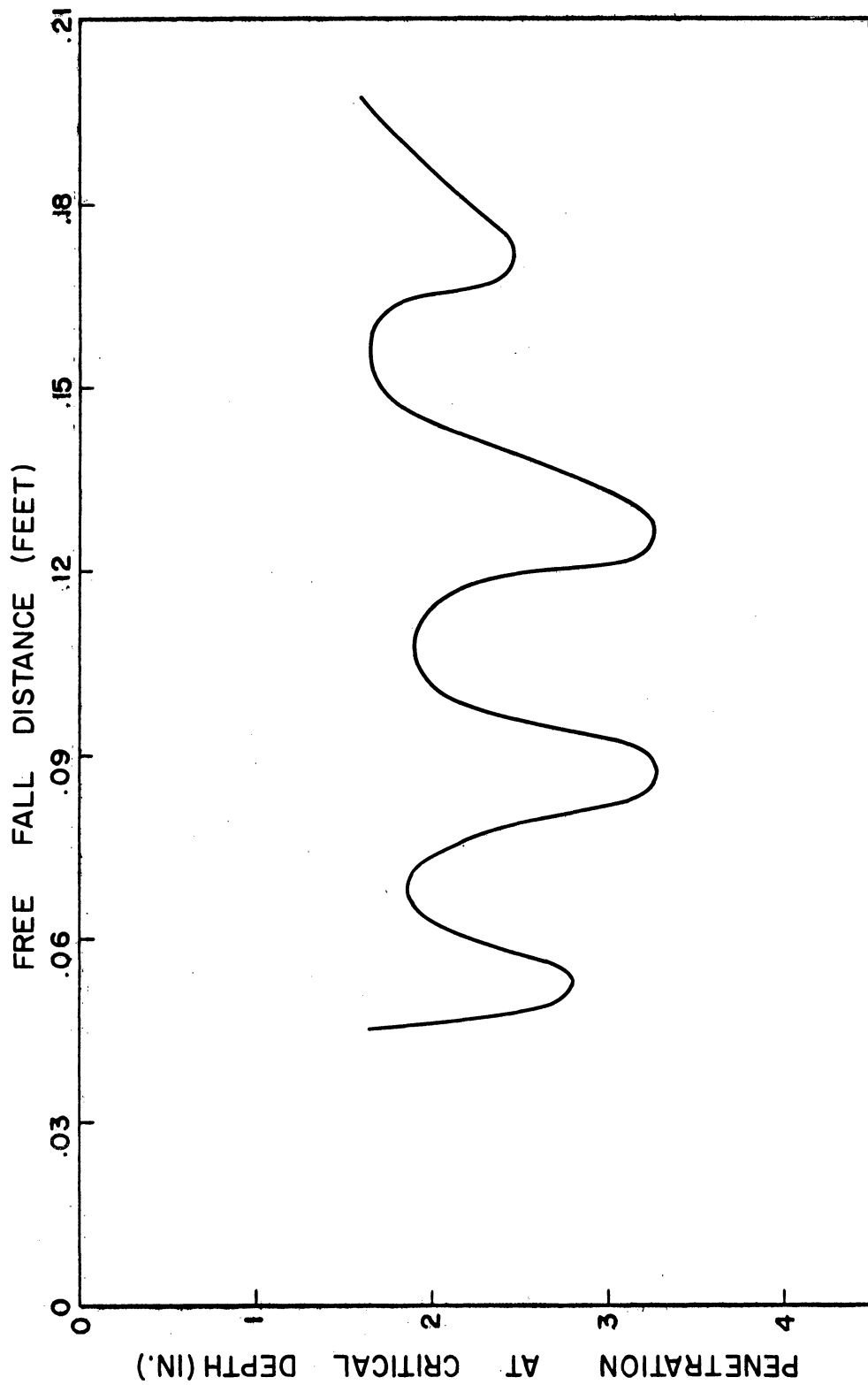
Figure 39. Variation of Ring Penetration with Free Fall Distance for D16B32.
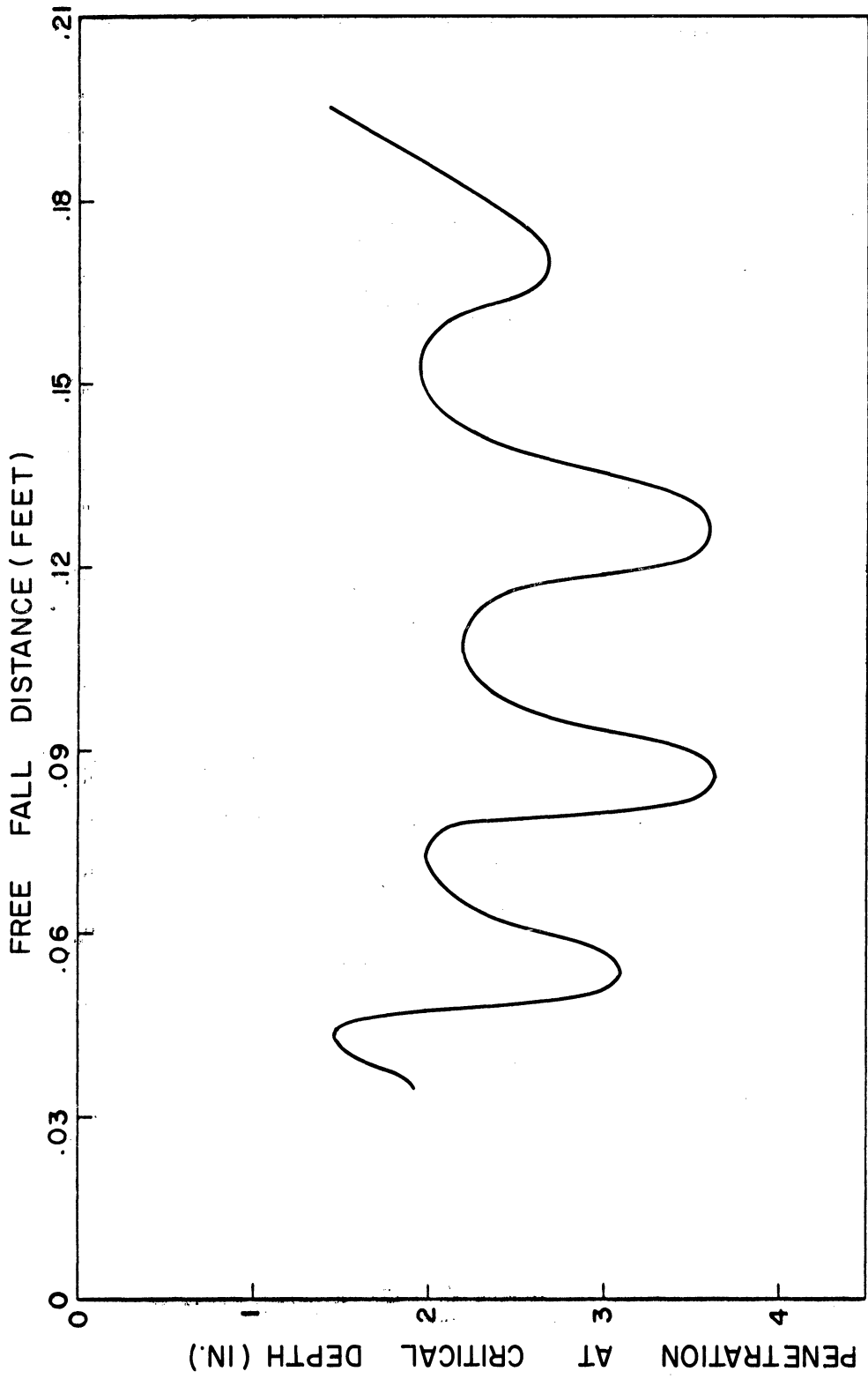
Figure 40. Variation of Ring Penetration with Free Fall Distance for DOB32.
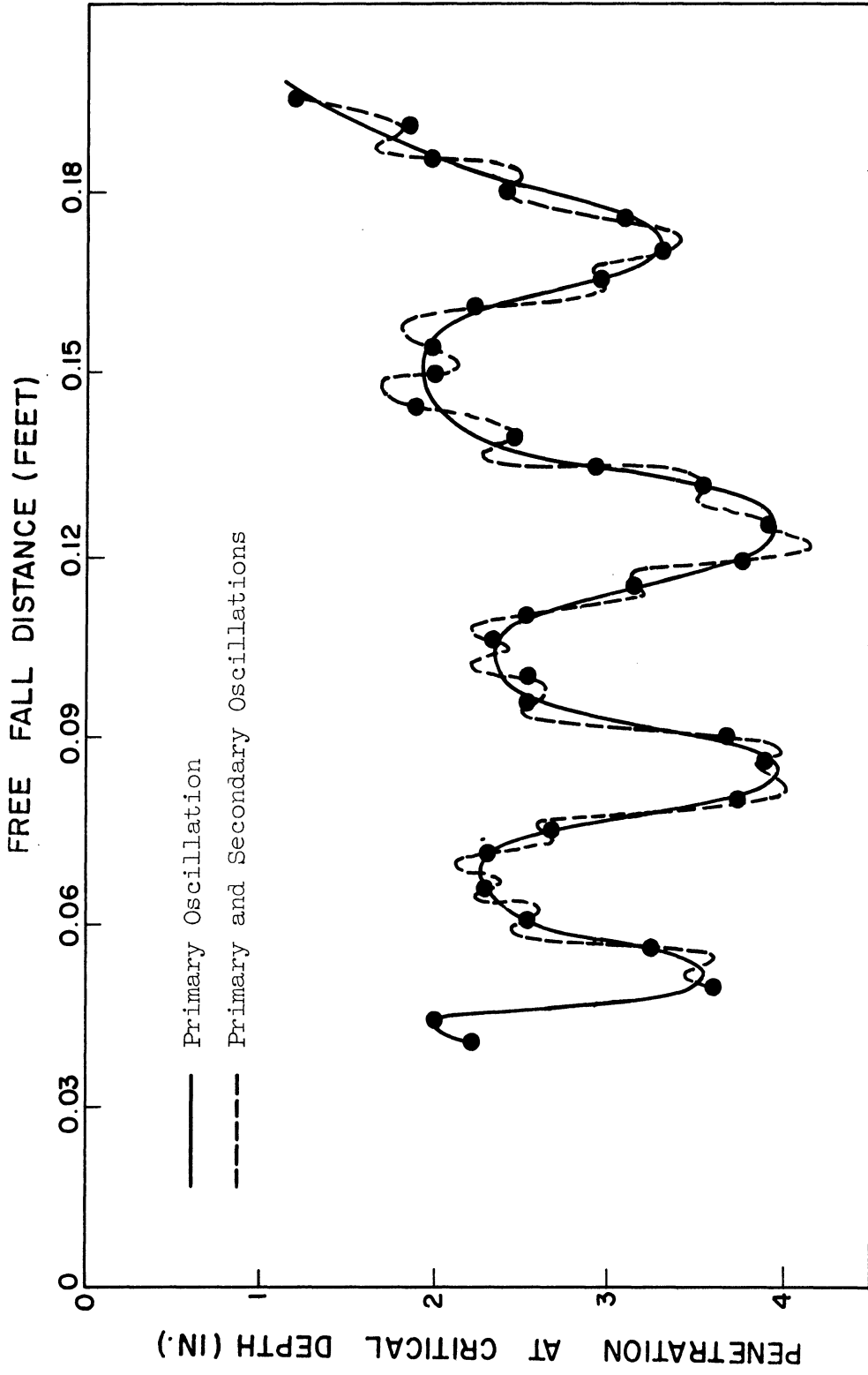
Figure 41. Variation of Ring Penetration with Free Fall Distance for DOB4 Showing Component Curves.
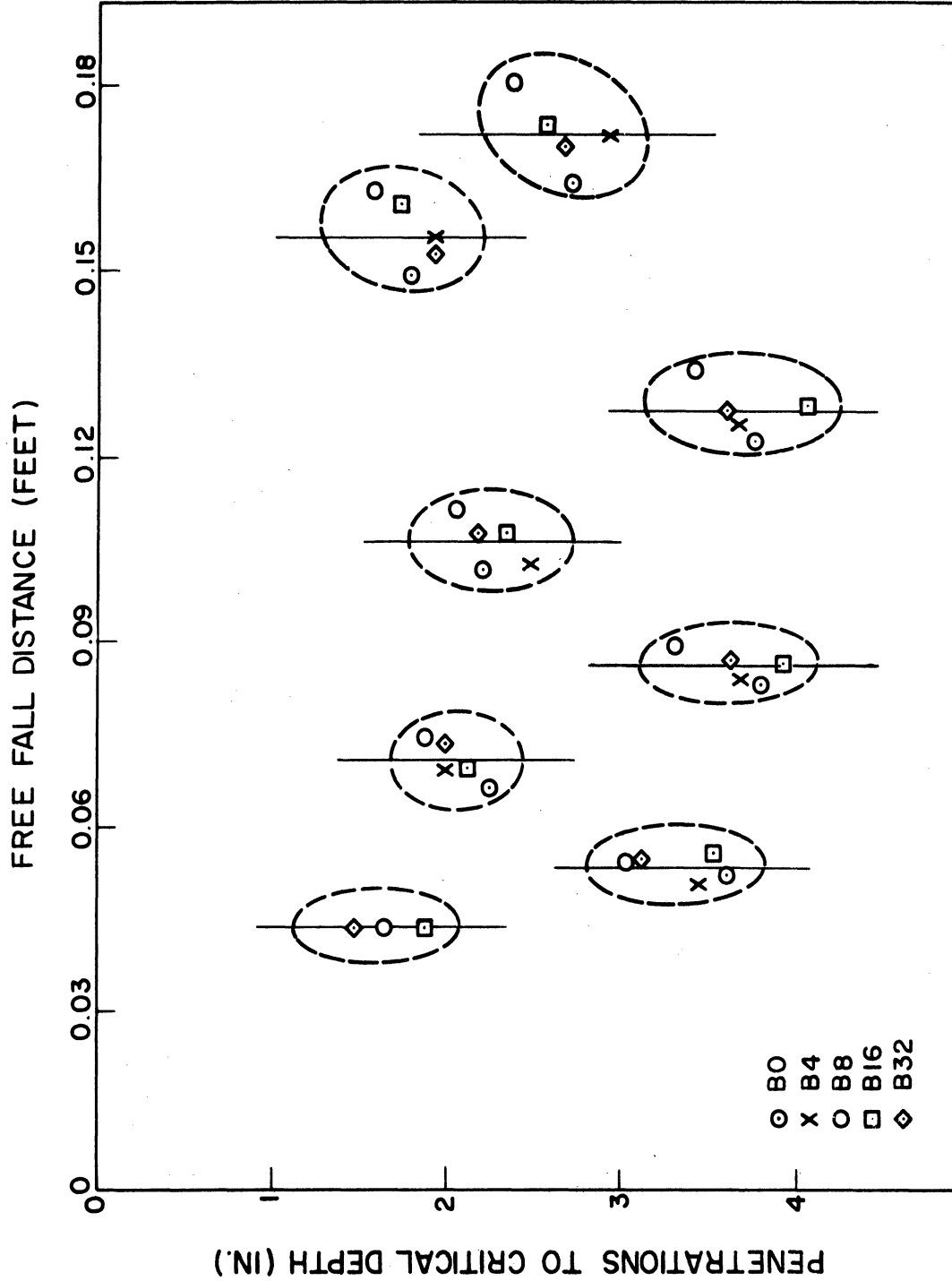
Figure 42. Composite of Results Showing Location of Relative Maximum and Minimum Penetrations for Drops D16 and Various Bases.
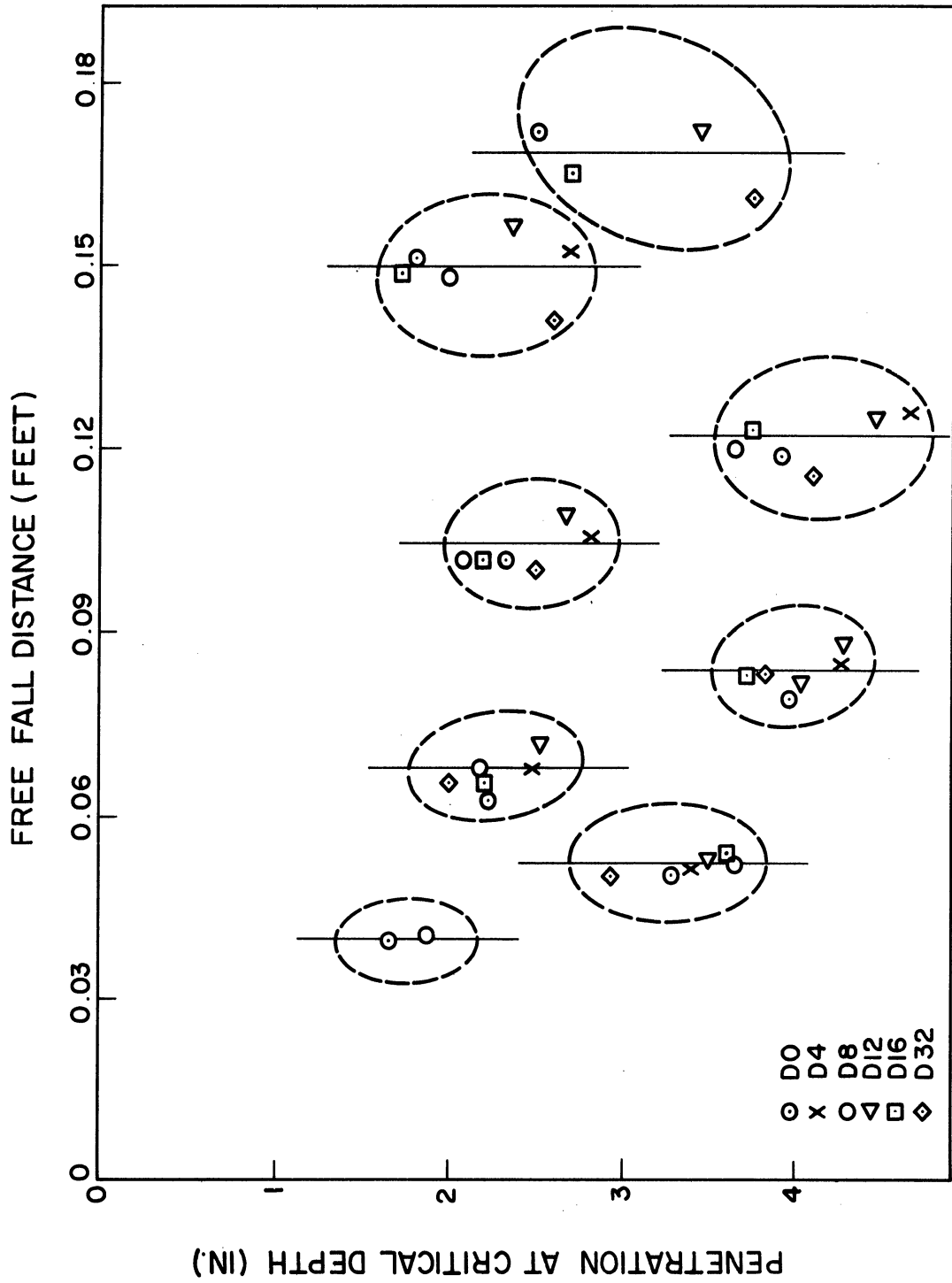
Figure 43. Composite of Results Showing Location of Relative Maximum and Minimum Penetrations for Base Bp and Various Drops
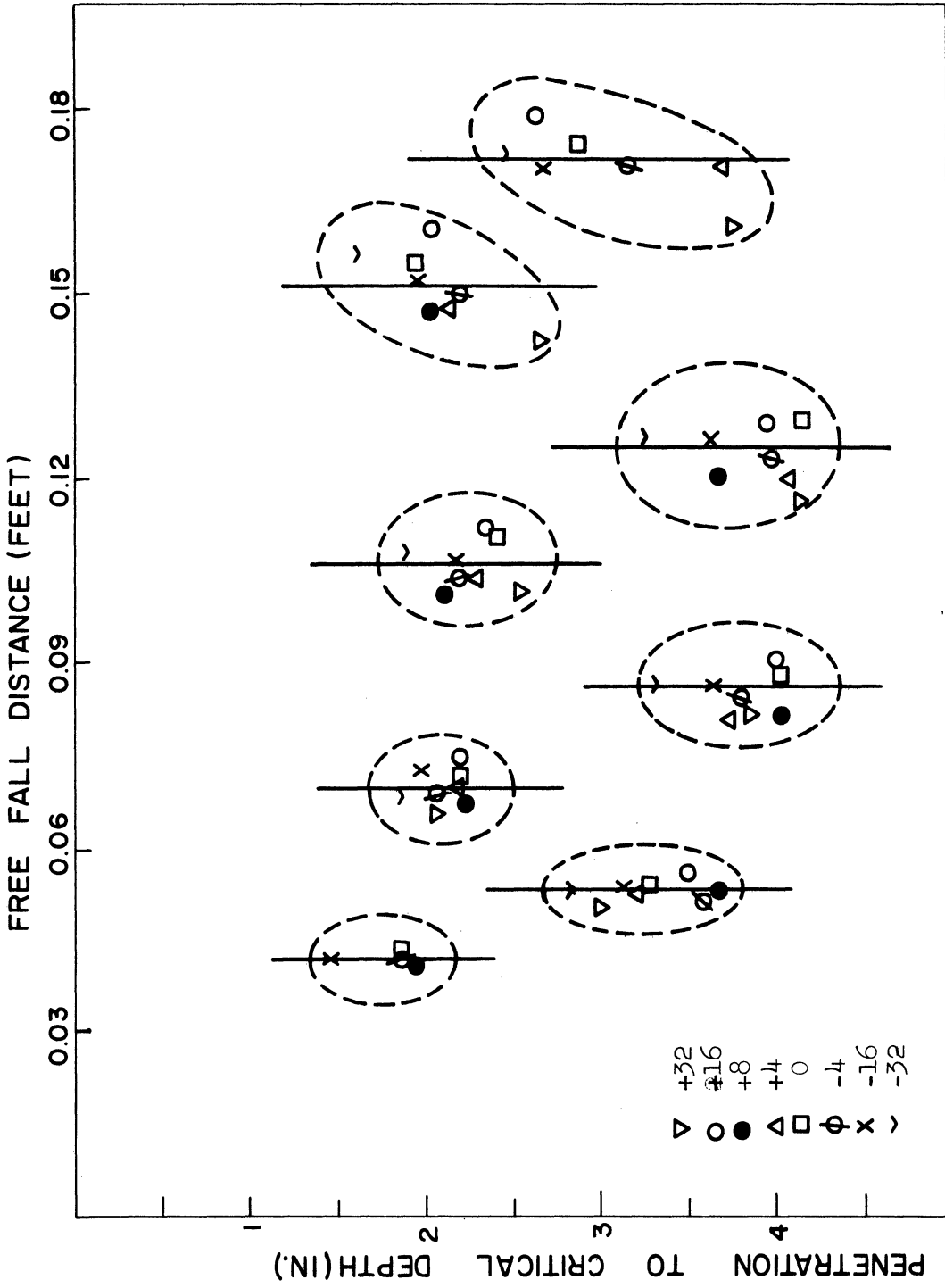
Figure 44. Composite of Results Showing Location of Relative Maximum and Minimum Penetrations for Various Density Differences.

combination (drop density-base density-free fall height) is held constant.
The location of the average free fall height to produce each local maxi-
mum and minimum critical depth is indicated by a short vertical line.
The variation from this average value tends to increase as the free fall
height increases but in general there is no obvious relationship between
the variation and the density combinations involved.

The spacing of these averages of the maximum and minimum points
is of note. The distance on the graphs from one maximum (of minimum) pene-
tration to the next increases as the free fall height increases. However,
the time is found to be constant from one maximum to the next over the
entire range. In addition, the period from one maximum to the next is di-
vided into unequal parts (with respect to time as well as free fall height),
an observation which agrees with the earlier observation that the period
of oscillation of the free falling drop is divided into two unequal parts
about the spherical shape taken as nodal points.

At any given maximum (or minimum) region the variation of pene-
tration is seen with respect to the combination of drop and base used.
However, no obvious relationship of the combinations to the variation in
penetration is evident.

b. Description and Discussion

The major interest of this study is in the behavior of
the rings once the transformation at the free surface is completed. In
brief, all rings descend into the base solution with diminishing velocity.
During the descent the rings suffer a loss of circulation, experience a
change in diameter, may be subject to oscillations, and may develop a
number of nodes. At a certain level, namely, the critical depth, the

ring may develop a number of secondary rings, depending on the combination of drop and base solutions used.

For purposes of classification and ease of reference, three types of rings will be defined, depending on whether the drop solution is of greater, equal or lesser density than the base solution. These will be designated hereafter as Types I, II and III, respectively.

1) Ring Diameter.

For Type I rings, the diameter of the ring at first increases in a nearly linear fashion with increasing penetration. As penetration increases, the ring spreads more rapidly with the linear relationship no longer being valid. The greater the density difference, the sooner the linear relationship ceases and the more rapidly the ring expands with increasing penetration. The greatest density difference used in this study, the D32B0 combination, resulted in a diameter-penetration relationship which exhibited little linearity even in the early stages of penetration. Reference to Figures 5 through 24 will show the region of linearity and its decrease with an increasing density difference.

The diameter of a Type II ring increases linearly with penetration to within about a ring diameter of critical depth. In this final region of penetration the diameter increases by 25 to 50 percent and the ring stops.

For Type III rings, the diameter increases linearly with penetration for a time but then begins to assume a constant value or even decrease with increased penetration. In this case, an increased density difference tends to lessen the range of penetration for which the linearity holds and accentuates the tendency for the diameter to contract as

critical depth is neared. In fact, some drops of the DOB32 combination were observed to produce rings whose inner diameter contracted to zero as critical depth was reached. This effect was observed visually by watching, from above and from the side, drops of the DOB32 type descend.

Two additional observations need to be made. First, there is a slight decrease in overall diameter slightly below the surface, as shown in most of Figures 5 through 24. There follows an increase and then the linear relationship of diameter with penetration. This feature was found in nearly all the photographs made in the region of transition from drop to ring. At the 1" level of penetration used for the reference level in the theoretical discussion to follow, the relationship was essentially linear in all cases.

Secondly, a comparison of many sets of negatives of various drop and base combinations indicate a definitely smaller ring diameter at the 1" level for rings of minimum penetration as compared to rings of maximum penetration. However, this difference is so small that its influence is neglected in the theoretical discussion.

2) Ring Velocity

The velocity of rings of minimum penetration is less than the velocity of rings of maximum penetration at any given level. For all rings the velocity decreases at a decreasing rate as the rings descend.

3) Critical Depth

Each ring will descend in the base solution to a level of penetration at which some clearly definable manifestation occurs. At this depth, the critical depth, the rings of Type II stop while rings of

Types I and III transform into a number of smaller rings of very low velocity. When the depth of penetration to the critical depth is related to the variables in the study, especially when related to the free fall height, interesting relationships appear.

The relationship of free fall height and depth of penetration to critical depth is periodic with features of a sine curve of increasing period. A study of Figures 25 through 41 clearly shows this relationship. A calculation of the period of the curve indicates that although the period is increasing with free fall height, it is actually constant with respect to the time of free fall. Additional calculations show that the intervals of free fall and time for the various periods satisfy the formula for a free falling body. Further it is noted that the frequency of the curves with respect to time is very well approximated by the expected frequency of oscillation of a free falling drop. The conclusion, one of the important ones of this study, <u>is that the oscillations of the falling drop have a direct and pronounced effect on the penetration of the ring formed.</u>

From a study of the individual frames of motion pictures of free falling drops, the times of appearance of distortions about the neutral configuration, (nominally spherical, except for drag effects), of the drop were found. Comparison with the free fall-critical depth curves further indicated that minimum penetration to critical depth occurs when the drop at contact with the free surface is in a neutral configuration but progressing from a vertically oblate to a horizontally oblate form. For maximum penetration to critical depth, the drop is again in a neutral configuration but progressing from a horizontally

oblate form to a vertically oblate form. For reference, the relationship of drop shape to points of maximum and minimum penetration to critical depth is indicated on Figure 37. The drops are at the neutral configuration shown as circles at maximum and minimum points and at the appropriate elliptical shapes as shown across the upper part of the figure. This variation of shape is typical of all figures of the series of penetration graphs.

For all drops of this study, it was found that rings would form for free fall heights corresponding to four or five times the period of oscillation of the falling drop. This appears to account for the periodic nature of the curves.

A possible effect of the secondary mode of oscillation of the free falling drop was evident upon occasion. In regions of minimum penetration to critical depth, the data points were sometimes seemingly random when using 0.005' increments of free fall height. When increments of 0.001' or 0.002' were used in these areas, a secondary oscillation was found to be superposed on the primary oscillation of the free fall-critical depth curve. Once the presence of such secondary oscillations was known, determination of the primary oscillation curve was more readily plotted from data collected. Figure 41 shows the data points at intervals of 0.005' with the primary curve corresponding. Also shown on this one figure is the secondary curve indicated by additional data points taken at smaller increments of free fall heights but not shown on the figure. The effect of the secondary oscillation, which is of smaller amplitude and greater frequency than the primary oscillation, is not shown on the other figures relating free fall height and critical

depth. The cause of these minor oscillations was not determined but are felt to be caused by modes of oscillation in the drop other than the primary mode. The effect would be small changes in drop characteristics as the surface is contacted from those that would prevail if only the primary mode of oscillation were present. This secondary effect was considered negligible within the general framework of the experimental program.

The variation of penetration to critical depth with free fall height is quite obvious from the figures. However, the variation of penetration at critical depth to either the density difference employed or the solutions used for the drop and base is not evidenced by composite results given in Figures 42 through 44 which show the location of relative maximum and minimum points of penetration for a given drop solution, a given base solution and a given density difference, respectively. Although the maximum and minimum points are localized within regions, and there is scatter within these regions, there is insufficient information to draw any conclusions as to the effects of the solutions used on the penetration to critical depth. A theoretical development will be made later in this thesis and results of numerical solutions presented. At that time, it will be seen that there is a definite relationship of penetration to critical depth and the density differences involved in the production of the ring. The variation of critical depth with density is numerically small and within the allowable tolerance in obtaining visually the critical depth, so that the figures of composite results do not reflect such changes.

Although the No. 20 needle was used almost exclusively, a few observations were made with other needle sizes. Figures 45 through 47 are presented only for the purpose of showing that the same general
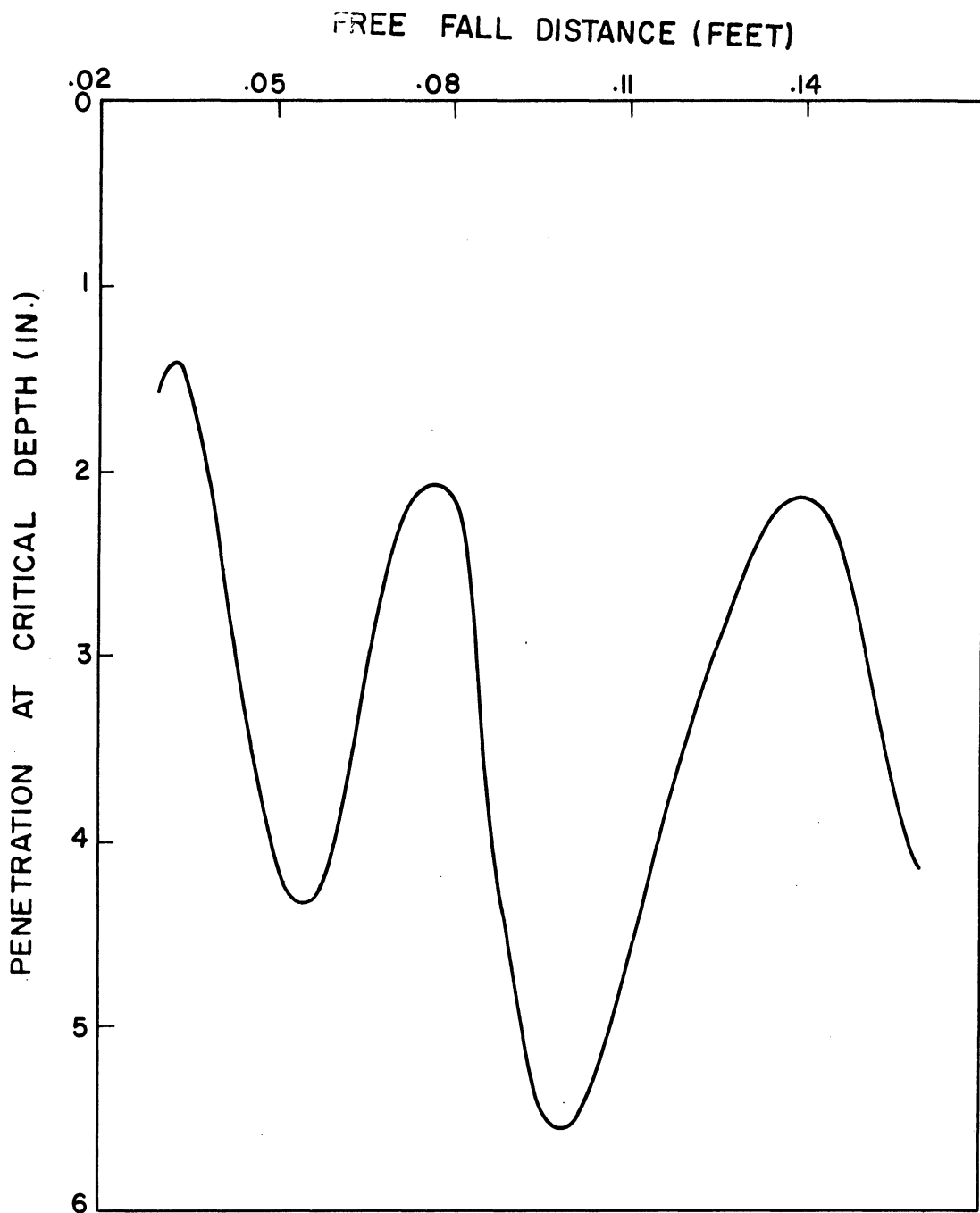
Figure 45. Variation of Ring Penetration with Free Fall
Distance for D16BO using No. 15 Needle.

FREE FALL DISTANCE (FEET)

Figure 46. Variation of Ring Penetration with Free Fall Distance for DOBO using No. 15 Needle.
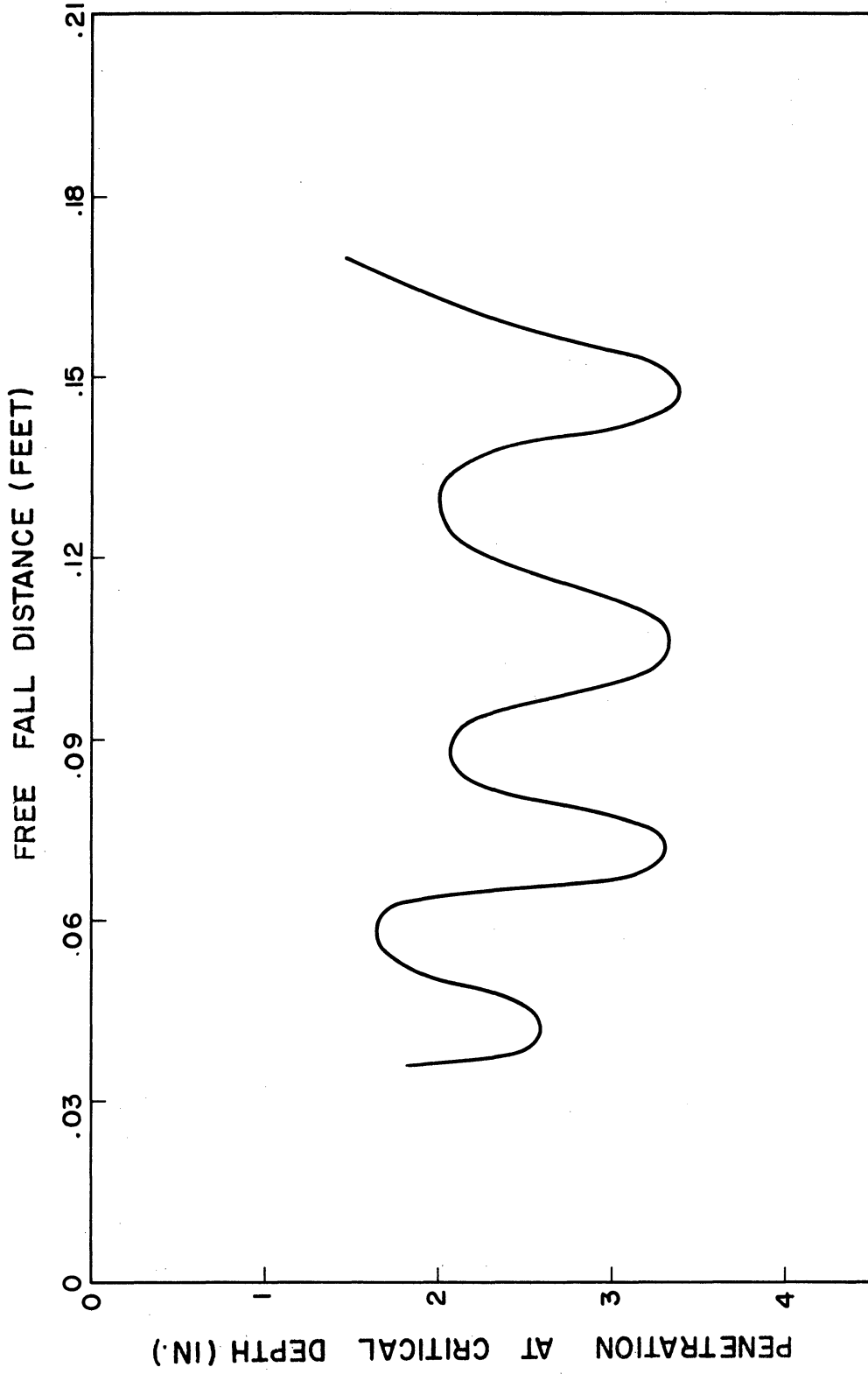
Figure 47. Variation of Ring Penetration with Free Fall Distance for D16B0 using No. 22 Needle.

patterns developed with rings from drops of other sizes. The time of os-
cillation is different and the critical depth relationship, although simi-
lar, varies in magnitude.

4) Circulation

In vortex ring theory (see Lamb[8]) a well known re-
lationship between the velocity of the ring V, circulation of the ring K,
ring radius R and core radius a is given by:

$$VR = \frac{K}{4\pi} (\ln \frac{8R}{a} - \frac{1}{4})$$

For this study, it was found from photographs that the core diameter at
the 1" level of penetration was about 0.07" for all rings and that core
diameter could be taken as decreasing linearly with depth of penetration
to about 0.06" at critical depth. Assuming this small variation in core
diameter and reading the values of V and R for various rings from indi-
vidual behavior graphs (Figure 25 through 41) the circulation for given
rings at given depths can be calculated.

Table I shows the calculated value of the circulation for vari-
ous rings at an initial penetration of 1" and at other depths of penetra-
tion. Average values of the circulation at each level are included.

Comparison of the values of circulation indicates several in-
teresting points. First, at the initial depth of 1" there is a range
of calculated circulation for each free fall height. However, the circu-
lation of rings which penetrate least to critical depth is on the aver-
age little more than half the circulation of rings of maximum penetra-
tion. The decrease of circulation is not found to be linear with depth
of penetration for the rings individually or collectively. Rather, it

TABLE I

VALUES OF $2Ra^2$ AND K FOR SELECTED PENETRATION DEPTHS FOR VARIOUS DROP-BASE-FALL COMBINATION.

Key: $2Ra^2 \times 10^6$ in^3 (upper value) / K in^2/sec (lower value)

Free Fall Height = 0.08' — Maximum Penetration Region

	1" Depth	1.5" Depth	2" Depth	3" Depth	3.5" Depth
D32B8	136 / .760		171 / .383	207 / .169	
D16B8	140 / .955		159 / .477	180 / .213	
D8 B8	160 / .878		177 / .427	189 / .157	
D4 B8	144 / .885		165 / .470	175 / .150	
D0 B8	144 / .777		177 / .396	184 / .034	
D32B0	136 / .671		183 / .282	252 / .113	
D16B0	136 / .935		159 / .490	180 / .213	200 / .138
D8 B0	160 / .853		171 / .402	189 / .157	219 / .094
D4 B0	151 / .910		165 / .470	180 / .150	185 / .063
Do B0	144 / .960		153 / .502	153 / .188	155 / .075
Average	145 / .853		168 / .445	190 / .157	190 / .092

Free Fall Height = 0.10' — Minimum Penetration Region

	1" Depth	1.5" Depth	2" Depth	3" Depth	3.5" Depth
D32B8	152 / .508	176 / .252	307 / .094		
D16B8	136 / .382	169 / .176	285 / .082		
D8 B8	144 / .445	162 / .144	196 / .050		
D4 B8	144 / .470	148 / .194	159 / .044		
DC B8	128 / .396	141 / .200	154 / .013		
D32B0	160 / .382	176 / .245	233 / .138		
D16B0	144 / .452	162 / .264	215 / .144		
D8 B0	144 / .364	162 / .207	202 / .107		
D4 B0	144 / .508	148 / .238	184 / .132		
DO B0	152 / .415	162 / .282	172 / .157		
Average	145 / .446	161 / .226	211 / .094		

is found from a plotting of the data of Table 1 that a quadratic curve is reasonable in approximating the variation of circulation with depth of penetration. Also, it is found that for rings of maximum penetration, the rate of decrease of circulation at the initial depth is very nearly the same for all rings. The data giving the circulation and rate of change of circulation are much more consistent for the larger values of the circulation. By working with the average values of circulation for rings of maximum and minimum penetration as well as the individual ring data, a quadratic curve was constructed which represented the rings of maximum initial circulation very well. Then by shifting of the origin, it was found that rings with other initial values of circulation could be represented by sections of this same curve. The actual equation used to represent rings of maximum initial circulation, 0.950 in^2/sec, was chosen as:

$$K = 0.067x^2 - 0.530x + 0.950$$

In general, the translation to rings of any initial circulation can be made with the general equation for a given circulation K_0 at initial depth:

$$K = 0.067x^2 - [0.053 - (0.950 - K_0)(0.0225)]x + K_0$$

Use of this equation indicates that as K_0 decreases, the depth at which circulation vanishes decreases which is in agreement with observations. Vanishing of circulation is here used to indicate the region of critical depth. The critical depth will later be more precisely located with respect to time. The equation represents well the average circulations calculated in table 1 at various levels of penetration for each fall height.

Figure 48 represents the general circulation relationship from which one may obtain the expected critical depth for any given initial circulation. The curve on which A and C lie represents circulation. For any point on curve OD , say B , horizontal and vertical lines through that point will intersect the circulation curve at two points, say A and C . Then AB represents initial circulation, AC the relationship of circulation and penetration from initial depth, and BC the distance from the initial depth to critical depth.

Critical depths predicted by the circulation relationship for given values of initial circulation are shown in Figure 49 by the solid curve. Data points of initial circulation versus critical depth as observed experimentally are shown. Agreement was considered satisfactory.

5) Time of descent

The time from surface contact of the drop to the arrival of the ring at critical depth was found to be 4.0 seconds for all rings regardless of density or free fall distance involved. This was observed visually and by precise studies of multiple image photographs. Many observations of critical depth were made by timing the ring for 4.0 seconds. The computations of critical depth in the analytic part of this study were based on this time of 4.0 seconds for the ring to reach critical depth.

Figures 50 through 52 show the effect of a given variable on the rings. A plot of the penetration versus time to that penetration is made using the penetration to critical depth (p_c) and the time to critical depth $(t_0 = 4.0$ seconds) to non-dimensionalize the variables. The figures indicate that for a given percentage of total descent time to reach critical depth, the percentage of total depth attained is increased

$$K = 0.067 \, x^2 - 0.53 \, x + 0.95$$

$$b = 0.08 \, a^2 + 0.06 \, a$$
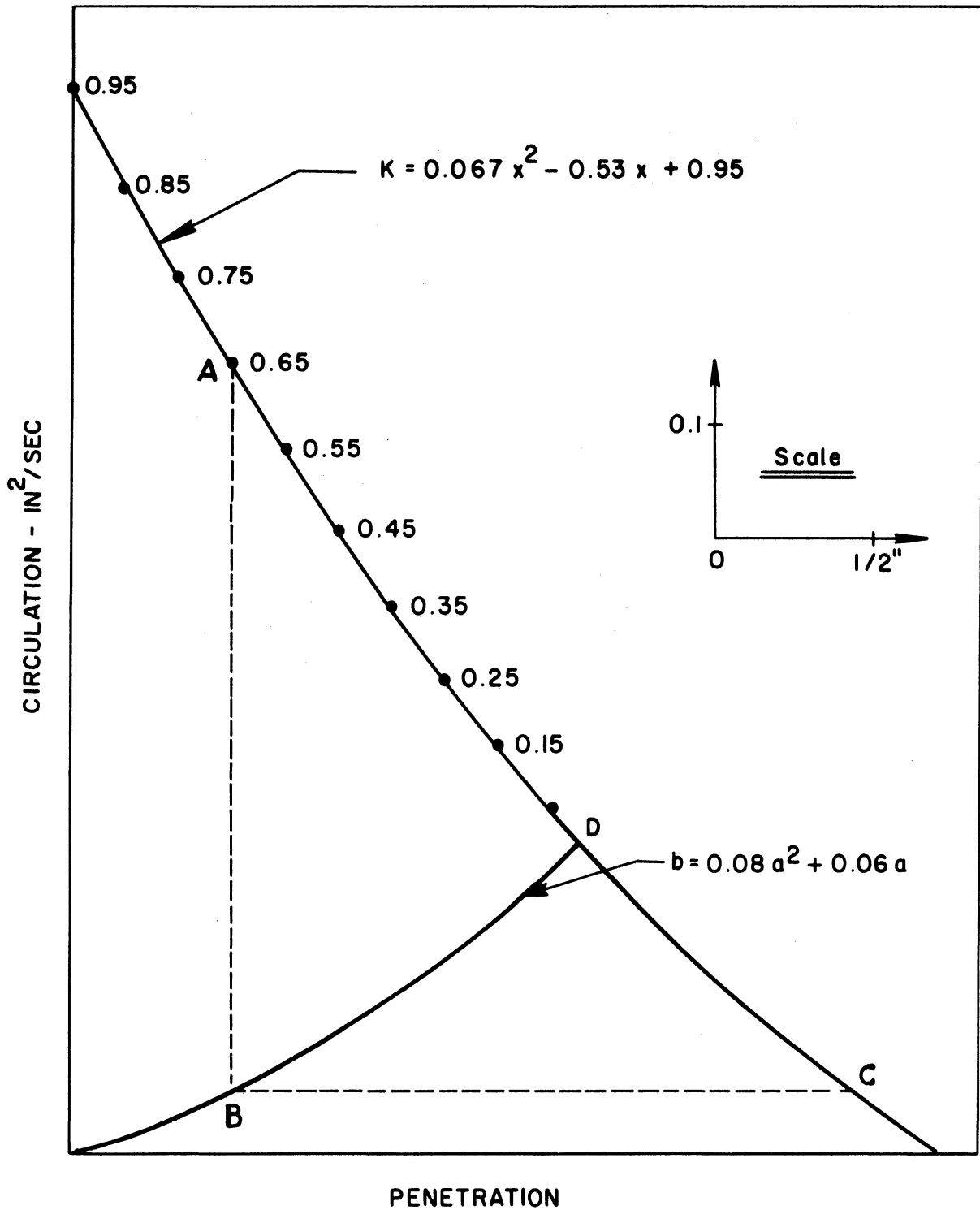
Figure 48. Initial Circulation and Expected Penetration
for Neutral Density Rings.
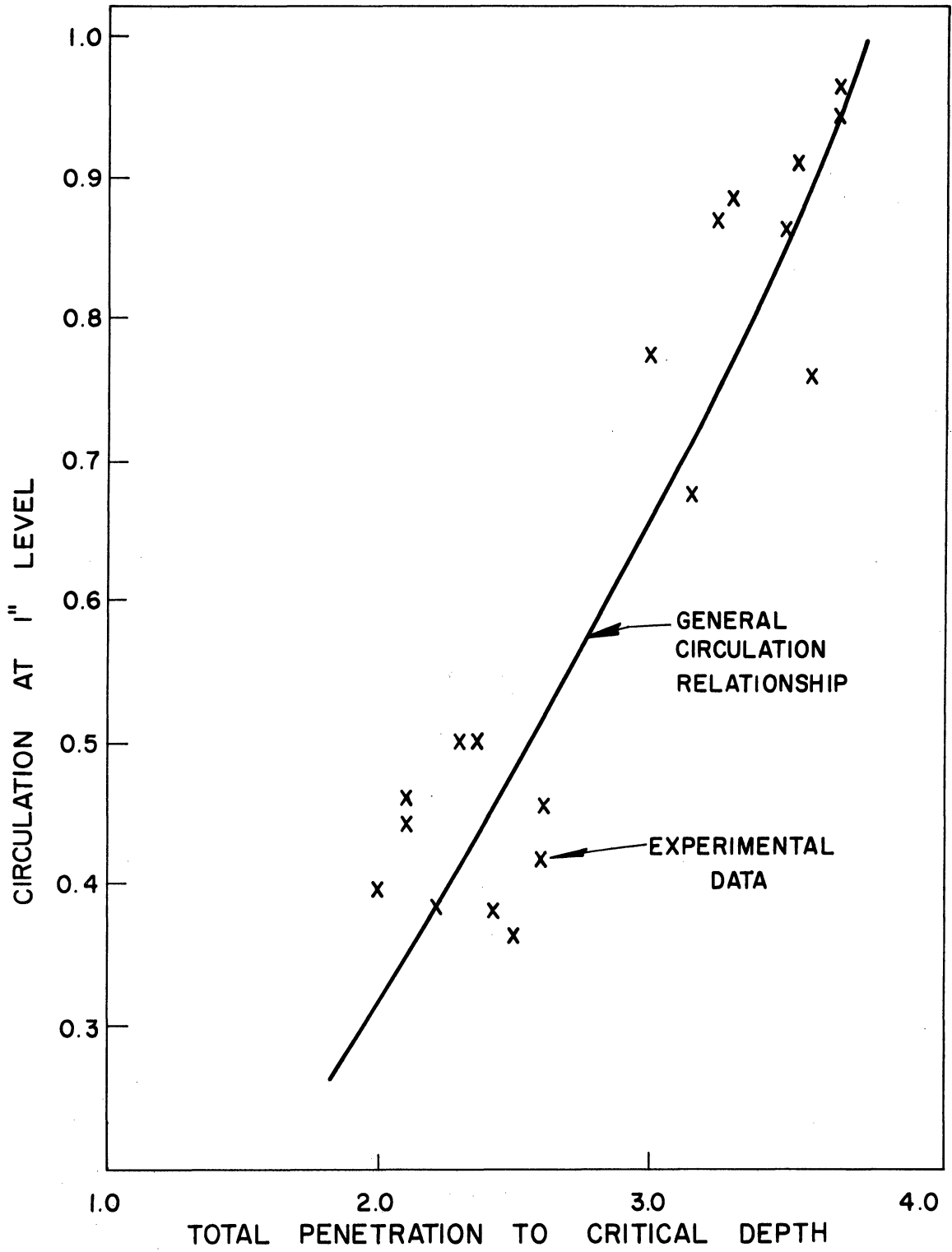
Figure 49.   Expected and Observed Penetration
to Critical Depth.

if the free fall is increased, if the base density is decreased, or if the drop density is decreased. Intermediate values of the variables fall between the bounding curves and are not shown.

6) Typical patterns

Figure 53 presents typical behavior patterns taken from multiple exposure photographs. Plate A shows a ring soon after surface penetration. The top image shows the nearly transformed ring and succeeding rings indicate uniform diameter and decreasing velocity. Images are 0.1 seconds apart. Plate B shows a Type I ring and the formation of secondary rings at critical depth. Images for Plates B through E are 0.5 seconds apart. Plate C shows a Type I ring with lesser density difference nearing critical depth. Note the more linear diameter relationship and the slower formation of secondary rings. Plate D shows a neutral density ring nearing critical depth while Plate E shows a Type III ring. In Plate E the overlapping of images shows that as the ring stops and secondary rings begin to form and rise. Plates F and G show secondary rings of Type I well after critical depth. Note that filaments still join the secondary rings.

4. Unusual Behavior Patterns

Two effects observed during the experimental study will be described and no explanation for their appearance will be attempted.

First, a small bubble appeared in the majority of the rings examined. It is first seen at the center of the core of the ring and remains at that position until the ring has slowed considerably as critical depth is approached. The bubble then slowly leaves the core center and begins to rise relative to the core center while moving toward the axis of the

ring along a path roughly 45° to 60° to the plane of the ring. As the

axis of the ring is neared, the path becomes vertical and the rate of

rise constant. A number of bubbles were observed and an average rate of

rise of 0.5 cm/sec determined. Lamb[8] gives the terminal velocity U

of a gas bubble of radius a ascending in water, with internal and gravity

effects considered, as $U = \rho g a^2/3\mu$. Application of the observed average

velocity of the bubbles indicates a bubble diameter of the order of 0.1 mm.

Visual observations are aided by the use of a magnifier or strong

sidelighting. Most multiple image photographs show the bubbles and indicate

a diameter of the order of size calculated. The pictures indicate that

the maximum depth which the bubbles attain is very nearly the critical

depth for the ring and might be used as a possible criterion for critical

depth. Although only one bubble was associated with most rings, multiple

bubbles were occassionally found. The small white dots in the lower

regions of Figure 53, Plates C and D are bubbles which have left the

core center.

A more detailed study of the bubble phenomenon would have to

be undertaken in order to establish any definite relationship with the

free fall height or the density difference of drop and base. Bubbles

were not always observed but no pattern of occurrence was evident.

The second unusual behavior pattern was found to be present in

nearly all drop-base combinations but was extremely limited in fall heights

producing it. Usually in the range of fall heights from 0.20' to 0.40'

one could, by trial and error, find a height from which the drop would hit

the surface, indent the surface, but remain as a sphere and "roll" about

on the surface for a split second before penetrating the surface. Such
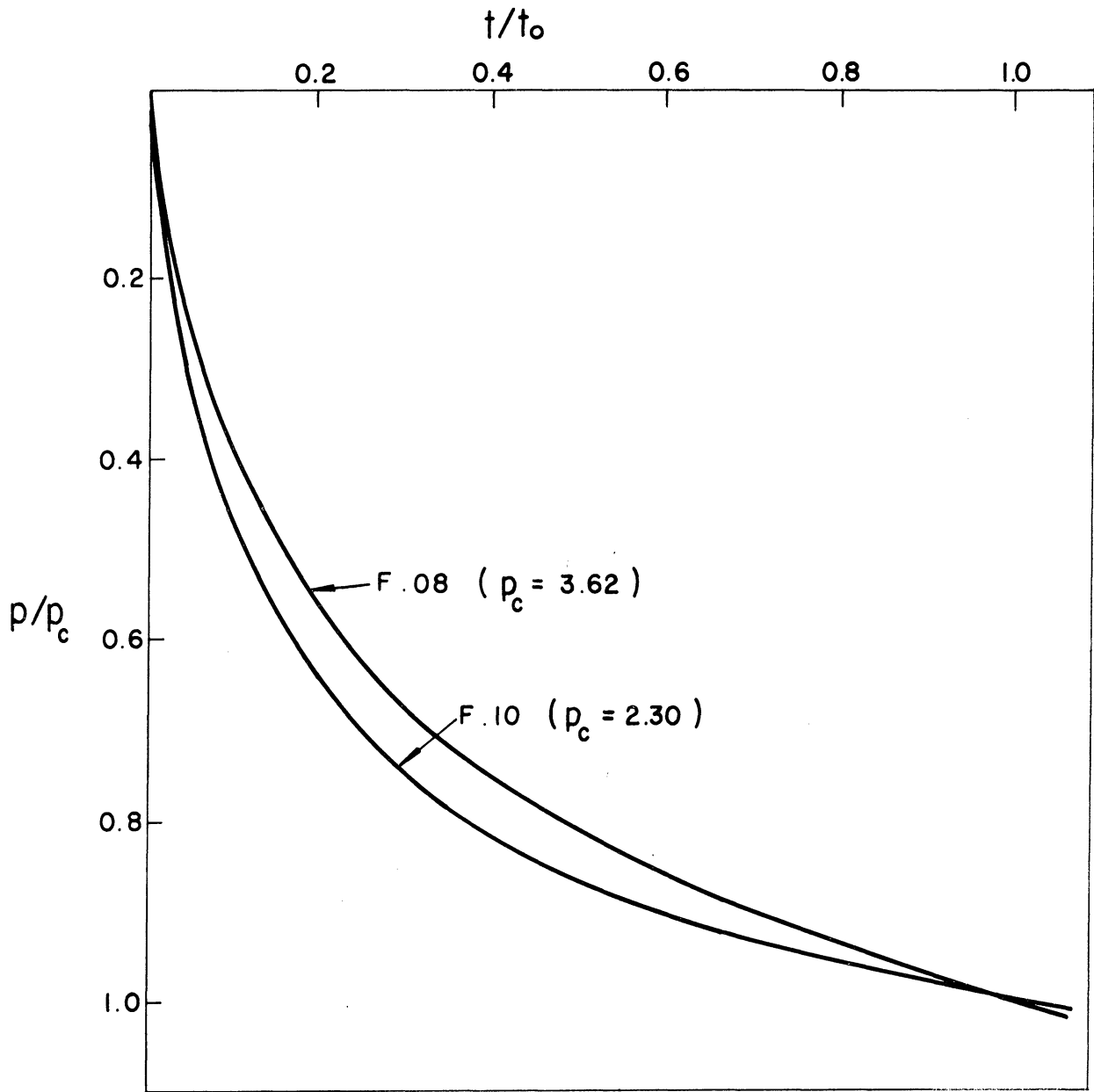
Figure 50. Effect of Free Fall Variation with D32B8.
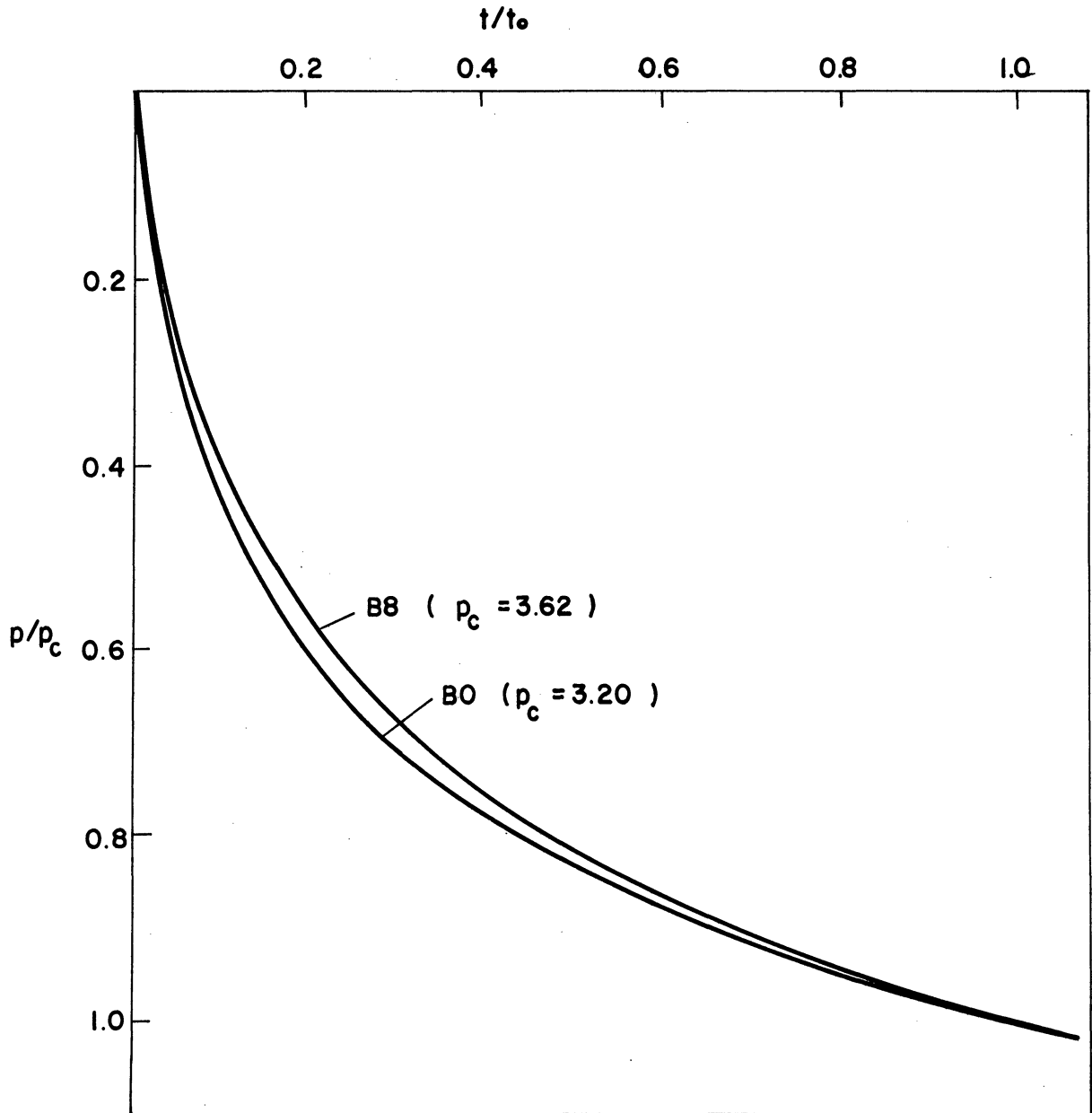
Figure 51. Effect of Base Variation with D32F.08.
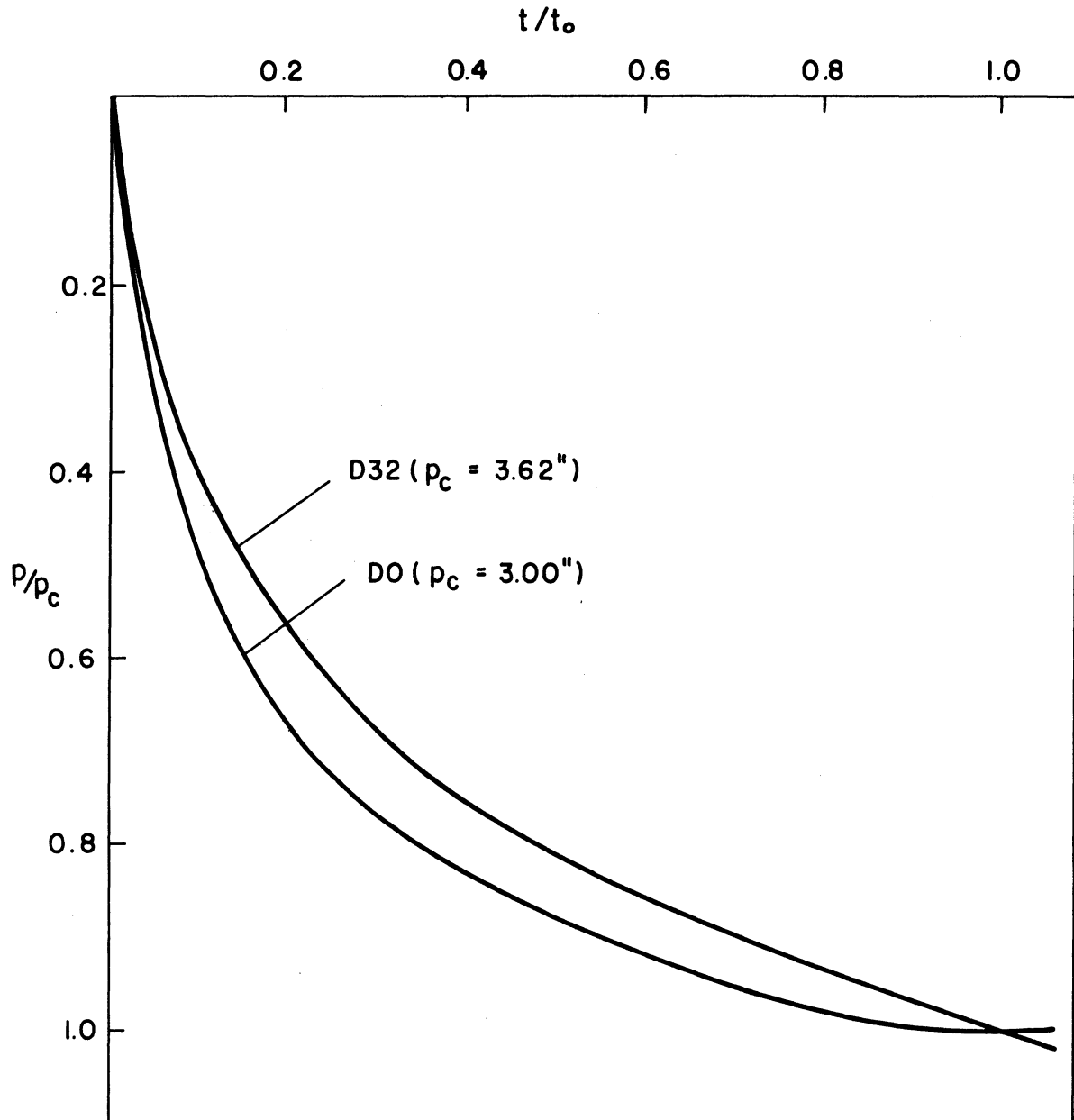
Figure 52.   Effect of Drop Variation with B8F.08.
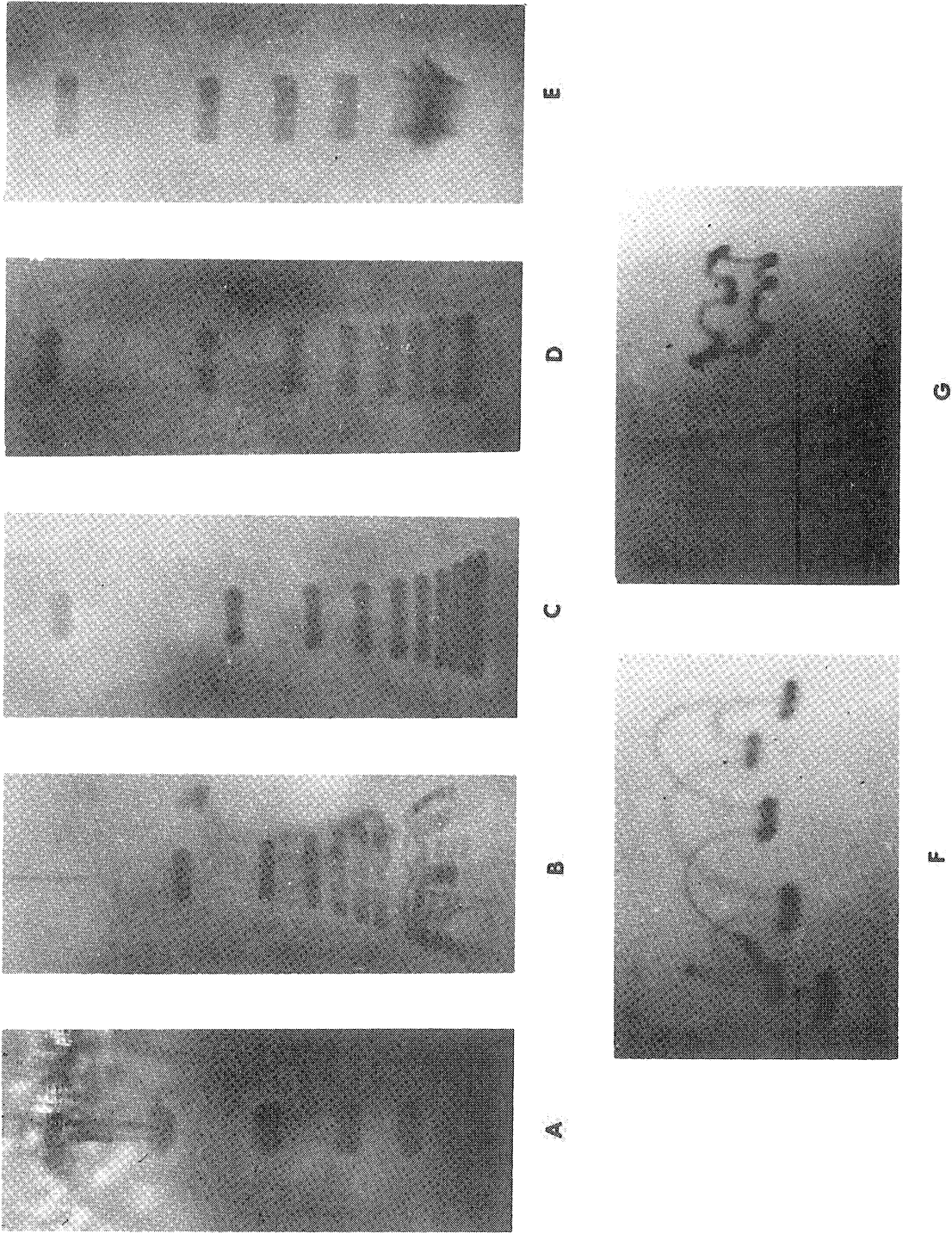
Figure 53. Ring Behavior as Exhibited by Multiple Exposure Film.

behavior was most prevalent in areas where drops had just recently pene-

trated and where there was a noticeable amount of dye residue at or near

the free surface indicating that surface tension forces are likely im-

portant. Reynolds[13] in a short note describing how such free standing

drops could be produced on the surface of a pond concluded that it be

essential that the surface of the water be free from scum and impurities

for the phenomena to occur. That free standing drops did not occur in

this study until several drops had fallen in rapid succession on a given

part of the surface seems to be in agreement with Reynolds' conclusion.

Figure 54 shows a series of frames from a high speed movie taken

at 2640 frames per second showing such an occurrence. The time during

which the drop stands on the surface is small but definite.

5. Range of Ring Formation.

The phenomena of vortex ring formation from falling drops is

limited to a very narrow range of free fall heights. If one begins with

the generating needle at a distance above the free surface which is less

than the diameter of the drop which can be formed, the drop will touch

the surface before reaching full size. At contact with the surface, the

drop merges with the base solution and leaves the needle. There is little

potential and kinetic energy associated with the drop but well formed

vortex rings form and descend to a critical level. This behavior is typi-

cal so long as the drop touches the surface before release with the depth

to the critical level increasing as the fall height increases.

For heights such that the drops barely release from the needle

before touching the surface, rings still form well and have good pene-

tration with the critical depth of a series of drops produced under
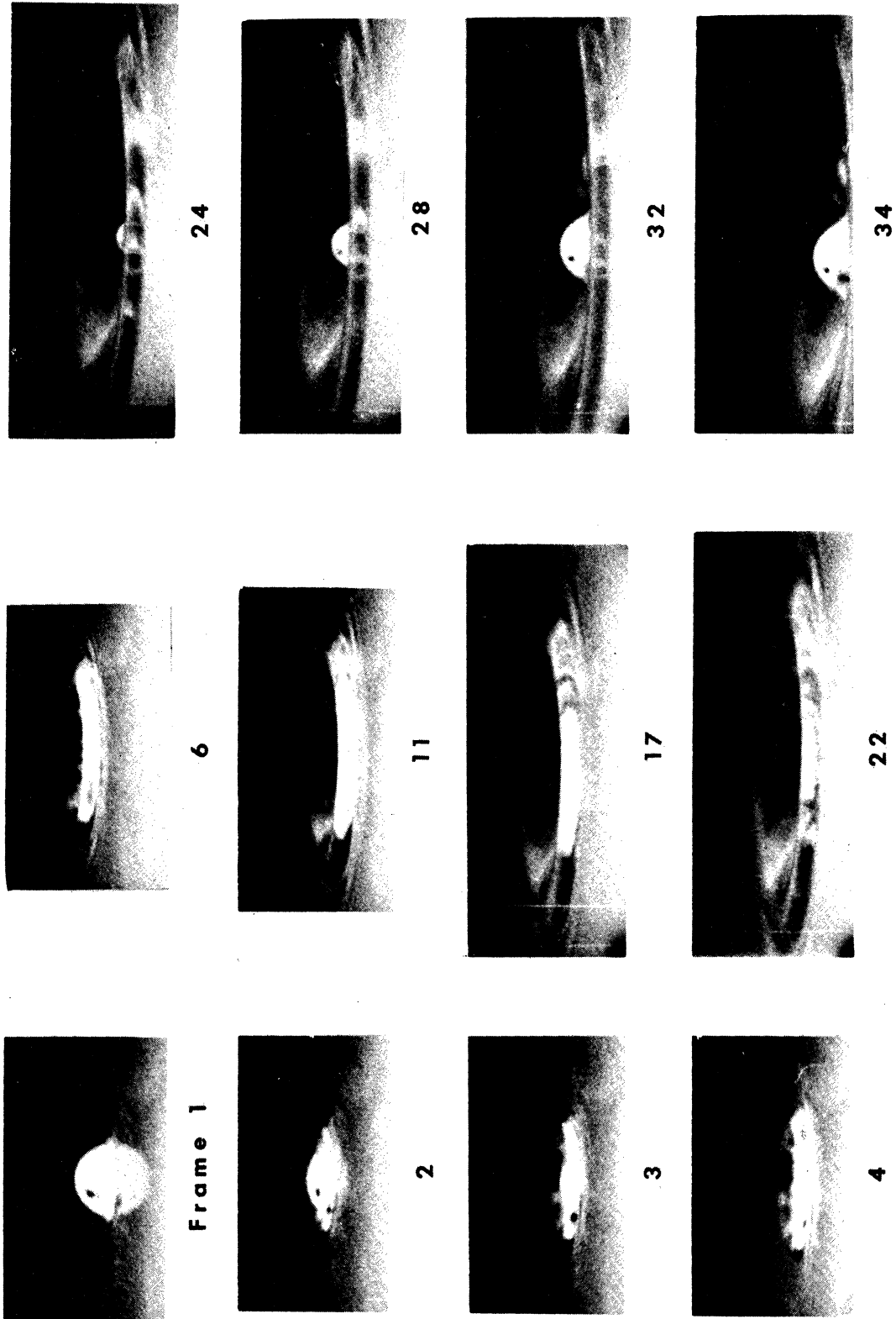
Figure 54. Surface Interaction of Drop from Free Fall of 0.205' as Viewed from Above.

identical conditions remaining quite uniform from drop to drop. However, as the fall distance increases, the resulting rings are erratic in behavior if indeed they form as rings at all. The number of abortions, or failures for rings to form, varies considerably in some cases for slight changes in generating conditions. Those rings which do form tend in many instances to have a wide range of penetrations to critical depth. At times the critical depths for a series of identical drops tend to concentrate at two levels as much as an inch apart. The drops are being subjected to strong oscillation effects, both of primary and secondary oscillation modes, during the first part of the free fall. Any slight variation in the shape of the drop coupled with the fact that the full period of the basic oscillation covers such a small free fall distance at the first stages of free fall combine to make the behavior of rings produced by small free fall quite sensitive. The experimental equipment and techniques used were not adequate to investigate the subtleties of this region. Hence the data presented in graphical form in section VI does not include free fall distances generally below about 0.040 or 0.045 feet. It was found that by the time this range of free fall heights had been reached, the rate of abortions diminished drastically and the critical depth observed for a series of identically produced rings was the same, within the allowable tolerance of $\pm$ 1/8". It should be noted that the end of the range of poorly defined or erratic rings in general came at or just past a region of minimum penetration to critical depth.

Once rings begin to form regularly and uniformly with increasing free fall heights, no further difficulties of the types described above occur until a free fall height of about 0.15' or more is reached.

A trend toward an increasing number of abortions develops, at times rather slowly, with increase in the free fall of the drop. Finally the rate of abortions becomes so high that few rings form, or rings produced by a different surface mechanism appear. Such rings are sometimes formed by a small drop which forms at the top of the spout which rebounds from the surface when free fall distances are large. For this study, the maximum fall distance used to produce rings for data was a matter of discretion and judgement for each individual case. No definite abortion rate was determined beyond which data were no longer taken but in general if more than half of the drops aborted no further information was recorded. As the upper limit of ring formation heights was approached, two characteristic features appeared. First, the penetration although varying sinusoidally tended to decrease with increasing free fall. Secondly, the turbulence observed near the rings increased and more residue from the drop was present now the surface.

For the No. 20 needle, it was found that the range of production of rings was from about 0.040' to from 0.15 to 0.21'. No effort was made to try to determine the reason for the range of the upper limit.

Figure 55 shows the surface interaction for a drop from a free fall distance of 0.205 feet. Under these conditions, abortions resulted in each instance. Two features are evident in the series which are different from the cases where rings form. First, the drop at contact seems to form a ring on top of the surface rather than causing an immediate depression in the surface. The center of the dyed mass disappears in the depression which forms soon but, quite different from the case where rings form, rises again sharply in the center. This node which rises is clearly

Frame 1   16   37

3   19   40

6   24   45

9   28   47

12   33   50
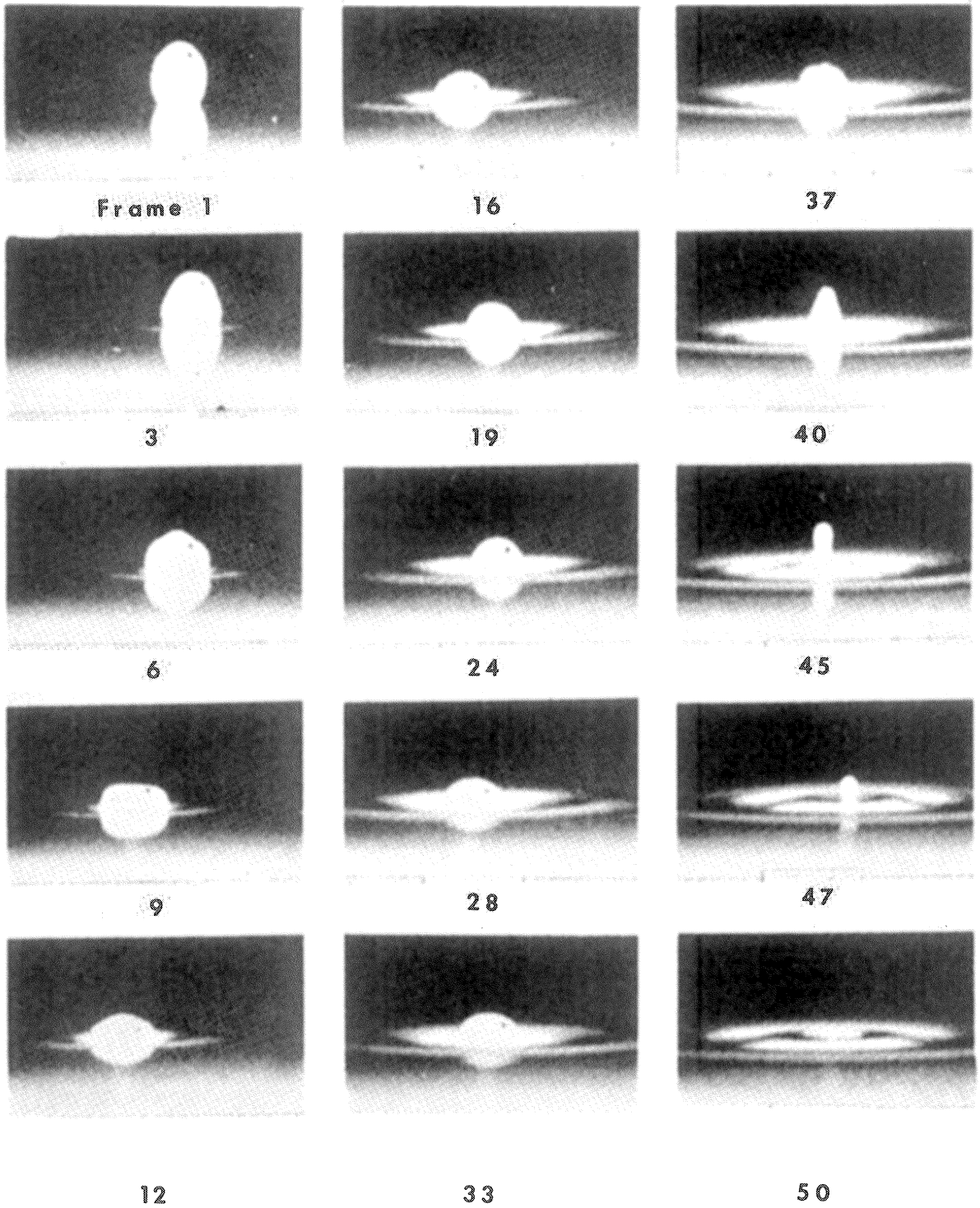
Figure 55.   Behavior of Drop which Remains Temporarily on Free Surface.

observed to be of dyed fluid and is a transition form to the sharp upward shaft with a spherical tip which is commonly shown in pictures of drops from higher distances. Increasing the fall height in the study produced such shafts for certain fall heights. However, the oscillation effects of the drop were evidently sufficient to cause the formation of a rounded tip or even a detached sphere to occur periodically as the fall height was increased.

It was under conditions similar to these that Reynolds[13] made his observations concerning the production of a multiplicity of vortex rings by drops of rain. Such a multiplicity was observed during this study with rings resulting from the original impact and then from the spout as it descended. As such rings were not of the same basic type as those described in the study, they were not included in any computations.

D. Measurements and Calibrations

As in any experimental study there was a need to control certain variables and provide reasonable satisfaction that this was actually accomplished. In addition the measurement of the desired properties of behavior as well as the possible error associated with these measurements must be considered.

Several measurements of length are involved in this study. Some of the measurements were obtained by photographic techniques and are quite precise. Other measurements taken visually were considered correct within an eighth of an inch of the recorded value. The various measurements and method of recording are discussed separately.

1. __Drop size__:

Obviously the size of the needle used to produce the drops is of prime importance in determining the size of drops. The bulk of the study was done with a standard Yale No. 20 hypodermic needle with outside diameter of 0.035" and inside diameter 0.025". Some additional isolated data were taken from rings formed by using a No. 22 and No. 15 needle to indicate what trends might be expected by such a change. Also a standard 1/4" copper tube was used as generator for a few observations.

The diameter of the drops generated was calculated by dropping a counted number of drops into a 5 milliliter graduate. For uniformity the rate of formation was maintained at several seconds between drops. The various solutions used in the study when used with a given needle produced drops of essentially the same size. From this fact it was assumed that the surface tension of the solutions used did not vary enough to be important. A deliberate lowering of the surface tension of the base solution was a part of the study but no use of drops of lower surface tension was attempted. It must be remembered that the maximum difference in salt concentration for the entire study was about 1.5 percent; that is, the density variation was quite small.

For the No. 20 needle the drop diameter was found to be 0.308 centimeters or approximately one-eighth inch. See Appendix __B__ for drop sizes from other generating needles.

2. __Fall height__:

As noted in the description of the apparatus, the fall height was maintained as uniform as possible for all sections of the tank surface. The vernier to which the needle was attached was readable to 0.001' but

the data from which the pentration patterns were plotted were for the most

part obtained by using 0.005' increments of fall height. However, in some

instances where there were regions of ring abortion or rapid change in pene-

tration smaller increments were used for more accurate plotting.

3. Penetration:

The penetration of the rings was by far the most difficult

measurement to obtain. Multiple exposure photographs provided very accurate

measurements pertaining to a portion of the descent of a single ring.

However, in order to obtain a complete record of a given set of conditions,

it was necessary to patch together information from two or three films.

This patching technique was quite satisfactory as overlapping regions of

the films could be compared and rejections made if the ring did not behave

as expected from visual observation. Using the film technique, the pene-

tration was easily measured within 0.01" of the actual.

Due to the large number of data points necessary for plotting the

penetration curves the photographic technique was used only for selected

combinations of drop solution, base solution and fall height. The bulk of

the data points were obtained by visually noting the depth of the critical

penetration. This was difficult as a matter of judgement as to when this

depth was reached was necessary. Early results were based strictly on

the beginning of formations of the secondary rings or the reaching of

what was considered negligible velocity. While the former criteria in-

volved a change of form the latter (i.e. negligible velocity) had no

such guidepoint and was much more difficult. Later in the study, after

composite films had been studied, it was found that the critical depth

occurred at what could be considered a constant time after the surface

interaction.

The presence of internal currents in the base solution was a constant source of concern. While making observations, the aftereffect of the currents was constantly checked and a mental note made of the sections of the tank where upward or downward currents were present. Strong currents can increase or decrease the penetration to the critical depth by as much as a half inch. For this reason regions of negligible current action were sought and a number of drops used to determine a penetration. Currents were observed even after the base solution had been allowed to set undisturbed for three days or more. Although never completely absent they fortunately could be detected and avoided.

4. Ring dimensions:

Visual observations were not adequate to obtain ring dimensions. The multiple exposure films were, on the other hand, quite suitable for obtaining very precise measurements. When preparing to film a ring, the camera was focused using the ground glass back in such a way that the image was full size. The films were than measured directly using either a comparator which gave measurements to 0.005" or an engineering scale graduated in intervals of 0.02". The overall diameter of the rings was judged to be obtainable with a tolerance of 0.005" in most cases. Although efforts were made to produce films of uniform density, this was not always accomplished and there may have been some discrepancy due to contrast variations. However, within one film the data obtained could be compared without regard to contrast problems, if indeed they are serious.

While the overall diameter of the rings was rather easily obtained from films, the measurements of core diameter were very difficult.

The core diamteres were first of all much smaller than the overall diameters so that a small error in measurement represented a large percentage change. The films did not always define clearly the top and bottom limits of the rings and average values were used based on a number of rings of different combinations of drop and base solutions. For the No. 20 needle there was no noticeable deviation from an average core diameter of 0.07" at one inch below the free surface for any combination used. For all rings the core diameter was found to be represented by an average value of 0.06" at critical depth. The variation between these two values was taken to be linear. The calculations of the values of Ra^2 were made on the basis of this variation of core diameter.

5. Velocity:

All velocities were obtained from the multiple exposure films and are therefore average velocities between successive images. The average velocity from the surface to the first image was not available in this same manner as the time involved was unknown. For these cases, extrapolation produced the values shown.

6. Salinity:

Control of the salinity of the solutions used was exercised by mixing large batches of stock solution which was then bottled and stored until needed. Dilution by volume with ordinary tap water provided the desired salinity.

7. Temperature Effects:

Although the possible effect of temperature on the solutions was recognized, it was not felt that the overall effect would materially

affect the results being sought. The ambient temperature of the surround-
ings were certain to change during the period of several days during
which a particular base solutions was kept for use and hence the solution
temperatures would be changed. To attempt a control of temperature would
have been impractical. However, in order that the base and drop solutions
be at approximately the same temperature the base was allowed to settle in
the same surroundings as the drop solutions, which were pre-mixed and
stored.

E. Effects of Surface Tension

The effect of surface tension was investigated in two ways. The
various drop solutions were checked for the size drops produced by the
same needle. (See Appendix B.) Since all solutions produced drops of es-
sentially the same size, it was concluded that surface tension within the
range of solutions of the study could be considered constant.

A second investigation was made using a base of B8 solution.
With normal surface tension, penetration to critical depth was checked
for the full range of ring formation using drop solutions D16, D8, and D0.
A wetting agent (here one cc. of Kodak Photo-Flo) was added to the base
and the penetrations to critical depth checked for the same three drop
solutions.

Figure 56 shows both sets of results using the DOB8 combination.
The dotted curve represents penetration with reduced surface tension while
the solid curve shows penetration with normal surface tension.

Three effects are evident. First, the penetration to critical
depth is reduced at all free fall heights at reduced surface tension.
Second, the tendency for drops to abort is very pronounced, especially

near regions of minimum penetration. This tendency to abort is present in the case of normal surface tension but not to the same degree. Thirdly, with reduced surface tension, the penetration curves tend to shift slightly to the left. The shift shown in the figure was the most serious of the three curves obtained.

It is concluded, therefore, that surface tension due to density differences of the solutions used was not a factor in determining the size of drops but that a change in surface tension can affect the formation and behavior of rings.
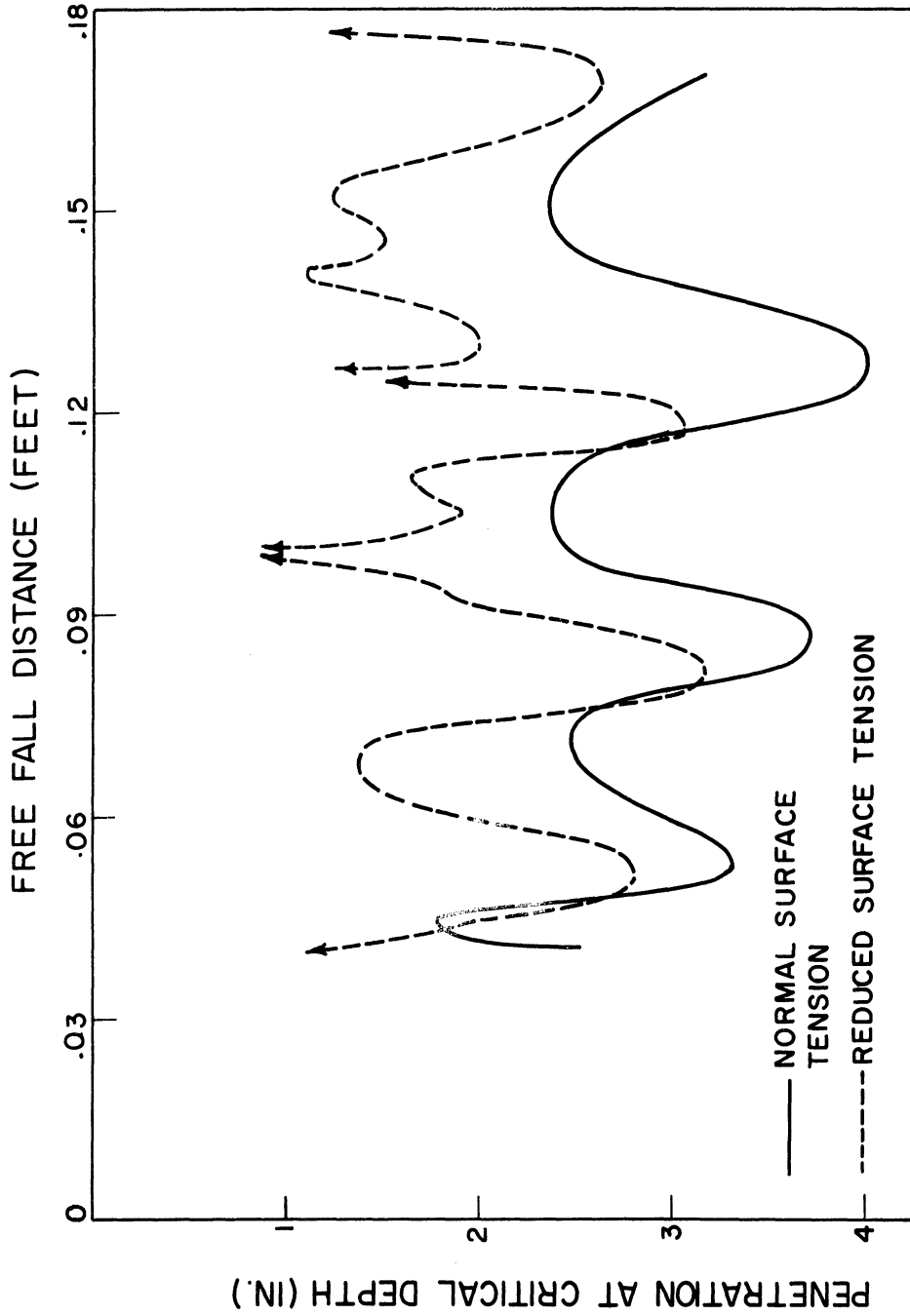
Figure 56. Variation of Penetration with Free Fall Distance using DOB8 for Normal and Reduced Surface Tension.

VI. ANALYTIC DEVELOPMENT

A. The Model Defined

The experimental results of this study indicate that a vortex ring model constructed to fit the conditions observed must possess the following characteristics.

1. The transformation to the vortex ring form is complete for all rings at an <u>initial depth</u> which is the same for all rings.

2. The size of the ring after transformation, i.e. at initial depth, is considered the same for all drops from a given needle.

3. The volume of the ring (as indicated by the dyed region) remains essentially constant during the whole of its descent and is considered to be the vorticity containing region of the ring.

4. The circulation associated with a ring decreases during descent. This should be related to the distance of penetration below initial depth in some rational way.

5. The rate of increase of diameter of Type I rings is greater than that for Type II rings while Type III rings have the least enlargement of diameter during descent.

Based on these characteristics, the model chosen consists of a torus of rotational fluid which descends into a base fluid. As the vortex ring descends into the base, there moves along with the ring an ellipsoidal volume of base fluid which surrounds the ring. (See Lamb[8]). The shape of this associated body is dependent on the relative diameter and core dimension of the ring and increases in volume as the ring descends. The increase in volume may be due to either entrainment of base

fluid by viscous effects or in a non-viscous manner by pressure distributions. Turner[18] attributes the growth of the volume associated with the rings of his study to non-viscous entrainment only. During the part of the descent for which the velocity is significantly large, such entrainment is probably dominant due to the intimate relationship of pressure and velocity. As the velocity decreases, viscous effects become more important and their role in ring enlargement and entrainment must be accounted for in a complete analysis.

The analysis of the behavior of the model is begun at an initial depth of penetration below the surface at which level the ring form is considered to be complete. At this initial depth the ring is considered to have a radius R and a core radius a . Both these dimensions change during descent but due to the assumption of a constant volume vorticity region the product Ra^2 remains constant.

B. Development of Theory and Methods and Criteria of Computation

A salient feature of the model chosen is the decay of circulation with increasing penetration. This is a point of major departure from the studies of Turner of the motion of vortex rings in uniform surroundings which were made under the assumption of constant circulation.

From ideal fluid vortex theory, it is known that momentum, P , of a vortex ring is given by the relationship:[8]

$$P = \pi\rho KR^2 \qquad (1)$$

where K is circulation and R the ring radius. The three variables P , R and K are all functions of time as well as depth of penetration.

Starting with the above relationship and the model chosen, a development of theory will be presented which will predict ring behavior (mainly, penetration below initial depth as it relates to ring diameter, ring velocity and time of descent) for various free fall heights of the drop from which the rings are formed and for various combinations of drop and base solutions.

Differentiation of Equation 1 with respect to time gives:

$$\frac{dP}{dt} = \pi\rho \left[2KR \frac{dR}{dt} + R^2 \frac{dK}{dt} \right] \qquad (2)$$

There will be present during descent a force F_m due to the motion of the ring and its associated mass. This could be thought of as being a drag force. In addition, there will be present a force F_b due to buoyancy when the densities of the drop and base solutions differ. Therefore:

$$\frac{dP}{dt} = \text{Forces acting on the body} = -F_m - F_b \qquad (3)$$

The buoyant force is given by: $F_b = (\Delta\rho)\Psi g \qquad (4)$

where $\Delta\rho$ is the density difference of the base and drop solutions, $(\rho_\beta - \rho_o)$ and Ψ is the volume of the original drop. The force due to the motion of the ring, F_m, is a combination of effects of acceleration and viscosity. As a first step it seems reasonable to assume this force to be of the form:

$$F = C_1 \rho V^2 A/2$$

with C_1 dimensionless and A the frontal area of the moving body.

The area A may be related to the ring radius by $\pi(C_2R)^2$ with C_2 a factor relating ring radius to that of the body of moving fluid. Hence, the force due to the motion of the ring may be expressed as:

$$F_m = \pi\rho C_m(VR)^2 \tag{5}$$

with $C_m = \dfrac{C_1 C_2^2}{2}$.

Equating relationships for dP/dt in Equations 2 and 3, and using Equations 4 and 5:

$$\pi\rho\left[2KR\frac{dR}{dt} + R^2\frac{dK}{dt}\right] = -\pi\rho C_m(VR)^2 - (\Delta\rho)Vg$$

Since $dR/dt = (dR/dx)(dx/dt) = V\,dR/dx$, and $dK/dt = (dK/dx)(dx/dt) = V\,dK/dx$, this equation may be written, when divided through by $\pi\rho RV$:

$$2K\frac{dR}{dx} + R\frac{dK}{dx} = -C_m(VR) - \frac{(\Delta\rho/\rho)gV}{\pi(VR)} \tag{6}$$

From vortex theory: [8]

$$V = \frac{K}{4\pi R}\left(\ln\frac{8R}{a} - \frac{1}{4}\right)$$

or

$$VR = \frac{K}{4\pi}\left(\ln\frac{8R}{a} - \frac{1}{4}\right)$$

Substitution into Equation 6 and division by $2K$ gives:

$$\frac{dR}{dx} + \frac{R}{2K}\frac{dK}{dx} = -C_m\frac{1}{8\pi}\left(\ln\frac{8R}{a} - \frac{1}{4}\right) - \frac{2(\Delta\rho/\rho)gV}{K^2\left(\ln\frac{8R}{a} - \frac{1}{4}\right)} \tag{7}$$

Equation 7 is a general relationship between the dimensions of the vortex ring model and the circulation of the ring.

In order to check the validity of assumptions and theory used to obtain Equation 7, the experimental data of this study will be applied.

The assumption of the region of vorticity being constant in volume implies that the product Ra^2 is constant. The initial conditions, at the initial depth taken one inch below the free surface, give values of Ra^2 shown in Table I with an average value $Ra^2 = 72 \times 10^{-6}$ in^3. Thus the quantity in the terms on the right hand side of Equation 7 becomes:

$$\ln 8R/a - 1/4 = \ln 8 + \ln R - \ln a - 1/4$$
$$= \ln 8 - 1/4 + \ln R - \ln(72 \times 10^{-6}/R)1/2$$
$$= 3/2 \ln R + 6.60$$

Substitution into Equation 7 gives:

$$\frac{dR}{dx} + \frac{R}{2K}\frac{dK}{dx} = - C_m \frac{3}{16\pi} (\ln R + 4.4) - \left(\frac{4gV}{3}\right) \frac{(\Delta\rho/\rho)}{K^2(\ln R + 4.4)}$$

For the No. 20 needle used, $\frac{4gV}{3} = 0.469$ in^4/sec^2, which upon substitution gives:

$$\underbrace{\frac{dR}{dx} + \frac{R}{2K}\frac{dK}{dx} = - \frac{3C_m(\ln R + 4.4)}{16\pi}}_{\text{Neutral Density Equation}} \underbrace{- 0.469 \frac{(\Delta\rho/\rho)}{K^2(\ln R + 4.4)}}_{\text{Buoyancy Term}} \qquad (8)$$

Equation 8 will be considered in two ways. First, for Type II rings (neutral density) the final term of Equation 8 is zero and the equation designated above as "Neutral Density Equation" applies. For Type I and Type III rings, a density difference is present and the full Equation 8 including the buoyancy term must be used.

Consider first the neutral density equation. At the initial depth, one inch below the surface, let $x = 0$ and measure penetration from this depth. The radius of the ring, R, is known and the variation

of radius with penetration is available from negatives. The two trouble-some variables of the equation are the motion coefficient, C_m , and the circulation K as a function of x . The motion coefficients cannot be calculated directly from data of the experiments. However, the relationship of circulation to ring velocity and ring dimensions does allow for calculation of circulation at given values of x . Table I is constructed of selected values of circulation. If now an empirical rela-tionship of circulation and penetration was found based on experimental data, the remaining variable of the neutral density equation, namely, C_m , can be found. By varying x until the circulation vanished, i.e. the ring stops, a set of values of C_m can be calculated. Calculation of the Reynolds number corresponding to each value of C_m gives sets of values from which a curve may be plotted.

Each term of the neutral density equation is non-dimensional. The term on the right hand side, involving C_m , is the term arising from the motion of the body of fluid connected with the ring. Theory con-nected with the motion of a body through a fluid shows that coefficients relating drag to the properties of the fluid and body are functions of the Reynolds number. In the present study, the physical quantities of importance which relate to drag on the ring are considered to be ρ , $\Delta\rho$, a , R , V , K and μ if one neglects possible surface tension effects. From these four independent dimensionless quantities:

$$\frac{\Delta\rho}{\rho} \; , \; \frac{R}{a} \; , \; \frac{K}{VR} \; , \; \frac{\rho VR}{\mu}$$

may be formed. Of these, R/a is related to K/VR by the circulation relationship previously given and $\Delta\rho/\rho$ is small and considered to enter

significantly only into the term involving the buoyant force. A non-dimensional force must depend, therefore, on K/VR and the Reynolds number $\rho VR/\mu$:

$$\frac{F_m}{\rho V^2 R^2} = C_m = f(\frac{K}{VR} , \frac{\rho VR}{\mu})$$

The experimental results indicate that there is little dependence on the value of K/VR . Hence the motion coefficients C_m will be considered as functions of the Reynolds numbers. Assuming that this relationship is valid for all rings of the study, the way is paved for the solution of the full Equation 8 including the buoyancy term.

In the solution of Equation 8, a value of $(\Delta\rho/\rho)$ is assumed corresponding to a specific combination of drop and base solutions. The empirical relationship of circulation and penetration is known, hence K and dK/dx are available. Observations indicate that for all rings of this study, initial conditions of $R = 0.05"$ at $x = 0$ may be assumed as being representative. Then from the circulation, the initial value of the product VR may be calculated and from this the Reynolds number at initial depth. Once the corresponding motion coefficient C_m at initial depth is calculated, Equation 8 may be solved for dR/dx at initial depth. Incrementing x and using the value of dR/dx just obtained will approximate the value of R at the new depth. Known and unknown quantities at this new depth are the same as those at initial depth and the process of calculation of a DR/dx at this depth is repeated. Also, the time interval between increments of depth may be approximated and total time of descent accumulated. This procedure can be repeated until the velocity, and hence K , vanishes. The result of this series of

calculations is, for a given initial ring radius and initial circulation, that one can predict the variation, with penetration, of ring diameter, ring velocity and time of descent.

The stability of the core of a ring is of interest. As the ring descends, the fluid is first observed rotating around a core of constant diameter. If the drop fluid is heavier than the base fluid, as the ring slows down a series of nodes begins to form around the circumference of the overall ring and may oscillate about some mean point. This is a first instability and results in several nodes which are only temporarily stable since these nodes soon move away from the axis of the ring, continue their descent, and form secondary rings. This is a type of instability found in the breakdown of a ring.

Taylor[16] showed that two fluids of different densities when accelerated in a direction perpendicular to their interface have a surface which is stable or unstable according to whether the acceleration is directed from the heavier to the lighter fluid or vice versa.

Applying this criterion, if the core is of light fluid (drop of less density than base) the situation is inherently stable with respect to centrifugal effects as heavier fluid is outside lighter fluid. However, if the core fluid is of greater density than the base, the situation is unstable and centrifugal effects would cause the core fluid to move outward. In this study it was observed that the core for all drop-base density combinations remained stable until the nodal instability close to critical depth.

The effects of surface tension were not included in Taylor's analysis but are important in the present case. In order to clarify

the discussion, three cases will again be considered as determined by the relative densities of drop and base.

For the case of the drop density greater than the base density, the Taylor instability is expected. The appearance of instability will be influenced by surface tension effects which are present. The observation is that an instability, probably of the Taylor type, does occur as disturbances on the ring produce nodes. The larger the density difference, the more abruptly the instability is manifest.

For neutral density, there is no possibility of instability of the Taylor type. No rings would be expected to form unless from some secondary influence. The observations made of rings of neutral density revealed that no secondary rings were formed.

If the drop is less dense than the base, the core is of light material and no Taylor instability exists. However, surface tension effects may be present. The observed behavior of rings of this type is for secondary rings to form at critical depth and rise toward the surface. These rings are considered to be the result of surface tension effects.

A possible explanation of the formation of nodes in the case of the drop density being greater than the base density is now presented. It is assumed that the major influences present are those due to the density difference and surface tension. As a ring descends and any disturbance is found on the interface of the ring with the base, the disturbance will grow according to the Taylor criterion. However, the surface tension effects may be large enough to balance or at least delay the growth of the instability. The centrifugal forces causing the Taylor instability

are large in the early stages of penetration and decrease as the ring

descends and the velocity decreases. The surface tension induces a

surface constraint, the magnitude of which will depend on the curvature

of the surface and the surface energy between the two fluids. As the

ring descends, the core diameter decreases and the surface tension

effects increase due to the increased curvature. Disturbances such as

those resulting from the Taylor instability cause the core diameter to

decrease in various regions around the circumference of the ring. These

constrictions are accentuated by the increased surface tension effects

due to increased curvature in the region. The result is the formation

of nodes similar to those found in the breakdown of a free falling

stream into a series of drops.

From these nodes the secondary rings eventually develop. The

dyed region connecting the nodes becomes very small but remains attached

between adjacent nodes as the nodes assume a ring form. The mechanism

for this transformation is not clear.

The rings of this study were found to remain coherent for a

considerable penetration depth for all density differences, even those

in which the drop density exceeded that of the base. The failure to

break up sooner may be due to either the stabilizing effects which the

surface tension has or to the fact that the total life of the rings

(about four seconds in this study) is less than the time needed for the

growth of any disturbance to become sufficiently large to cause break

up of the ring. Morton and Turner both noted that rings of low density

difference, although in their case the core was lighter than the base,

were subject to instabilities leading to the break up of the ring. How-

ever, the time to break up was larger.

VII. DISCUSSION

A. Comparison with Experimental Results

Once the model has been chosen and theory developed on the basis of observations and assumptions, the development must be shown to be compatible with data of the experiments. The procedure outlined in the previous section for the solution of the general Equation 8 was followed using data points from Figures 5 through 24.

The variation of radius with penetration for the DOBOF.08 combination was chosen as best representing a typical ring of neutral density. This ring does have R=0.05" at initial depth, x=0, and varies linearly with penetration for the first part of the descent. A program in MAD language was written to calculate the motion coefficients and corresponding Reynolds numbers for penetrations from initial depth to critical depth by increments of 0.1". The derivatives, dR/dx, of the neutral density equation were found by a method of passing a curve through four consecutive points and obtaining the derivative at the desired point. Values of R and x were known throughout. The circulation was given by the relationship developed before:

$$K=0.067x^2-0.053x+0.950$$

From these values, the values of C_m and Reynolds number were calculated for each x value until the circulation vanished. This set of values was stored for use in determining motion coefficients for all subsequent computations.

As a check on the values of C_m and Reynolds number from the above calculations, the relationship of radius and penetration for the case DOBOF.10 was introduced with the corresponding circulation equation:

$$K=0.067x^2-0.410x+0.450$$

and the values of C_m and Reynolds numbers calculated for this case. A plot of values for the two cases, nearly extreme values for the experiments, is shown in Figure 57. Agreement of results increases with decreasing Reynolds numbers (i.e. with increasing penetration and consequent decreasing velocity). The motion coefficient is related to the total drag on the ring and associated body, this drag being due to a combination of acceleration and viscous effects. Calculations show that for the same Reynolds number, the accelerations in the case of the lesser initial circulation are in order of magnitude of twice those for the maximum initial circulation. The contribution of acceleration effects to the value of C_m being different, it is reasonable that differences be found. As acceleration effects vanish in both cases, the values of C_m approach a common value.

The values of C_m and Reynolds numbers obtained from the maximum circulation were used for all rings that were formed in such a way as to give maximum penetration (Cf. Figure 58). When buoyancy affected the motion there could have been an effect on C_m due to the slightly different deceleration pattern. This effect was considered to be minor and was not corrected for in the calculations. Values of C_m between the two extremes shown in Figure 57 could be used in a general situation, using the value of the local accelerations as a guide in selecting the values. Average accelerations are shown at various sections of the curves of Figure 57.

With the motion coefficients available, the full Equation 8 was solved for various density differences and with various values of initial circulation. The program produced the values of the ring
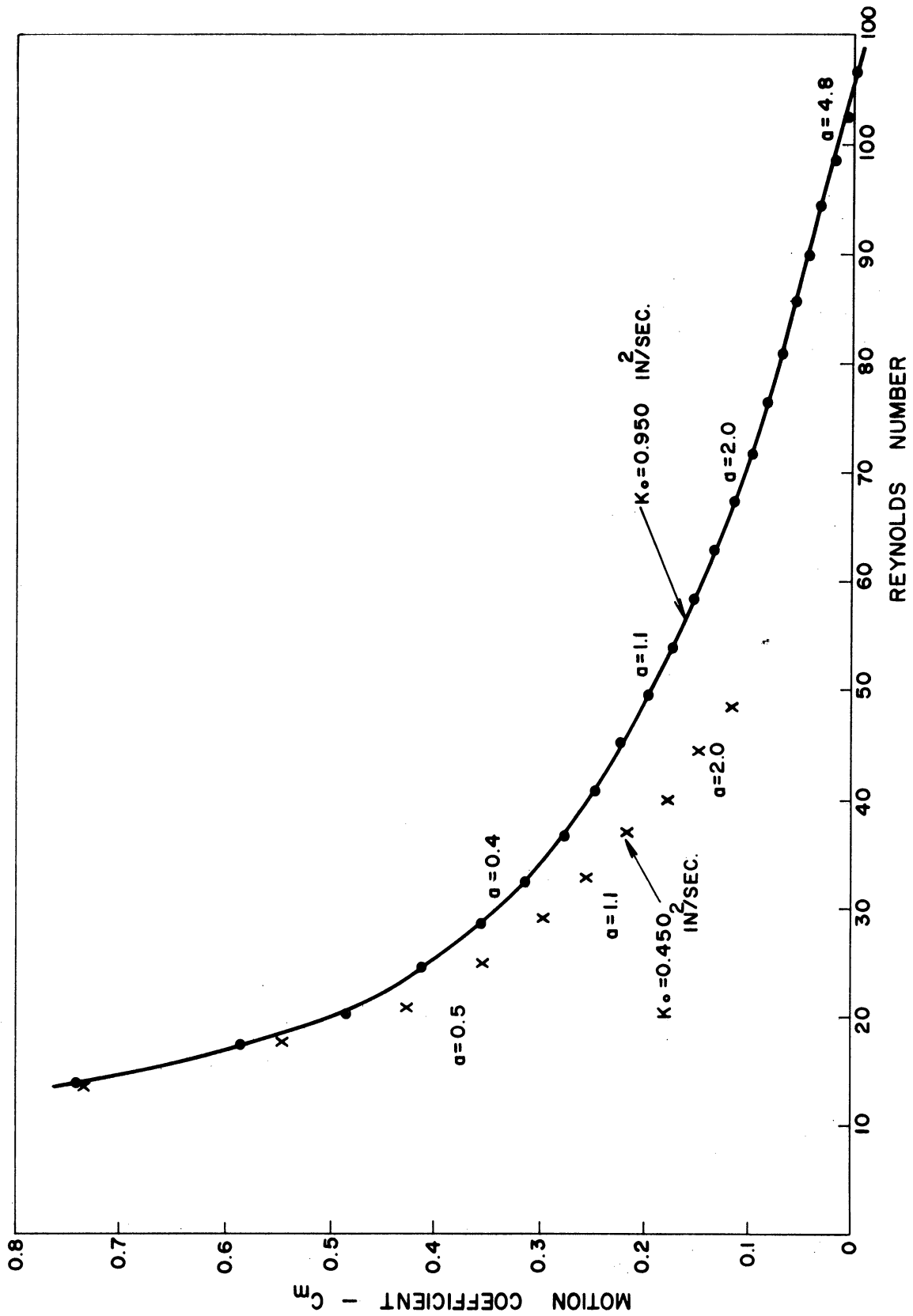
Figure 57. Motion Coefficients Versus Reynolds Numbers.

radius, the velocity of the ring, the time from first surface contact

to the point of penetration and other data used for checking purposes.

This was done for increments of penetration from initial depth to the

depth at which circulation vanished.

To illustrate the conclusions which may be drawn from the

numerical solutions of Equation 8, Figures 58 and 59 are presented.

Figure 58 shows the effect of holding the initial circulation

constant at K_o=0.950 in ^{2}/sec. and varying the density difference.

The indication is that for increasing density difference, if positive,

the ring radius increases more and more rapidly with increasing

penetration. The critical depths shown are calculated at 4.0 seconds

after free surface contact. As the density difference increases, there

is a small but definite decrease in critical depth. For negative density

differences, the rate of change of radius decreases and at a decreasing

rate as the difference is increased. For the lower parts of penetration

curves and negative density differences, the radius actually decreases.

With other initial values of circulation, similar graphs and observa-

tions result.

Figure 59 shows various initial circulations for the case of

neutral density. The effect of decreased circulation at initial depth

is to reduce the critical depth and to reduce the final ring radius.

The variation of critical depth with circulation is quite large and is

the basis of the penetration curves presented in Figures 25 through 41.

As indicated previously, the variation in critical depth with density

difference is so small that it does not appear on these figures. The

variation is within the tolerance for visual determination of critical

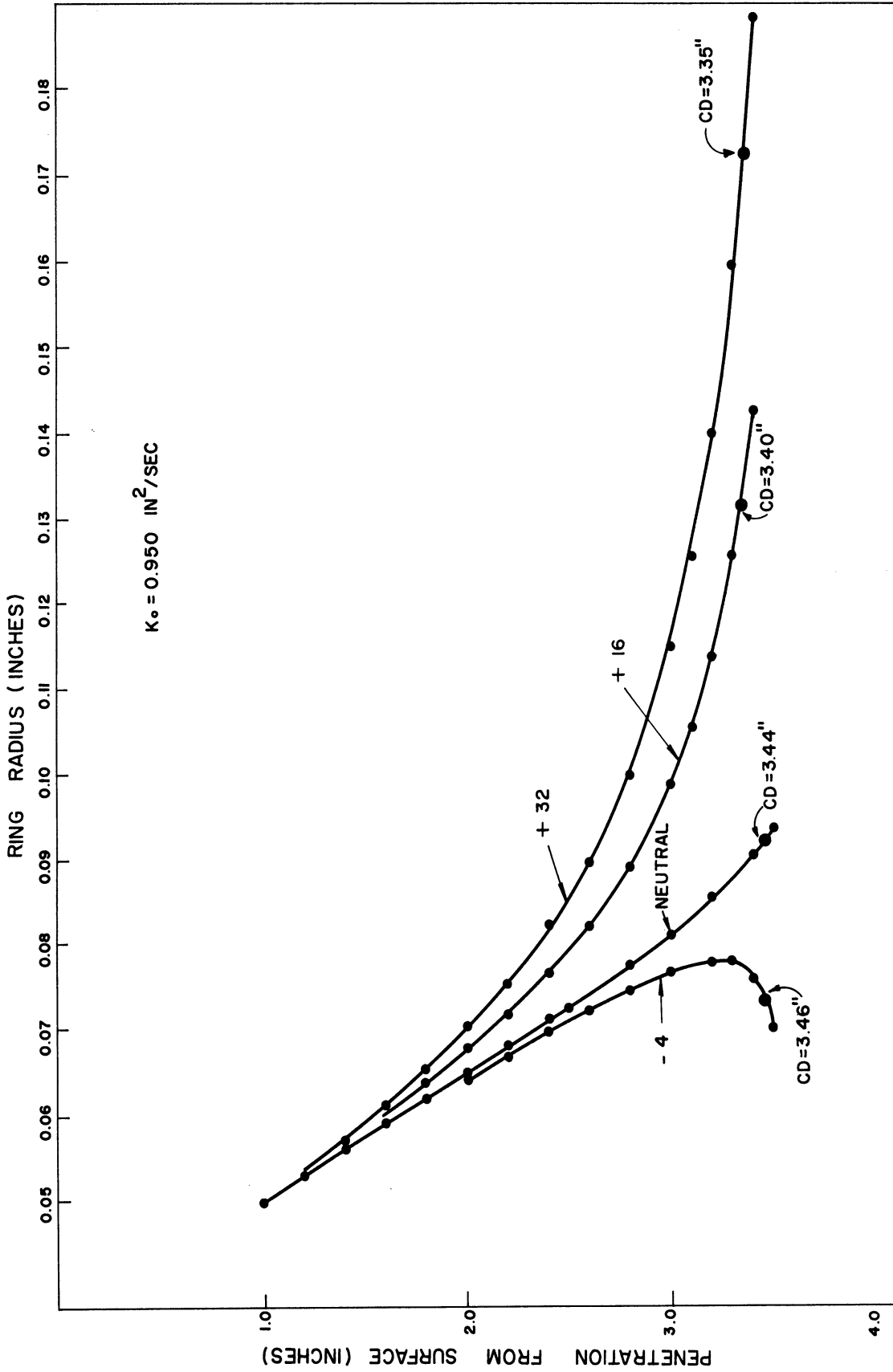depth. It is noted that calculations indicate that the slope of the

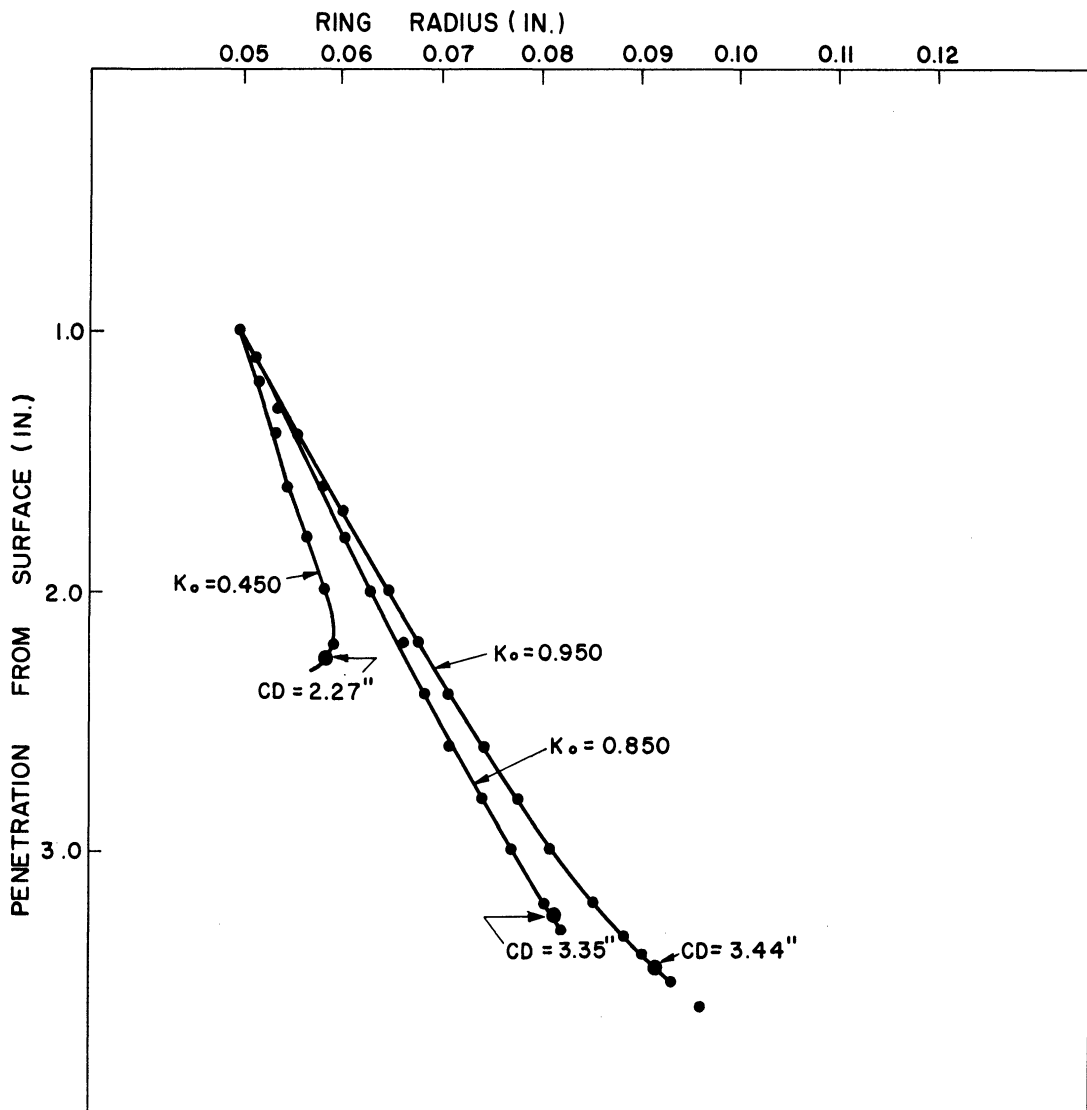Figure 58.   Variation of Ring Radius with Density Difference; $K_o = 0.950$.

Figure 59. Variation of Ring Radius with Initial Circulation; Neutral Density Case.

radius versus penetration curve at initial depth decreases for decreasing

circulation. This is partially due to the use of motion coefficients

from the maximum initial circulation for all circulations. Interpolation

to get appropriate curves for C_m and Reynolds numbers for each initial

circulation would remove this effect. Similar plots based on other

density differences exhibit similar characteristics.

It is to be expected that observed and calculated data be in

reasonable agreement. As an example, Figure 60 presents the experimental

curves as shown in Figure 11, (with a D4B8F.08 combination used to form

rings) with numerically calculated points added. In this instance,

agreement of experimental data and calculated data is very good except

for the lower section of the diameter curve. For rings of Type III,

the diameter was usually observed to decrease as critical depth was

neared, a characteristic this particular experimental ring did not

display.

In comparing the calculated values with experimental data,

agreement was found to be generally good. Note that the linear part of

the relationship of radius and penetration decreases with increasing

density difference, an observation made in the experiments. The cal-

culations of critical depth at 4.0 seconds gives values in excellent

agreement with observations. Comparisons of calculated curves with

individual curves of Figures 5 through 24 vary in agreement. Some are

very good while others compare poorly. In the cases of poor agreement,

it should be recalled that the calculations of initial circulation

were made from average velocities and could be in error in particular

cases. Also, the individual curves might have been affected by internal

currents or a ring which was atypical in some manner unknown at the
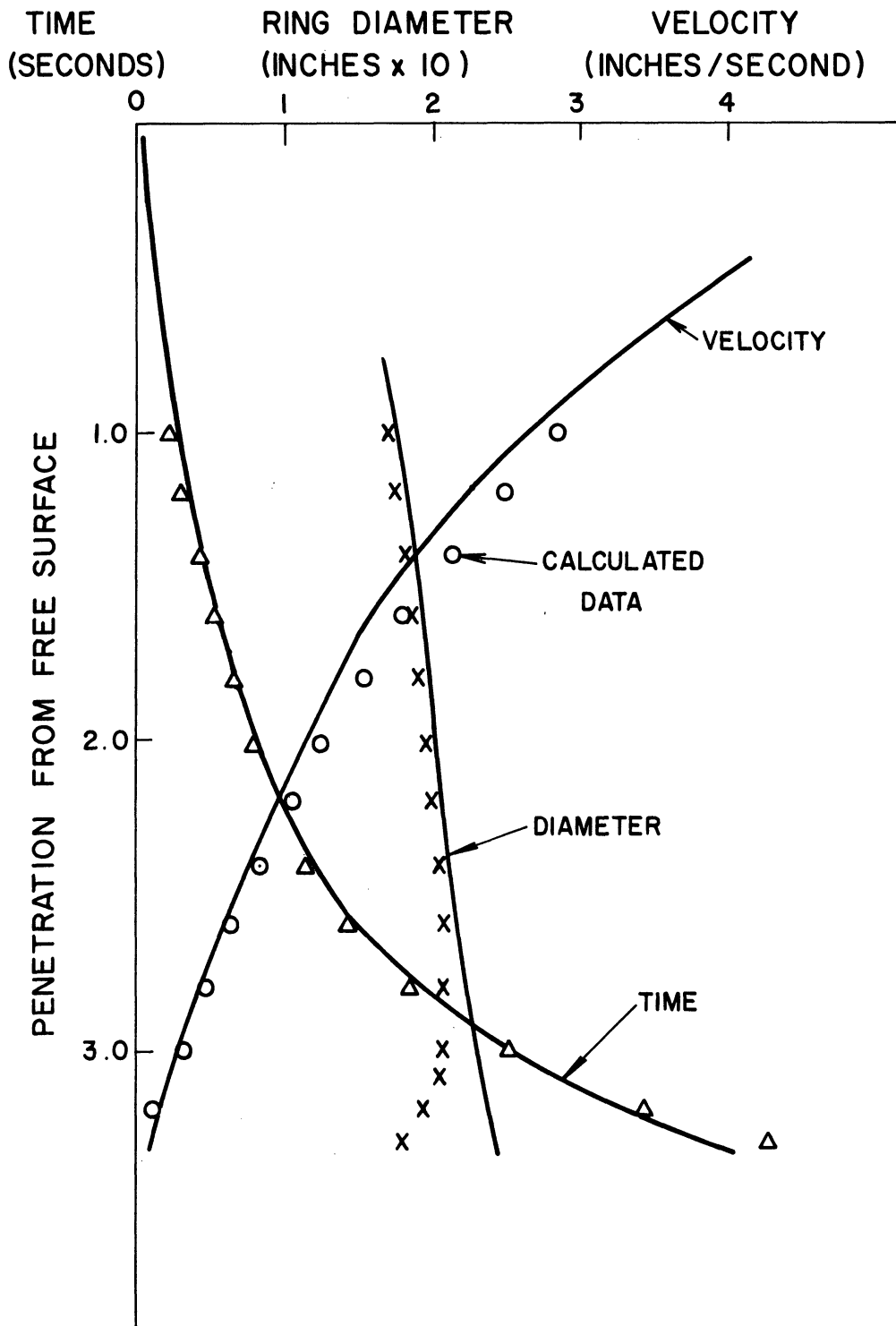
time of photographing.

Figure 60.   Calculated and Observed Data
for D4B8F.08 Rings.

B. Comparison with Previous Studies

      The basic framework within which this and previous studies were made differs in several ways. In the first place, the maximum density difference of drop and base solutions of this study was about 1.5% on either side of neutral density. Turner used density differences of up to 20% with the ring solution always buoyant with respect to the base solution. However, Turner noted that results using density differences of less than 4% were inconclusive due to the unstable nature of the rings produced. It was in this region, however, that this entire study was made.

      The magnitude of physical properties of rings which Turner used in his experimental work was much greater than those of this study. The buoyant mass used to form the rings which Turner used was approximately 400 times that of this study, the initial velocity of the rings of Turner was about 10 times the maximum initial velocity of this study and the constant circulation assumed by Turner was of the order of 15 times the average initial circulation of rings of maximum penetration of this study. That is, Turner studied rings of much greater momentum.

      The basic assumption of constant circulation of buoyant vortex rings in uniform surroundings as used by Turner is not used in the analysis of this study. The implication from the assumption of constant circulation and the assumption of a similarity solution is that the ring radius varies linearly with penetration. This result of Turner was not found to be generally true in this study. The relationship of ring radius and penetration was found to be nearly linear for much of the descent of rings of neutral density. However, for rings of Types I and III the linear relationship was not found satisfactory.

The actual values of the circulation of this study are seen to vary over the entire descent of the ring and to vanish at critical depth.

A second assumption suggested but not used by Turner is based on observations made by Bowen. Bowen's observations indicated that for a certain class of vortex rings arising in clouds generated by detonations, the vorticity containing region is constant. The values of Ra^2 for the rings of this study included in Table 1 indicated that rings of this study are of this type. The variations of Ra^2 are greatest for those rings of greatest density difference. However, for rings of greatest density difference, the formation of nodes which eventually develop into the secondary rings makes the measurement of core diameters very difficult as the rings descend. An increase in the values of Ra^2 based on the core diameter is therefore not surprising for these cases and the assumption of a constant volume vorticity containing region is quite appropriate.

VIII. SUGGESTED EXTENSIONS

This study has been primarily directed toward the general behavior exhibited by vortex rings formed by free falling drops hitting a free surface. A number of interesting features appeared which might form the basis of further investigations. Some are of an experimental nature while some require analytic research.

The experimental part of the program might profitably be expanded to include a variety of drop sizes rather than the one size used in this study. A few observations made with other size drops did indicate that although the properties of the ring were the same for these drops, there could be significant changes in the magnitudes and significance of certain properties. For instance, the development of secondary rings is likely to vary, turbulent tendencies of rings vary and the critical depths found to vary with penetration and time.

The use of a stratified base solution, or of a base composed of two distinct layers of fluid of different densities would be of interest. A few early observations of rings approaching an interface within the base indicated that penetration of the interface was dependent on the properties of the ring, in some unknown fashion. Saunders[14] conducted a similar experiment with much larger, turbulent rings.

Finally, the density range, which was quite limited in this study, might be extended to investigate limits on density for which present observations hold. It is especially obvious that rings of larger density differences spread more rapidly and that secondary ring development is more distinct.

Analytically, several areas are of interest. The internal motion of the drop and the configuration at impact with the free surface were found to be highly important in the formation of rings. The mechanism by which the transformation from drop to ring is made, if properly analysed, might contribute to a knowledge of the dynamics of falling drops. In a similar vein, the failure of drops to form rings for various fall heights needs further study.

The circulation of a ring after transformation might analytically be related to generating conditions. This would provide refined circulation relationships with depth and possibly lead to an explanation of the periodic nature of the circulation-penetration curve, especially for the larger free fall heights.

The dynamics and kinematics of the internal motion of the vortex rings are not clear. It is felt that the behavior of the air bubbles found at the core of the rings might aid in determining the forces and internal motion within the body of fluid surrounding the ring proper.

The stability of the descending ring might be investigated to determine the mechanism by which the secondary rings form. This would likely involve a study of surface tension effects in the core of the ring.

IX. CONCLUSIONS

From the results of this study, several conclusions may be drawn concerning the characteristics and behavior of vortex rings formed by free falling drops interacting with a free surface.

1. The rings of this study are of a different nature from those assumed by Turner. Rings of this work are considered laminar while those of Turner were turbulent. Furthermore, the assumptions and conclusions of the similarity solution assumed by Turner were not found appropriate to this study.

2. The assumption of a constant volume of the vorticity containing region proposed by Bowen is supported by the results of this study. It was found that the volume of the dyed region did remain essentially constant during descent of a ring.

3. Vortex rings formed by free falling drops interacting with a free surface form only for a limited range of free fall heights. This range is bounded above and below by regions in which formation is either erratic, non-existent or of a different basic mechanism of formation.

4. The extent of penetration of rings into the base solution is highly dependent in at least two ways on the free fall height of the drop. If the momentum of the drop, which is a function of free fall height, is too great, no coherent rings appear. Also, the shape of the oscillating drop as it hits the surface has radical effects on the penetration of the ring formed. The shape of the drop is found to change rapidly with free fall height.

5. The penetration of the rings is related to the initial circulation and the density difference of the solutions used. In

general the larger the circulation or smaller the density difference, the greater the penetration.

6.   On the basis of the last two points, the circulation of the ring formed is highly dependent on the shape of the drop when it hits the surface.

7.   Two important dimensionless parameters appeared during the study. The parameter $\Delta\rho/\rho$ was found to be important in determination of the buoyant force and the Reynolds number in determining the motion coefficients for use in evaluating the drag term.

8.   The variation of diameter of a ring during descent is quite dependent on the relative densities of the drop and base solutions. The slope of the penetration-diameter curve in the region close to initial depth is nearly constant for all rings and the curve tends to be linear for a time after initial depth. For increasing density difference, however, the region of linearity decreases and the ring expands in diameter more rapidly than for the neutral density case, if the difference is positive. For negative differences, the ring tends to expand less rapidly and even contracts near critical depth.

9.   The time to reach critical depth was found to be very close to 4.0 seconds for all rings of this study. This was observed regardless of the density differences or circulation at initial depth.

10.   Other phenomena of the study: secondary rings form from rings of non-neutral density.

11.   A theory model can be constructed to predict the motion of the ring with satisfactory accuracy.

APPENDIX A

OSCILLATION OF FREE FALLING DROPS

Although a study of the motion of free falling drops is not a direct part of this study, the following frame by frame presentation in Figure 61 clearly shows the oscillation which is present in the falling drop. The arrangement is such that a complete oscillation is shown in each column. By looking across a row, the similarity of shape for consecutive periods can be seen.

It should also be noted that the time from the spherical shape to the vertically oblate form and back to the spherical shape is longer than for the half cycle through the horizontally oblate form. The drop shown was for a free fall distance of 0.105' and is shown hitting the surface as a sphere in progress to the horizontally oblate form. This produces minimum penetration.

A free fall of 0.085' produced maximum penetration for the D8B0 combination used. Surface contact occurred approximately at frame 29 (fifth down in the fourth column) as the drop was spherical and progressing to a vertically oblate form.

The frames shown were taken at 480 frames per second, or an elapsed time between frames of approximately 0.002 seconds.
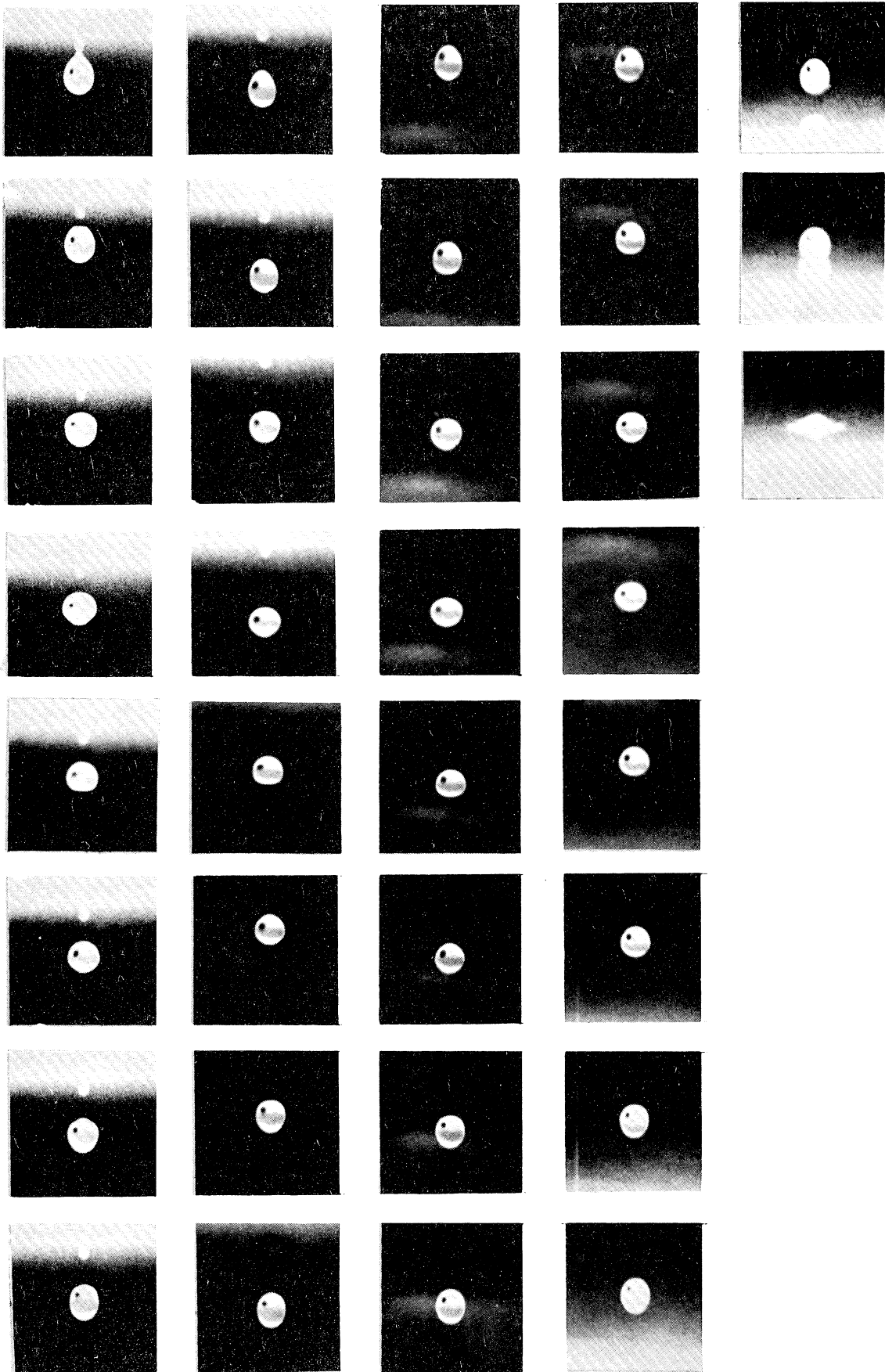
Figure 61. Oscillations of a Free Falling Drop from 0.105'.

APPENDIX B

DETERMINATION OF DROP PROPERTIES

To determine the diameter of a sphere with the same volume as the average volume of the drop, a series of drops were caught in a 5 ml. graduate. The first milliliter was found to be inaccurate and not used in the calculations. The following presents the values for two needle sizes.

	N20D16	N20D16	N20D0	N15D16	N15D0
seconds/drop	9	0.9	4.1	4	5
drops: 0-1 ml.	50	50	51	24	25
drops: 1-2 ml.	69	66	69	36	36
drops: 2-3 ml.	67	64	69	35	35
drops: 3-4 ml.	66	62	66	34	34
drops: 4-5 ml.	66	64	67	35	35
Average:	67	64	68	35	35
Diameter: cm.	0.308	0.310	0.308	0.378	0.378

From this, it was concluded that drop size is independent of drop solution for the range of densities of the study provided the drops were not too closely spaced. Also, an increase in needle size, (i.e. diameter, not needle number size), increases the drop size.

From the drop diameter, the expected frequency of oscillation is easily calculated by the relationship:

$$f = 3.87 \, a^{-3/2} \text{ cycles/sec.}$$

where a is the radius of the drop in centimeters. For the two cases above:

No. 20 needle   a = 0.154 cm.   Frequency = 64.5 cycles/sec.

Period = 0.0155 seconds

No. 15 needle   a = 0.189 cm.   Frequency = 47.1 cycles/sec.

Period = 0.0212 seconds

BIBLIOGRAPHY

1. Anders, Edward, "Diamonds in Meteorites," <u>Scientific American</u>, (Oct., 1965), 26.

2. Basset, A.B., <u>Hydrodynamics</u>, Vol. 2, Dover Publications, New York, 1961.

3. Charters, A. C., "High Speed Impact," <u>Scientific American</u>, (Oct., 1960), 128.

4. Cone, D. D. Jr., "The Soaring Flight of Birds," <u>Scientific American</u>, (April, 1962), 130.

5. Hicks, W. M., "On the Steady Motion and Small Vibrations of a Hollow Vortex," <u>Philo. Transaction</u>, Vol. 175, Part 1, (1884), 161.

6. Hicks, W. M., "Researches on the Theory of Vortex Rings," <u>Philo. Transaction</u>, Vol. 176, Part 2, (1885), 725.

7. Hughes, R. R., and Gilliland, E. R., "The Mechanics of Drops," <u>Chem. Eng. Prog.</u>, Vol. 48, No. 10, (Oct., 1952), 497-504.

8. Lamb, Horace, <u>Hydrodynamics</u>, Dover Publications, New York, 1945.

9. Morton, B. R., Taylor, G. I., and Turner, J. S., "Turbulent Gravitational Convection from Maintained and Instantaneous Sources," <u>Proc. of Royal Society</u>, A234, (1956), 1.

10. Morton, B. R., "Weak Thermal Vortex Rings," <u>Journal of Fluid Mechanics</u>, 9, (1960), 107.

11. Rayfield, G. W., and Reif, F., "Evidence for the Creation and Motion of Quantized Vortex Rings in Superfluid Helium," <u>Physical Review Letters</u>, Vol. 11, No. 7, (Oct., 1963), 305-308.

12. Reif, F., "Quantized Vortex Rings in Superfluid Helium," <u>Scientific American</u>, Vol. 211, No. 6, (Dec., 1964), 116.

13. Reynolds, Osborne, <u>Papers on Mechanical and Physical Subjects</u>, Vol. 1, Cambridge University Press, 1900.

14. Saunders, Peter M., "Penetrative Convection in Stably Stratified Fluids," <u>Tellus</u>, 2, (1962), 177.

15. Scorer, R. S., "Experiments of Convection of Isolated Masses of Buoyant Fluid," <u>Journal of Fluid Mechanics</u>, 2, (1957), 583.

16. Taylor, G. I., "The Instability of Liquid Surfaces When Accelerated in a Direction Perpendicular to their Planes. I," <u>Proc. Royal Society</u>, A201, (1950), 192.

17. Thomson, J. J., "On the Vibrations of a Vortex Ring, and the Action upon each other of Two Vortices in a Perfect Fluid," Philo. Transaction, Vol. 173, Part 2, (1882), 493.

18. Turner, J. S., "Buoyant Vortex Rings," Proc. Royal Society, A239 (1957), 61.

19. Turner, J. S., "A Comparison between Buoyant Vortex Rings and Vortex Pairs," Journal of Fluid Mechanics, 9, (1960), 419.

20. Woodward, Betsy, "The Motion in and Around Isolated Thermals," Quarterly Journal of Royal Meterological Society, 85, (1959), 144.